Combined *operando* Raman/UV-Vis-NIR spectroscopy as a tool to study supported metal oxide catalysts at work

Het toepassen van *operando* Raman / UV-Vis-NIR spectroscopie voor het bestuderen van metaaloxide katalysatoren onder reactiecondities

(met een samenvatting in het Nederlands)

Proefschrift

ter verkrijging van de graad van doctor aan de Universiteit Utrecht op gezag van de rector magnificus, prof. dr. W.H. Gispen, ingevolge het besluit van het college voor promoties in het openbaar te verdedigen op maandag 19 juni 2006 des middags te 4.15 uur

door

Stanislaus Josephus Tinnemans

geboren op 14 februari 1978, te Deurne

Promotor:	Prof. dr. ir. B.M.W. Weckhuysen
Co-promotoren:	Dr. T.A. Nijhuis
	Dr. T. Visser

Contents

ISBN-10: 0-393-4209-1

ISBN-13: 978-90-393-4209-1

Omslag: audivisuele dienst, Departement Scheikunde, Universiteit Utrecht

The research described in this thesis was financially supported by NWO

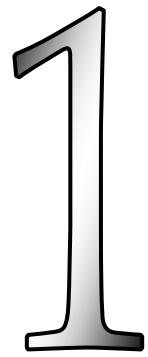

General Introduction

Introduction

In 1666 Newton was the first to show that 'white' light from the sun consists of a series of colors by means of a glass prism. The resulting spectrum was displayed on a screen. This analysis of light was the beginning of the field of spectroscopy. Throughout the centuries thereafter, different spectroscopic techniques have been developed. All these methods have in common that they use radiation (as light is a form of electromagnetic radiation) to interact with a sample. As the sample interacts with the incoming beam, the resulting outgoing beam provides characteristic information about the sample. A human eye is a kind of spectrometer. If one looks at a piece of red paper, the following process occurs. Daylight (white light) interacts with the paper surface. The complementary color is absorbed and the remaining light is reflected and reaches the eye. In this case, this means that green is absorbed and since this is the complementary color of red, the paper is seen as red.

Figure 1.1 shows part of the electromagnetic spectrum classified into the commonly known regions.[1]

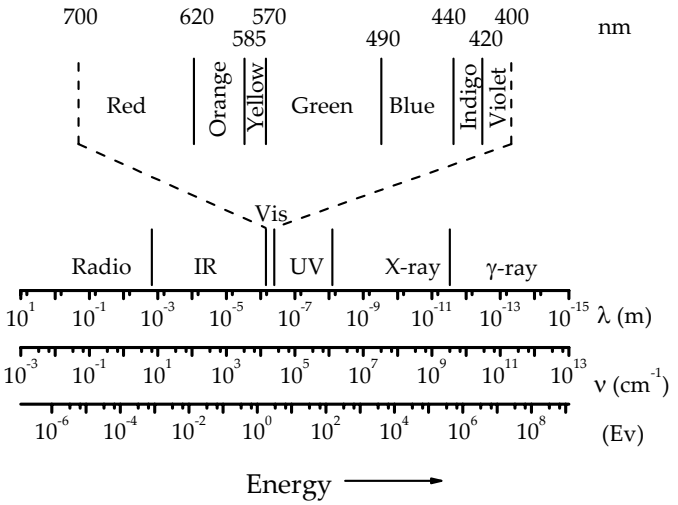

Figure 1.1 *Electromagnetic spectrum showing the different electromagnetic regions.*

Spectroscopy and catalysis

Light can interact with matter and in this process it can be absorbed, reflected or scattered. Measuring the absorbed or scattered radiation provides chemical information about the substance under investigation. These substances can be gasses, liquids as well as solids. One specific type of solids are catalysts. A catalyst is a substance that increases the reaction rate without being consumed in a reaction.[2] Examples of well-known catalysts are enzymes in a body, but also the catalyst in the

exhaust gas system of a car. The definition implies that a catalyst has an endless life. This is not completely true since catalysts have to be replaced due to a loss of activity after a period of time.

To understand the behavior of this type of materials it is important that the characteristic features are investigated. This makes it possible to create new catalysts or improve existing ones. Spectroscopy can help in this process because for instance it is possible to learn why a catalyst is performing excellent, or on the contrary is not working at all in a reaction.

The catalyst is typically characterized at different stages during its catalytic cycle. This means at different steps during its preparation process, but also after reaction when it might be deactivated. A combination of this information helps in understanding the catalytic behavior during reaction. However, the active species are not necessarily identified in this way. It is possible that during reaction the catalyst changes and that the initially identified structures are the most abundant, but not representative for the activity. Think of single frames in a film. Separately they may create an impression, but sufficient frames together in the right order result into a movie. Ideally catalyst scientists would like to take movies or 'motion pictures'[3] inside a catalytic reactor when it is operating, providing a detailed insight in the working principles of the catalyst hence enabling the design of more active and / or selective substances. Such approach of catalyst design is in most cases still a dream since the experimental tools currently available for making 'motion pictures' inside a catalytic reactor are very rudimentary.[4,5]

Efforts of people to increase the understanding of catalytic systems resulted in the development of *in-situ* spectroscopy. In contrast with 'conventional' static spectroscopy, additional criteria are met. It can be defined as spectroscopy under reaction conditions.[6] A different definition states that an *in-situ* spectroscopic study is the study of a sample that is in the position where it has been treated or is being treated.[7] The first definition is easy to understand. By applying (different) spectroscopic techniques under reaction conditions, it is made sure that the obtained information is relevant for e.g. the active site. The second definition is more general and is applicable in all situations where a changing condition during the measurements is involved. For instance, monitoring the heating of a catalyst in a vacuum environment is called *in-situ*, but also gas flowing over a catalyst at temperatures far from normal operating temperatures or experiments during which the pressure is changed. Another example is an experiment in a specially designed optical cell, which has no resemblance with a typical industrial reactor.

Recapitulating, the term *in-situ* spectroscopy is not always used rigorously, since the experimental conditions may differ from relevant reaction conditions.
To illustrate the interest in this field of spectroscopy the number of scientific papers published in literature on this subject over the last 45 years are plotted in Figure 1.2.

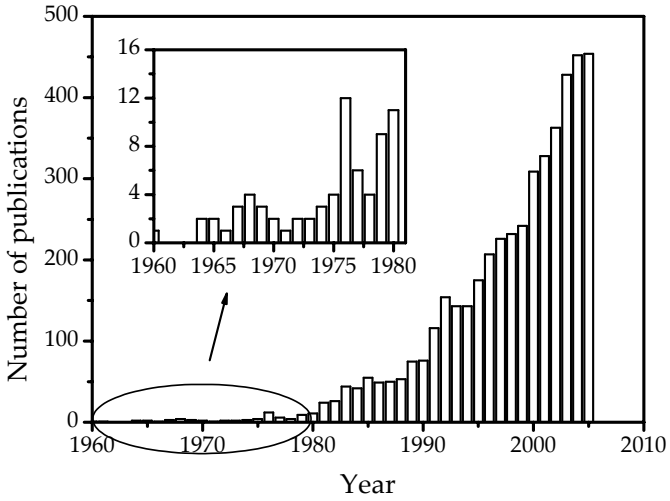

Figure 1.2 *Number of scientific publication retrieved via SciFinder using the keywords 'in situ' and 'spectroscopy' and 'catalysis' (2-1-2006).*

The first publications on *in-situ* spectroscopy date from 1954 by Eischens and describe the interaction of CO with Cu, Pt, Pd and Ni supported on SiO_2.[8,9] From 1954 to 1980 only a few papers per year appeared in literature. After 1980 a rapid increase in the amount of papers is visible indicating that from that year onwards a growing interest in the use of *in situ* spectroscopic techniques in the field of catalysis is present. Comparing the relative increase to the increase in publications on 'catalysis' in general, revealed that especially in the period 1995-2005 more research on 'in situ' and 'spectroscopy' is conducted. To distinguish '*in-situ* spectroscopy' from 'spectroscopy under true catalytic operation', the term *operando* was introduced to emphasize that the spectroscopic measurements are performed under reaction conditions.[10]
Measuring under reaction conditions has more value if time resolved techniques can be applied. In this way the formation and disappearance of species inside a reactor can be monitored. Ideally, one would like to measure at timescales corresponding to the breaking and formation of chemical bonds in molecules at the active site, but most of the *operando* techniques nowadays applied are only working in the second or

subsecond regime. In other words, only differences in relative population of active sites and / or reactive intermediates can be assessed.
For measuring under reaction conditions it is important that these conditions are as close to industrial practice as possible, i.e. realistic pressures and temperatures. This implies that the experimental set-up can be regarded as a 'true' catalytic reactor. Ideally the spectroscopic device is brought inside the reactor unaltering the processes taking place inside.

In the last decade several *operando* set-ups have been built in various laboratories combining the application of a spectroscopic technique with on-line activity measurements.

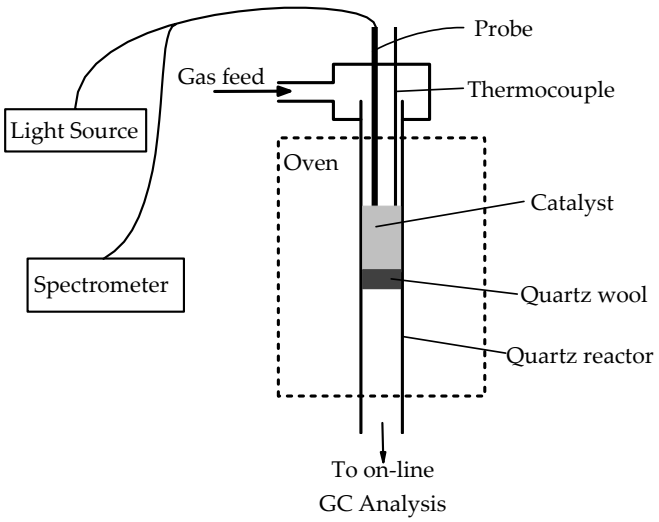

Figure 1.3 *Scheme of an operando UV-Vis-NIR set-up for measuring supported metal oxide catalysts operating in gas-phase reactions at elevated temperatures up to 700 °C and ambient pressures.*[11]

Figure 1.3 shows as an example a set-up, which allows measuring time resolved UV-Vis-NIR spectra of a catalytic solid during a gas-phase reaction. More specifically, this set-up has been used to study the dehydrogenation of light alkanes over supported metal oxide catalysts as well as the decomposition of NO_x over Cu-ZSM-5 zeolites.[5,11-14]

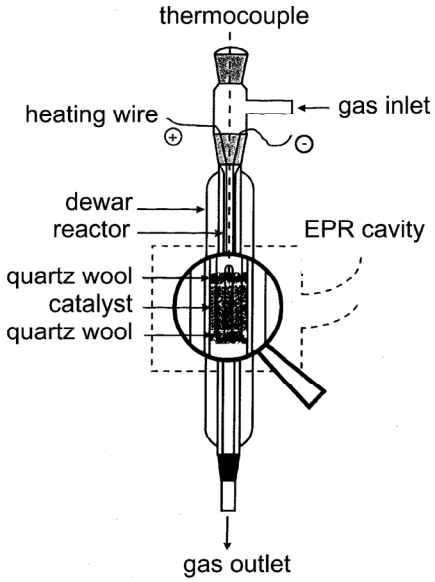

Figure 1.4 *Scheme of an operando EPR set-up for measuring supported metal oxide catalysts operating in gas-phase reactions at temperatures up to 550 °C and ambient pressures.*[15]

Another example, shown in Figure 1.4, is an *operando* EPR cell developed in the group of Brückner (Berlin, Germany). It has been used to study the behavior of vanadium phosphate catalysts during the oxidation of n-butane, the dehydrogenation of alkanes over supported chromium oxide catalysts and the selective catalytic reduction of NO_x over supported manganese oxide catalysts.[16-21] Both designs only allow for the measurement of one spectroscopic technique. It would be more advantageous to look at catalytic systems from different perspectives by making use of multiple characterization techniques.[22] However, one has to keep in mind that adding additional spectroscopic techniques is most valuable if they provide complementary information. Combining complementary information leads to a more detailed understanding of the catalytic system and hence a better assessment on what is happening in the reactor. With these considerations in mind, it is fair to say that in the last years many attempts have been made by several research groups to combine multiple spectroscopic techniques into one set-up.

Overview of operando set-ups making use of multiple spectroscopic characterization techniques

Table 1.1 provides an overview of the currently available *operando* set-ups equipped with two or three spectroscopic techniques, which can be used simultaneously for catalyst characterization.[15,22-38] This table shows the time resolution that can be achieved (in the second or sub-second regime), the obtained information and the application domain (homogeneous and heterogeneous catalysis). To the best of our knowledge, the first combination of techniques reported in the open literature was X-ray diffraction (XRD) with X-ray absorption spectroscopy (EXAFS).[27-29,35] Such set-ups have been developed independently of each other by the groups of Thomas (Cambridge, UK) and Topsoe (Lyngby, Denmark) in the 90's. The nice feature of this combination is the complementarities of the techniques; *i.e.*, XRD provides long-range ordering information of the catalytic solid under investigation, whereas EXAFS is sensitive to the short-range ordering of the materials. Besides catalytic reactions, the set-up is also suitable to study crystallization processes of *e.g.* zeolite materials. Unfortunately, the time resolution was in the order of 30 seconds to minutes. Recent developments in X-ray detection systems may lead to substantial improvements.

Since this first coupling of techniques, many other set-ups have been developed. Most combinations involve the use of vibrational (IR as well as Raman) and electronic (UV-Vis-NIR) spectroscopies. Certainly, from a technical point of view these are the most simple to make, whereas in the case of magnetic resonance techniques (NMR and EPR) more technical hurdles have to be taken to make the combined set-up working. Bruckner reported in 2001 the combination of EPR and UV-Vis-NIR spectroscopy together with on-line GC analysis.[15] With this set-up transition metals (especially Cr and V) have been investigated during for instance alkane dehydrogenation reactions.

The basis of this thesis is a set-up, which combines time-resolved UV-Vis-NIR and Raman spectroscopy to study heterogeneous catalysts in gas phase reactions, and is equipped with both on-line gas chromatography and mass spectrometry for product analysis. Very recently, two experimental set-ups have been built making use of three spectroscopic techniques. These techniques can be applied simultaneously to the sample under (identical) reaction conditions. An *operando* UV-Vis, Raman and EPR set-up has been constructed by the group of Brückner (Berlin, Germany), which allows studying supported vanadium oxide catalysts during oxidative dehydrogenation of propane[24]. The other 'three technique set-up' combines UV-Vis-NIR,

Tabel 1.1 *Existing combinations of characterization techniques for studying homogeneous (Homo) and heterogeneous (Hetero) catalysts at work.*

Techniques	Time (s)	Information to be obtained	Domain	Ref.
XRD	30	⇒ Long-range structural order	Hetero	27-29,35
XAFS	10-30	⇒ Short-range structural order		
EPR	60-300	⇒ Paramagnetic transition metal ions	Hetero	15,22
UV-Vis-NIR	0.01-1	⇒ Electronic d-d and charge transfer transitions of TMI		
Raman	2-120	⇒ Vibrational spectra of metal oxides and organic deposits, such as coke	Hetero	32,33
UV-Vis-NIR	0.01-1	⇒ Electronic d-d and charge transfer transitions of TMI		
ED-XAFS	0.01-1	⇒ Coordination environment and oxidation state of M and M^{n+}	Homo	36
UV-Vis-NIR	0.0008	⇒ Electronic d-d and charge transfer transitions of TMI		
Raman	2-120	⇒ Vibrational spectra of metal oxides	Hetero	30
FT-IR	0.01-1	⇒ Vibrational spectra of adsorbed species, such as NO		
NMR	7200	⇒ Identification of organic molecules formed via chemical shift values	Hetero	37
UV-Vis-NIR	0.01-1	⇒ Electronic transitions ($\pi^* \leftarrow n$ and $\pi^* \leftarrow \pi$) of organic molecules		
ED-XAFS	6	⇒ Coordination environment and oxidation state of M and M^{n+}	Hetero	31
FT-IR	0.01-1	⇒ Vibrational spectra of adsorbed species, such as CO and NO		
FT-IR	0.01-1	⇒ Vibrational spectra of reaction mixtures and adsorbed molecules	Homo and hetero	26,34
Phase behavior monitoring		⇒ Video monitoring of phase behavior		
FT-IR	0.01-1	⇒ Vibrational spectra of reaction mixtures and adsorbed molecules	Hetero	25
UV-Vis-NIR	0.01-1	⇒ Electronic transitions of the catalyst material		
EPR	60-300	⇒ Paramagnetic transition metal ions	Hetero	24
UV-Vis-NIR	0.01-1	⇒ Electronic d-d and charge transfer transitions of transition metal ions		
Raman	2-120	⇒ Vibrational spectra of metal oxides and organic deposits, such as coke		
UV-Vis-NIR	0.05-1	⇒ Electronic d-d and charge transfer transitions of transition metal oxides	Hetero	23
Raman	0.05-1	⇒ Vibrational spectra of metal oxides and organic deposits, such as coke		
ED-XAFS	0.003-1	⇒ Coordination environment and oxidation state of metals and metal ions		

Raman and ED-XAFS in one spectroscopic-reaction cell and has been developed in our group.[23]

One would anticipate at first sight that making combinations of two or three spectroscopic techniques is rather straightforward. In principle one could couple all the techniques mentioned in Table 1.1 in one catalytic reactor, creating a kind of dream machine. Unfortunately, this instrument will simply not work because each spectroscopic technique has its own sensitivity towards a specific catalytic system or towards the reactants or solvents used. For instance, every technique has a concentration range in which useful data can be gathered. If these ranges do not overlap, the additional value of combining techniques is limited.[39] Often a compromise in which all techniques are not hampered too much has to be chosen.

In other words, one should first consider the catalytic application, the characteristics of the catalytic material as well as the reaction medium before starting to assemble the most appropriate techniques in one reactor system. One could even argue that a reaction mechanism proposed based on experimental data obtained for a catalytic system at low concentrations could be different from that obtained at high concentrations.

As already mentioned briefly above, the development of a combined *operando* Raman and UV-Vis-NIR set-up will be discussed in this thesis. This combination is able to provide information on both vibrational and electronic transitions and therefore is complementary. The possibility for providing new information about supported metal oxide catalysts at work is explored with the dehydrogenation of propane over Cr / Al_2O_3 catalysts as the case study. To provide the reader a better understanding of the applied techniques, the basic theory will now be briefly discussed.

Theoretical background on Raman spectroscopy

In 1928, C.V. Raman and K.S. Krishnan published the observation that if (sun)light is passed through some filters and focused on a liquid, the observed radiation not only consists of the same wavelength as the incident beam (elastic scattering), but also of scattered radiation of lower frequency (inelastic scattering).[40] This observation was in line with theoretical predictions of A. Smekal in 1923.[41] Later it was shown that also light with a higher frequency is present.

The inelastic scattered radiation contains information specific for the compound under investigation. In Raman spectroscopy three different types of scattering are

important namely the Rayleigh, the Stokes and the anti-Stokes scattering.

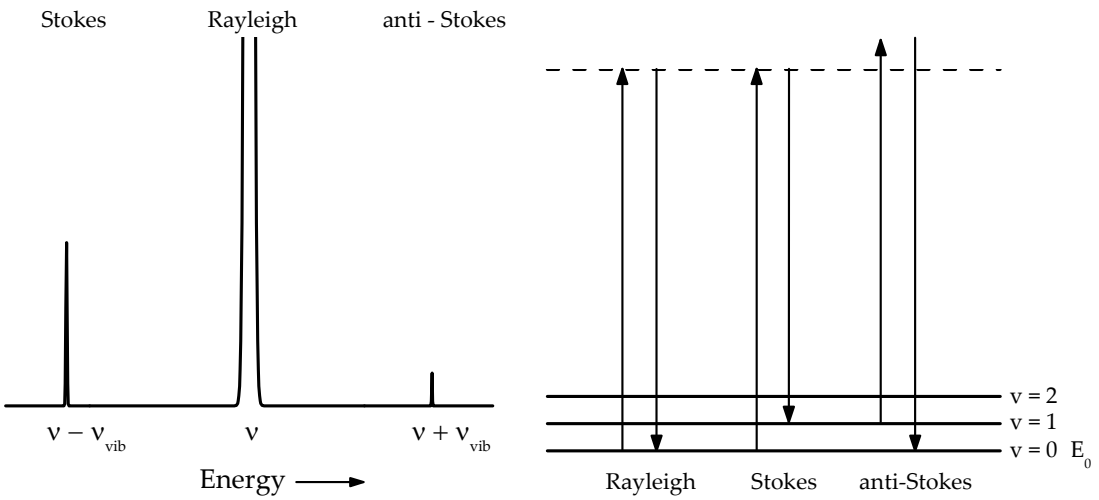

Figure 1.5 *Theoretical Raman spectrum (left) and an energy diagram (right) showing the principal energy transfers related to Raman spectroscopy.*

The left part of Figure 1.5 shows a typical Raman spectrum. In the right part the corresponding energy transitions are illustrated. The first type of radiation is Rayleigh scattering. In this process photons are elastically scattered and have the same energy as the incident beam. Molecules are excited in a virtual state and upon relaxation return to their original ground state. The release of energy during relaxation equals the energy primarily absorbed. However, there is a very small possibility, depending on the wavelength of the incident beam, that the energy of the scattered radiation is of a different energy i.e. light is inelastically scattered. Most often, this radiation will be of lower energy. In Raman spectroscopy this is called the Stokes radiation. In Figure 1.5 (right) this is illustrated in the middle part where a molecule is illuminated and falls back to an excited state. On the other hand, a molecule can release radiation of higher energy if the final energy level of a molecule is lower than the original one, the so called anti-Stokes radiation. A molecule, already in an excited state, is illuminated and upon relaxation falls back into its ground state. In this process, energy is transferred from the molecule into the radiation.
From Figure 1.5 (right) it is clear that the same vibration is involved in both the Stokes and anti-Stokes shift, namely $\nu_1 \rightarrow \nu_0 = \nu_0 \rightarrow \nu_1$.

After defining the terms Stokes and anti-Stokes radiation, it is important to understand the changes that are induced in the molecules. The amount of energy transferred is typical for transitions between vibrational levels. This does not mean that every vibration in a molecule is Raman active. Only those vibrations can be seen with Raman spectroscopy in which the polarizability of the molecule is changed.
The electric field of the incident radiation (E) interacts with a molecule and may induce a dipole moment (μ) of magnitude

$$\mu = \alpha E \qquad \text{(eq. 1.1)}$$

In this equation, the polarizability is represented by α.
The incident radiation is a time varying quantity and if molecules are subjected to a beam of radiation of frequency (ν) the electric field experienced by each molecule varies according to

$$E = E_0 \sin(2\pi\nu t) \qquad \text{(eq. 1.2)}$$

resulting in

$$\mu = \alpha E = \alpha E_0 \sin 2\pi\nu t \qquad \text{(eq. 1.3)}$$

In Equation1.3 the induced dipole (μ) will emit radiation of its own oscillating frequency and this explains the observed Rayleigh scattering. If molecules undergo some internal motion like rotation or vibration, the polarizability can be changed periodically and if a vibration of frequency ν_{vib} is involved, one can write

$$\alpha = \alpha_0 + \beta \sin(2\pi\nu_{vib} t) \qquad \text{(eq. 1.4)}$$

In this equation α_0 represents the equilibrium polarizability and β the rate of change of polarizability with the vibration.
Combining Equations 1.4 and 1.3 result in

$$\mu = \alpha E = (\alpha_0 + \beta \sin(2\pi\nu_{vib} t)) E_0 \sin 2\pi\nu t \qquad \text{(eq. 1.5)}$$

This can be rewritten as

$$\mu = \alpha_0 E_0 \sin 2\pi\nu t + \tfrac{1}{2}\beta E_0 \{\cos 2\pi(\nu - \nu_{vib})t - \cos 2\pi(\nu + \nu_{vib})t\} \quad \text{(eq. 1.6)}$$

From Equation 1.6 one learns that the induced dipole has, besides the Rayleigh component, also two components at a frequency of $\nu \pm \nu_{vib}$. Note that these Stokes and anti-Stokes frequencies are only present if $\beta \neq 0$.
The ratio between anti-Stokes (AS) and Stokes (S) transitions can be derived from the Maxwell-Boltzmann distribution of states[42]:

$$\frac{N_{upper}}{N_{lower}} = \frac{AS}{S} = \frac{(\nu + \nu_{vib})^4}{(\nu - \nu_{vib})^4} e^{-\Delta E/kT} \quad \text{(eq. 1.7)}$$

In this equation ΔE represents the energy difference between the relaxed and excited state, k the Boltzmann constant and T the temperature.
From Equation 1.7 it becomes clear that at moderate temperatures Stokes transitions are more likely to occur than anti Stokes transitions. As a result a Stokes band is more intense than the corresponding anti-Stokes band, see Figure 1.5 (left).

In principle light of every wavelength can be used to obtain a Raman spectrum. However, to prevent overlapping spectra monochromatic light is used. In the early days sources like a mercury arc were used. With the development of the laser in combination with the improvements of the filters, more intense sources became available. By applying laser technology the number of photons reaching the sample was increased and so increasing the amount of Stokes (and anti-Stokes) radiation. The result is a better sensitivity. From Equation 1.7 it becomes clear that the excitation wavelength is also of influence on the Raman scattering. For instance, if the wavelength of the laser is reduced by a factor 2 (from 1064 nm (9398.5 cm^{-1}) to 532 nm (18797 cm^{-1})), the Stokes (and anti Stokes) bands are 16 times (2^4) more intense. This implies that it is best to use short wavelength lasers, since then the Raman efficiency is best. However, other phenomena are responsible for an influence on the sample and should therefore be taken into consideration. For instance fluorescence may occur.[43] This is when in the decay from the virtual excited state light is emitted by the sample. Also trace amounts of impurities can be responsible for this effect. Fluorescence is very intense compared to the weak Raman effect and as a result the

Raman bands cannot be discriminated. Changing the wavelength of the laser to a longer wavelength can sometimes be used to solve problems with fluorescence.[44] The explanation is that at a longer wavelength the energy transitions, responsible for the fluorescence, are no longer possible. An alternative is using a deep UV laser ($\lambda < 250$ nm).[45] The reason for the absence of fluorescence in using these high energy lasers is not known. The disadvantage, however, is that photochemical processes may lead to undesired side-reactions. Laser heating can also be a problem during measurements. Especially blue and black samples are capable of absorbing light strongly and as a result blackbody radiation may occur. Also the structure of the sample may change due to this increased temperature.[46]

Theoretical background on UV-Vis-NIR diffuse reflectance spectroscopy

In contrast to Raman spectroscopy, where vibrational information is obtained, UV-Vis-NIR spectroscopy probes the electronic transitions in a compound. Well-known examples are the $\pi^* \leftarrow \pi$ and $\pi^* \leftarrow$ n transitions in organic molecules and the d-d and charge-transfer (CT) transitions of inorganic materials.[47]

In solution, the absorption of a compound can easily be measured through the liquid, i.e. in transmission. The obtained signal can be described by Beer's Law:

$$A = \varepsilon c l \qquad \text{(eq. 1.8)}$$

This equation states that the absorption of a compound (in solution) is dependent on its concentration (c), the path length through the cel (l) and an extinction coefficient (ε). Solid materials, like heterogeneous catalysts, are most often not transparent and as a result transmission spectroscopy cannot be applied on these samples. By using UV-Vis-NIR diffuse reflectance spectroscopy (UV-Vis-NIR DRS) this problem can be avoided. This technique is based on the transmission and diffuse reflection of light by small particles. When light interacts with small particles it is either specular reflected or diffuse reflected. In specular reflection the light is reflected on the surface with the same angle as that of the incoming beam. Diffuse reflected light penetrates the surface and after partial absorption and multiple scattering, appears again on the surface. The reflected beam bears the structural and chemical information.

A theory for this phenomenon was initiated in the beginning of the 20th century by Schuster[48] and later further developed by Kubelka and Munk[49].

The result is the Schuster-Kubelka-Munk or Kubelka-Munk function:

$$F(R_\infty) = \frac{(1-R_\infty)^2}{2R_\infty} = \frac{K}{S} \qquad \text{(eq. 1.9)}$$

With this equation the diffuse reflection of a sample (R_∞), measured as the light intensity reflected from the powdered sample divided by the light intensity measured from an ideally reference standard, can be related to an apparent absorption (K) and apparent scattering coefficient (S). This equation is valid under the following conditions:

1. The intensity of the scattered light must be equal in all directions, i.e. isotropic light scattering.
2. The sample is irradiated with diffuse monochromatic light.
3. The sample should be of infinite thickness, typically > 2 mm.
4. The concentration of absorbing centers should be low and evenly distributed throughout the sample.
5. Fluorescence should be absent.

In practice this means that randomly shaped particles containing low amounts of light absorbing centers should be used. An extended theory was introduced by Klier.[50] In this theory a true absorption (α_ν) and true scattering (σ_ν) coefficient are related to K and S via:

$$\alpha_\nu = \eta K \text{ and } \sigma_\nu = \chi S \qquad \text{(eq. 1.10)}$$

From Equations 1.9 and 1.10 it follows that:

$$\frac{\alpha_\nu}{\sigma_\nu} = \frac{(1-R_\infty)^2}{2R_\infty} \cdot \frac{\eta}{\chi} \qquad \text{(eq. 1.11)}$$

It was shown that in the limit for small absorptions (K/S = 0 - 0.3) η and χ are equal to 1/2 and 4/3, respectively, and thus η/ χ has a fairly constant value of 3/8. This implies that at low concentrations a quantitative determination of the concentration (C) is possible via:

$$F(R_\infty) = \frac{(1-R_\infty)^2}{2R_\infty} = \frac{K}{S} = \frac{\alpha C}{K} = kC \qquad \text{(eq. 1.12)}$$

In this equation, α and k are proportionality constants. This equation states that if S is constant for a given wavelength, a linear relation is present between signal and concentration. With this extended theory it is thus possible to measure UV-Vis-NIR DRS in a quantitative manner, provided that the mentioned conditions 1 to 5 are met.

Raman and UV-Vis-NIR spectroscopy applied on supported chromium oxide catalysts

In this thesis the developed *operando* Raman and UV-Vis-NIR set-up is used to characterize supported chromium oxide catalysts. Most oxide supports give only weak backgrounds in Raman spectroscopy. This allows the probing of Cr-O vibrations. Since the vibrations of Cr^{6+} have a large influence on the polarizability of the molecule, these compounds are easier to measure than those of the lower oxidation states of chromium such as Cr^{3+}. The information obtained with UV-Vis-NIR DRS contains characteristic information on the oxidation state and coordination environment of the supported chromium catalyst. Table 1.2 summarizes the most important features of chromium observable with Raman and UV-Vis-NIR spectroscopy.

Tabel 1.2 *Overview of band assignments of supported chromium oxide catalysts for Raman and UV-Vis-NIR spectroscopy in solids.*

Spectroscopic technique	Type of signature	Location of the bands	Type of Chromium specie	Reference
Raman	Cr - O - Cr	550 cm^{-1}	Cr_2O_3	51-59
	Cr=O	980 – 990 cm^{-1}	dehydrated monochromate	
		1000 – 1010 cm^{-1}	dehydrated polychromate	
		850 – 880 cm^{-1}		
UV-Vis-NIR	Charge transfer	330 – 370 nm	chromate	60-66
		240 – 270 nm		
		435 – 480 nm	polychromate	
		330 – 370 nm		
		240 – 280 nm		
	d-d transitions	590 – 670 nm	(pseudo-) octahedral Cr^{3+}, including Cr_2O_3	
		770 – 1000 nm	(pseudo-) octahedral Cr^{2+}	
		1000 – 1430 nm	(pseudo-) tetrahedral Cr^{2+}	

Outline of the thesis

The goal of this PhD project was the development of an *operando* Raman and UV-Vis-NIR set-up and to explore its possibilities in providing new information about supported metal oxide catalysts at work. In **Chapter 2** it is shown that with these techniques valuable complementary information can be obtained. Also an extensive description of the set-up is provided and its value is shown with the dehydrogenation of propane over a supported chromium catalyst as a model reaction. Although interesting spectroscopic information is obtained, it would be of more interest if the novel set-up could be used in a quantitative manner to determine the amount of coke formed on the catalyst during dehydrogenation. In **Chapter 3** two methods are presented for the on-line determination of the amount of coke on the catalyst. The first method is the application of an internal standard, whereas the second method corrects for the changing color of the catalyst during reaction. In **Chapter 4** these two methods are compared to monitor the amount of Cr^{6+} present during a series of reduction experiments.

During the conducted dehydrogenation experiments it appeared that coke, formed on the catalyst, influences the activity and selectivity, in this way taking part in the reaction. Proposed roles for coke are a carbon pool mechanism or an adsorption effect. The research described in **Chapter 5** was conducted to discriminate between these two effects. Furthermore, an investigation towards a possible reaction mechanism is described. The thesis ends with a summary and a look into the future of *operando* spectroscopy.

References

1. Ohanian, H. C. *Physics (second edition expanded)*; W.W. Norton & Company: New York, **1989.**
2. Atkins, P. W. *The Elements of Physical Chemistry*; Oxford University Press: Oxford, **1999**
3. This term is borrowed from an instrumental development at the end of the 19th century in the field of cinematography. E.J. Muybridge (1830-1904) developed the first moving picture projector. This projector is often coined the Zoopraxiscope, since the first objects of which he made moving pictures were animals, such as horses. Projecting images drawn from photographs, rapidly and in succession on a screen, operates the Zoopraxiscope. The photographs were painted onto a glass disc, which rotated, thereby producing the illusion of motion. From this point forward in time, Muybridge's work began to clearly show that the possibility of actual moving pictures or cine-photography was a reality and even not so far from perfection.

4. Haw, J. F., Ed.; *In-situ spectroscopy in Heterogeneous Catalysis*; Wiley-VCH: Weinheim, 2002, pp 4.
5. Weckhuysen, B. M., Ed.; *In-situ Spectroscopy of Catalysts*; American Scientific Publishers: Stevenson Ranch, 2004, pp 1.
6. Weckhuysen, B. M.; Van Der Voort, P.; Catana, G., Eds.; *Spectroscopy of Transition Metal Ions on Surfaces*; Leuven University Press: Leuven, 2000.
7. Banares, M. A. Raman Spectroscopy. In *In-situ Spectroscopy of Catalysts*; Weckhuysen, B. M., Ed.; American Scientific Publishers: Stevenson Ranch, 2004; pp 59.
8. Mapes, J. E.; Eischens, R. P., *J. Phys. Chem.*, **1954**, *58*, 1059.
9. Eischens, R. P.; Plisken, W. A.; Francis, S. A., *J. Chem. Phys.*, **1954**, *24*, 1986.
10. Weckhuysen, B. M., *Phys. Chem. Chem. Phys.*, **2003**, *5*, 4351 Operando spectroscopy is the shortened version of spectra of an operando or working catalyst. This name has been proposed by M. A. Banares, E. Gaigneaux, G. Mestl and B.M. Weckhuysen in 2000 in Washington DC during the ACS meeting.
11. Puurunen, R. L.; Beheydt, B. G.; Weckhuysen, B. M., *J. Catal.*, **2001**, *204*, 253.
12. Puurunen, R. L.; Weckhuysen, B. M., *J. Catal.*, **2002**, *210*, 418.
13. Groothaert, M. H.; Lievens, K.; van Bokhoven, J. A.; Battiston, A. A.; Weckhuysen, B. M.; Pierloot, K.; Schoonheydt, R. A., *Chem. Phys. Chem.*, **2003**, *4*, 626.
14. Groothaert, M. H.; Lievens, K.; Leeman, H.; Weckhuysen, B. M.; Schoonheydt, R. A., *J. Catal.*, **2003**, *220*, 500.
15. Bruckner, A., *Chem. Comm.*, **2001**, 2122.
16. Bentrup, U.; Bruckner, A.; Rudinger, C.; Eberle, H. J., *Appl. Catal. A-Gen.*, **2004**, *269*, 237.
17. Bruckner, A., *Phys. Chem. Chem. Phys.*, **2003**, *5*, 4461.
18. Bruckner, A. Electron Paramagnetic Resonance. In *In-situ Spectroscopy of Catalysts*; Weckhuysen, B. M., Ed.; American Scientific Publishers: Stevenson Ranch, 2004; pp 219.
19. Bruckner, A.; Martin, A.; Kubias, B.; Lucke, B., *J. Chem. Soc. Faraday Trans.*, **1998**, *94*, 2221.
20. Bruckner, A.; Martin, A.; Lucke, B.; Hannour, F. K., *Stud. Surf. Sci. Catal.*, **1997**, *110*, 919.
21. Bruckner, A.; Martin, A.; Steinfeldt, N.; Wolf, G. U.; Lucke, B., *J. Chem. Soc. Faraday Trans.*, **1996**, *92*, 4257.
22. Bruckner, A., *Catal. Rev.-Sci. Eng.*, **2003**, *45*, 97.
23. Beale, A. M.; Van der Eerden, A. M. J.; Kervinen, K.; Newton, M. A.; Weckhuysen, B. M., *Chem. Comm.*, **2005**, *24*, 3015.
24. Bruckner, A., *Chem. Comm.*, **2005**, 1761.
25. Burgi, T., *J. Catal.*, **2005**, *229*, 55.
26. Caravati, M.; Grunwaldt, J. D.; Baiker, A., *Phys. Chem. Chem. Phys.*, **2005**, *7*, 278.
27. Clausen, B. S.; Grabaek, L.; Steffensen, G.; Hansen, P. L.; Topsoe, H., *Catal. Lett.*, **1993**, *20*, 23.
28. Couves, J. W.; Thomas, J. M.; Waller, D.; Jones, R. H.; Dent, A. J.; Derbyshire, G. E.; Greaves, G. N., *Nature*, **1991**, *354*, 465.

29. Grunwaldt, J. D.; Molenbroek, A. M.; Topsoe, N. Y.; Topsoe, H.; Clausen, B. S., *J. Catal.*, **2000**, *194*, 452.
30. Le Bourdon, G.; Adar, F.; Moreau, M.; Morel, S.; Reffner, J.; Mamede, A. S.; Dujardin, C.; Payen, E., *Phys. Chem. Chem. Phys.*, **2003**, *5*, 4441.
31. Newton, M. A.; Jyoti, B.; Dent, A. J.; Fiddy, S. G.; Evans, J., *Chem. Comm.*, **2004**, 2382.
32. Nijhuis, T. A.; Tinnemans, S. J.; Visser, T.; Weckhuysen, B. M., *Phys. Chem. Chem. Phys.*, **2003**, *5*, 4361.
33. Nijhuis, T. A.; Tinnemans, S. J.; Visser, T.; Weckhuysen, B. M., *Chem. Eng. Sci.*, **2004**, *59*, 5487.
34. Schneider, M. S.; Grunwaldt, J. D.; Burgi, T.; Baiker, A., *Rev. Sci. Instrum.*, **2003**, *74*, 4121.
35. Shannon, I. J.; Maschmeyer, T.; Sankar, G.; Thomas, J. M.; Oldroyd, R. D.; Sheehy, M.; Madill, D.; Waller, A. M.; Townsend, R. P., *Catal. Lett.*, **1997**, *44*, 23.
36. Tromp, M. *Development of time resolved XAFS spectroscopy techniques, Ph. D. Thesis*; Utrecht University: Utrecht, **2004.**
37. Hunger, M.; Wang, W., *Chem. Comm.*, **2004**, 584.
38. Tinnemans, S. J.; Mesu, J. G.; Kervinen, K.; Visser, T.; Nijhuis, T. A.; Beale, A. M.; Keller, D. E.; van der Eerden, A. M. J.; Weckhuysen, B. M., *Catal. Today*, **2006**, *113*, 3.
39. Kervinen, K.; Korpi, H.; Mesu, J. G.; Soulimani, F.; Repo, T.; Rieger, B.; Leskela, M.; Weckhuysen, B. M., *Eur. J. Inorg. Chem.*, **2005**, 2591.
40. Raman, C. V.; Krishnan, K. S., *Nature*, **1928**, *121*, 501.
41. Smekal, A., *Naturwiss.*, **1923**, *11*, 873.
42. Long, D. A. *Raman Spectroscopy*; McGraw-Hill Inc.: Great Britain, **1977**
43. Knozinger, H.; Mestl, G., *Top. Catal.*, **1999**, *8*, 45.
44. Jeziorowski, H.; Knozinger, H., *Chem. Phys. Lett.*, **1976**, *42*, 162.
45. Asher, S. A.; Johnson, C. R., *Science*, **1984**, *225*, 311.
46. Bowie, B. T.; Chase, D. B.; Griffiths, P. R., *Appl. Spectrosc.*, **2000**, *54*, 164A.
47. Atkins, P. W. *Physical Chemistry (6th edition)*; Oxford University Press: Oxford, **2001**, p. 502.
48. Schuster, A., *J. Astrophys.*, **1905**, *21*, 1.
49. Kubelka, P.; Munk, F., *Z. Techn. Phys.*, **1931**, *12*, 593.
50. Klier, K., *J. Opt. Soc. Am.*, **1972**, *62*, 882.
51. Vuurman, M. A.; Wachs, I. E.; Stufkens, D. J.; Oskam, A., *J. Mol. Catal.*, **1993**, *80*, 209.
52. Vuurman, M. A.; Wachs, I. E., *J. Phys. Chem.*, **1992**, *96*, 5008.
53. Vuurman, M. A.; Stufkens, D. J.; Oskam, A.; Moulijn, J. A.; Kapteijn, F., *J. Mol. Catal.*, **1990**, *60*, 83.
54. Vuurman, M. A.; Hardcastle, F. D.; Wachs, I. E., *J. Mol. Catal.*, **1993**, *84*, 193.
55. Kim, D. S.; Wachs, I. E., *J. Catal.*, **1993**, *142*, 166.
56. Kim, D. S.; Tatibouet, J. M.; Wachs, I. E., *J. Catal.*, **1992**, *136*, 209.
57. Jehng, J. M.; Wachs, I. E.; Weckhuysen, B. M.; Schoonheydt, R. A., *J. Chem. Soc. Faraday Trans.*, **1995**, *91*, 953.

58. Hardcastle, F. D.; Wachs, I. E., *J. Mol. Catal.*, **1988**, *46*, 173.
59. Deo, G.; Wachs, I. E., *J. Phys. Chem.*, **1991**, *95*, 5889.
60. Zecchina, A.; Garrone, E.; Ghiotti, G.; Morterra, C.; Borello, E., *J. Phys. Chem.*, **1975**, *79*, 966.
61. Weckhuysen, B. M.; Wachs, I. E.; Schoonheydt, R. A., *Stud. Surf. Sci. Catal.*, **1994**, *91*, 151.
62. Weckhuysen, B. M.; Verberckmoes, A. A.; Buttiens, A. L.; Schoonheydt, R. A., *J. Phys. Chem.*, **1994**, *98*, 579.
63. Weckhuysen, B. M.; De Ridder, L. M.; Schoonheydt, R. A., *J. Phys. Chem.*, **1993**, *97*, 4756.
64. Ghiotti, G.; Garrone, E.; Della Gatta, G.; Fubini, B.; Giamello, E., *J. Catal.*, **1983**, *80*, 249.
65. Fubini, B.; Ghiotti, G.; Stradella, L.; Garrone, E.; Morterra, C., *J. Catal.*, **1980**, *66*, 200.
66. Krauss, H. L.; Rebenstorf, B.; Westphal, U., *Z. Anorg. Allgem. Chem.*, **1975**, *414*, 97.

2

The development of an *operando* Raman / UV-Vis-NIR set-up for monitoring supported chromium oxide catalysts during propane dehydrogenation.

Abstract

The implementation of *operando* Raman and UV-Vis-NIR spectroscopy into a novel reactor system is described. This set-up is capable of monitoring heterogeneous catalysts under reaction conditions. The potential of the set-up is demonstrated for the catalytic dehydrogenation of propane. It is shown that these spectroscopic techniques provide qualitative information on the changing oxidation state of the catalyst and the coke formed during reaction. This information can be linked to catalytic data as measured with on-line micro GC and mass spectrometry.

Introduction

Propene is an important building block in chemical industries. Products are for instance polypropene, propene oxide, oxo alcohols, acrylonitrile and cumene.

The demand for propene in the period 1990 – 2010 is continuously increasing.[1] This is illustrated in Figure 2.1.

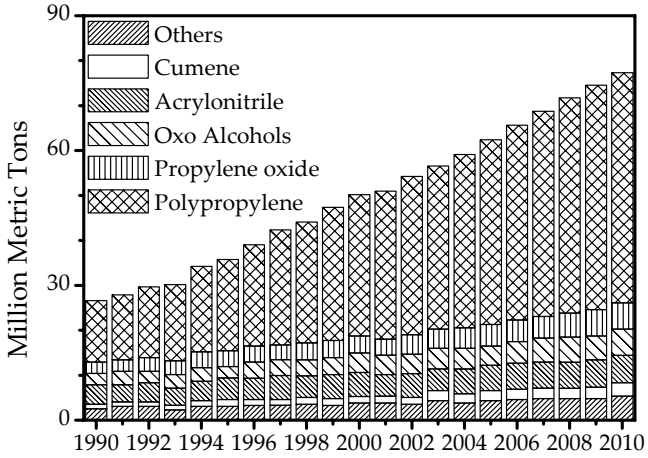

Figure 2.1 *Global propene consumption in the period 1990-2010.*[1]

From Figure 2.1 it is clear that the demand for propene has increased significantly over the last decade and the expectations are that this trend will continue in the years to come. The Figure also illustrates that the expected increase in demand for propene from ca $60 \cdot 10^6$ ton in 2005 to about $80 \cdot 10^6$ ton in 2010 can be mainly contributed to the increasing demand for polypropene. This increasing demand for polypropene originates from the increasing need of plastics in Asia and more specifically in China.[2,3]

Conventional sources to produce propene are ethane steam crackers (67%) and fluidized catalytic crackers (FCC, 30%). However, the requested amounts of propene is outgrowing the production capacity and this makes new production facilities vital.[4-6]

Large expansions for propene production are currently being constructed in the Middle East and north-east Asia.[2,4,7] However this does not completely satisfy the demands. Current technology is producing a lot of (low value) side-products, making new technology required. Via the application of a new (improved) catalyst in FCC, the propene yield can be increased from about 6 to 25 wt%.[6,7] Also the application of less common technologies such as the direct dehydrogenation of propane can reduce the propene shortage.

Propane dehydrogenation offers some specific advantages to propene derivative producers. First, the only product is propene. Companies specifically interested in producing propene are not interested in producing ethene or higher olefins (C_4^+ co-products) that are made from naphtha crackers, or gasoline and fuels from refineries. Second, some of the best locations for propene derivative plants do not have good access to propene. These sites represent a high demand for propene (derivatives), i.e. near China. Given the high cost of shipping and storing propene, dehydrogenation of propane is generally more cost-effective than buying propene for these locations.[6,8]
Until now the direct dehydrogenation has found limited use because the economics are heavily dependent on the price of the feedstock, i.e. the price of propane. However, the economics have changed and the price difference between propane and propene is now making the dehydrogenation more attractive. As a result the amount of propene produced via dehydrogenation is expected to double during the next five years from 1.2 to 2.4 · 10^6 metric tons per year when new plants come in production in Saudi Arabia (Al-Jubail).[6,9]

Currently there are five industrial dehydrogenation processes available. These are the Catofin process, the Oleflex process, Steam active reforming (STAR), fluidized bed dehydrogenation (FBD) and the Linde process. To the best of our knowledge only the Catofin and Oleflex processes are currently commercially applied for the dehydrogenation of propane. The different methods will be briefly described in the next paragraphs.
The first process available for the dehydrogenation of propane is the Catofin or Houdry process (ABB Lummus).[5,6,10-13] The process is widely used in the dehydrogenation of iso-butane to iso-butene, an important primary product in the production of methyl tertiary butyl ether (MTBE). With the pressure on this market due to the banning of MTBE from fuels for environmental reasons, new applications for the Catofin process are developed. An example is the dehydrogenation of propane. A Catofin plant usually contains five cyclically shallow bed operated reactors containing a chromium oxide on alumina catalyst. The process is typically run at a temperature around 575 °C and at a subatmospheric pressure of 0.2-0.5 bar. Each reactor undergoes a cycle of typically 12 minutes of propane dehydrogenation, 3 minutes purge/evacuation, 12 minutes of catalyst regeneration using air and 3 minutes of purge/evacuation optionally followed by a catalyst reduction. The five reactors are switched in such a manner that the overall plant operates in a continuous

manner, with always 2 reactors dehydrogenating, 2 regenerating and 1 under purge. This is illustrated in Figure 2.2.

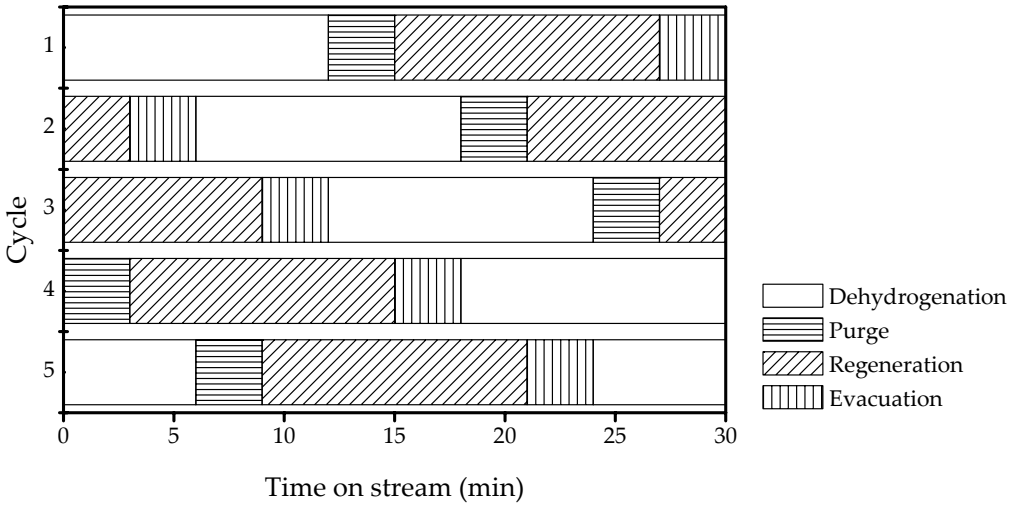

Figure 2.2 *Typical cycle timing for a five reactor system.*

Operating a 5 reactor plant in accordance with Figure 2.2 has the advantage that the product stream is relatively constant. This is beneficial for the propene processing plants downstream, since then a constant stream of reactant is provided.

During the dehydrogenation cycle the catalyst activity changes. This is mainly caused by two effects: 1) the formation of coke on the catalyst and 2) the reduction of Cr^{6+} to Cr^{3+}. In the regeneration cycle the coke is combusted and the chromium is partially re-oxidized. The heat is used to reheat the catalyst to the desired temperature. Currently the cycle times for the Catofin process are fixed and based on the heat exchange in the process. During the lifetime of the catalyst (typically 2 years), the reaction temperature is gradually increased to maintain the desired conversion level.

A competitive process for the direct dehydrogenation is UOP's Oleflex process.[5,6,8,10-12,14,15] The process can be separated into three different sections: the reactor section, the catalyst regeneration section and the product recovery section. The reactor section consists of three or four radial flow reactors, connected in series, containing a supported platinum catalyst. The last reactor is coupled to both a continuous catalyst regeneration unit (CCR) and the product regeneration unit. In the last reactor, the catalyst is separated from the product stream. Subsequently it is regenerated with air to burn off carbonaceous products. Afterwards, it is deployed again in reactor 1. The product stream is separated into products and the not reacted propane is

reintroduced into the feed. The catalyst is typically a Pt / Sn on alumina catalyst. Typical reaction temperatures of the Oleflex process are 525 - 705 °C at pressures of 1-3 bar.

The third process makes use of STeam Active Reforming (STAR).[6,12,16-18] This process was developed by Phillips Petroleum Co, and is now licensed by Uhde (Germany).

By adding oxygen to the feed, the equilibrium is shifted towards the product side, since the oxygen reacts with part of the hydrogen formed during dehydrogenation. The catalyst contains Pt as active phase promoted with tin on a support of zinc aluminate or magnesium aluminate with calcium aluminate as binder. The reaction is operated at 6 – 9 bar and 500 – 600 °C. There are two major requirements for this catalyst. First it has to be stable in the presence of steam and oxygen second it should maintain its activity for dehydrogenation and does not convert hydrocarbons in carbon oxides and hydrogen. Since small amounts of coke are formed on the catalyst it is necessary to regenerate the catalyst after 7 hours for a period of 1 hour in oxygen / air. By using multiple reactors similar to Figure 2.2 the product stream is kept as constant as possible. The process has commercially been proven by the dehydrogenation of 1-butene to butadiene and the dehydrogenation of butane. A pilot-plant study for the dehydrogenation of propane has been performed.

The fluidized bed dehydrogenation (FBD) is licenced by Snamprogetti and Yarsintez.[5,11,15,18] In this process the pure alkane feed bubbles through the staged fluidized bed reactor at 1.1 - 1.5 bar. Since coke is formed on the alumina supported chromium catalyst a regeneration of the catalyst is required. Therefore part of the catalyst is continuously moved to a regenerator and back. Typical operating temperatures are 550 – 600 °C. This process is commercially used for the dehydrogenation of isobutane and isopentane.

The last process described in this context is the Linde process (Linde, BASF).[5,15,18] This process is performed in three fixed bed reactors. Two operate under dehydrogenation conditions while the third is regenerated by combusting the coke on the catalyst with a steam / air mixture. The catalyst in this process is a CrO_x / Al_2O_3. The process is operated at a temperature of 590 °C and is kept at nearly isothermal conditions, to minimize thermal cracking and coke formation. A pilot plant study for the dehydrogenation of propane has been performed.

An overview of important parameters for all five described processes is provided in Table 2.1.

Table 2.1

Comparison of current industrial technologies for the dehydrogenation of propane. [5,11,15]

Process	**Catofin**	**Oleflex**	**STAR**	**FBD**	**Linde**
License holder	ABB Lumus/ United Catalysts	UOP	Uhde	Snamprogetti Yarsintez	Linde (BASF)
Catalyst	CrO_x / Al_2O_3	Pt / Sn / Al_2O_3	Pt / Sn on Zn or Mg Al_2O_3 / Ca Al_2O_3	CrO_x / Al_2O_3	CrO_x / Al_2O_3
Operating mode	Cyclic	Moving bed	Cyclic	Fluidized bed	Cyclic
Reactor type	Adiabatic	Adiabatic	Isothermal	Adiabatic	Isothermal
Number of reactors	5	4	8	1	3
Typical cycle time	0.5 h	Continuous	8 h	Continuous	9 h
T (°C)	525 – 677	525 – 705	482 – 621	520 – 600	590
P (bar)	0.1 – 0.7	1 – 3	3 – 8	1.1 – 1.5	>1
Propane conversion (%)	65	40	30 – 40	40	50
Selectivity towards propene (%)	85	90	80 – 90	89	91
Capacity Mtons/yr	0.7	1.25			

The applied catalysts provide an opportunity for a spectroscopic investigation of catalysts under reaction conditions. Spectroscopy is an excellent manner to track the state of a CrO_x / Al_2O_3 catalyst during the catalytic dehydrogenation process. Especially a combination of UV-Vis-NIR and Raman spectroscopy, performed simultaneously is capable of providing a much better insight in the catalyst health. With UV-Vis-NIR spectroscopy the oxidation state of the chromium oxide catalyst can be determined while Raman spectroscopy is excellent in tracking the different types of coke on an active catalyst.[19]

Therefore, the aim of this work was to develop an *operando* Raman / UV-Vis-NIR set-up in which the Catofin process could be investigated under typical operating conditions, i.e. at elevated temperatures.

Construction of an *operando* Raman / UV-Vis-NIR set-up

Two set-ups combining the advantages of both Raman and UV-Vis-NIR spectroscopy have been developed, while on-line product analysis was integrated in these systems via connection of a mass spectrometer and a micro GC.[20] A schematic representation of the first newly developed system is presented in Figure 2.3.

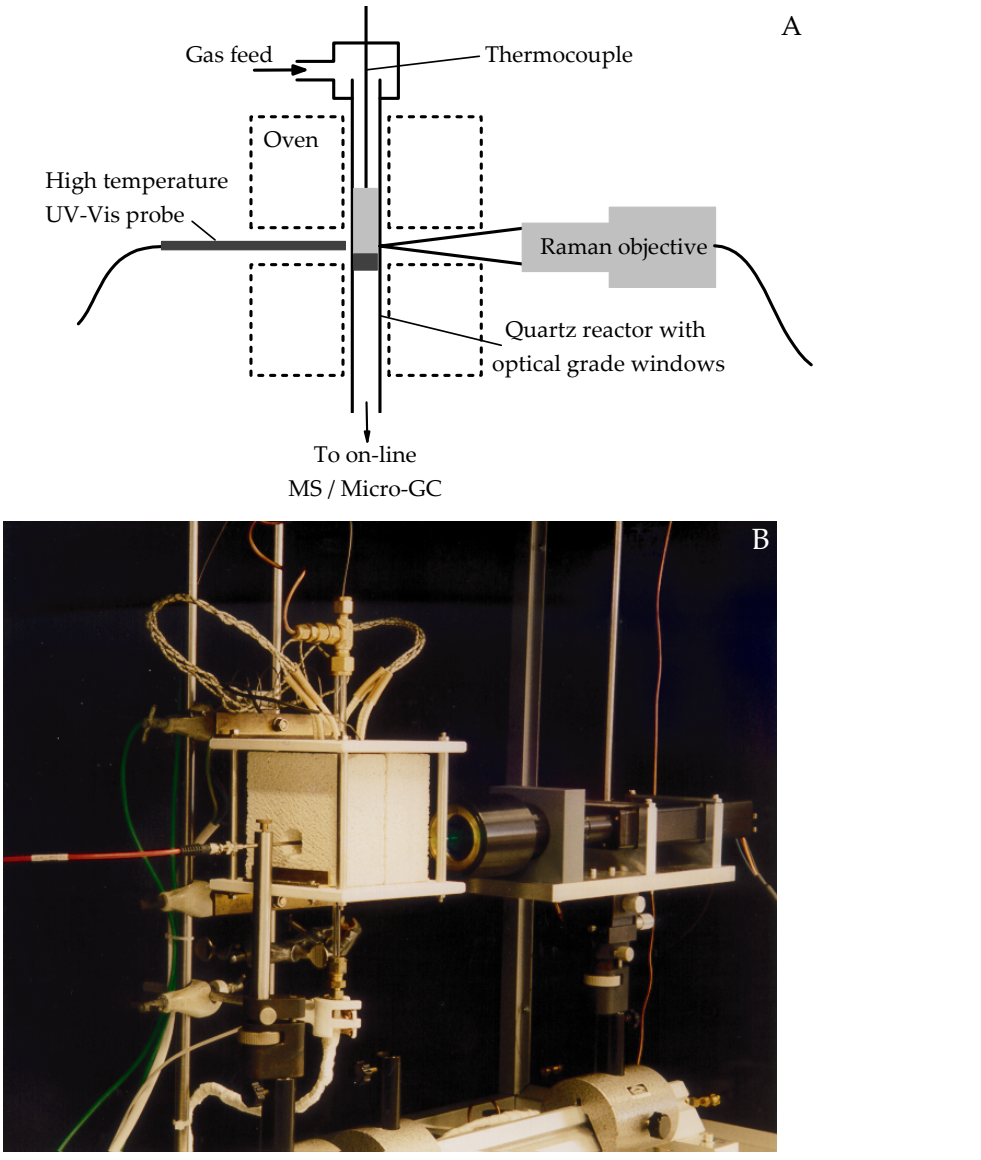

Figure 2.3 *Schematic presentation (A) and picture (B) of the reactor set-up with combined UV-Vis-NIR and Raman spectroscopy.*

The set-up consists of a 6 mm diameter quartz reactor tube with a special square section in which the tube wall is made of optical grade quartz windows. These quartz windows are necessary for focusing the UV-Vis-NIR and Raman light sources and obtain better spectroscopic data. Typically, 300 mg of catalyst is placed in the reactor as a packed bed supported on quartz wool just below the optical windows. Catalyst extrudates were milled to a typical particle size of 50 μm. The bed height is ca. 15 mm. The reactor is placed vertically in the center of a 10 cm long tubular oven block; a coated thermocouple can be inserted in the catalyst bed to directly monitor the catalyst temperature. The metal oven block has on opposite sides two horizontal 8 mm holes directed at the catalyst bed. One of the holes is used to aim an Avantes FCDUV400-G-01CHT UV-Vis-NIR reflection probe at the catalyst bed. This high-temperature probe contains three 400 μm optical fibers closely packed in a triangle. One fiber is connected to an Avantes Avaspec 2048 spectrometer and another fiber is connected to an Avantes halogen-deuterium light source (DH-2000). The third fiber is a spare one, to be used if one of the other two breaks. The measuring range of the spectrophotometer is 175-1120 nm. However, effectively the system only provides a usable signal to noise ratio above 220 nm, partly caused by the low transmittance of the optical fibers below this wavelength. The second hole in the oven is used for focusing a Raman laser at the catalyst. Raman spectra were measured with a Kaiser RXN spectrometer equipped with a 532 nm laser (frequency doubled Nd-YAG). A 5.5" non-contact objective was used for beam focusing and collection of scattered radiation, which was detected by a CCD. The laser output power at the focusing spot is typically 60 mW.

The gas leaving the reactor is analyzed using a Pfeiffer Omnistar quadrupole mass-spectrometer (MS). All m/z components in the gas from 14 to 44 amu were analyzed. The scanning time per mass was 50 ms, making the effective time resolution of the mass spectrometer 7.5 s. By performing a deconvolution procedure using the known fragmentation patterns of the reactants and all possible products, it is possible to convert the mass signals quantitatively to concentrations. A more facile quantification of the product gas is possible with the on-line Varian CP-4900 micro-gas chromatograph (GC) system equipped with a Poraplot-Q and Molsieve 5A column. This GC system is capable of performing analyses at less than 90 s intervals.

After the development of this first combined Raman / UV-Vis-NIR set-up, a different set-up was constructed which has the additional advantage that UV-Vis-NIR spectra can be gathered as function of the catalyst bed height. A schematic picture of this set-up is presented in Figure 2.4.[21]

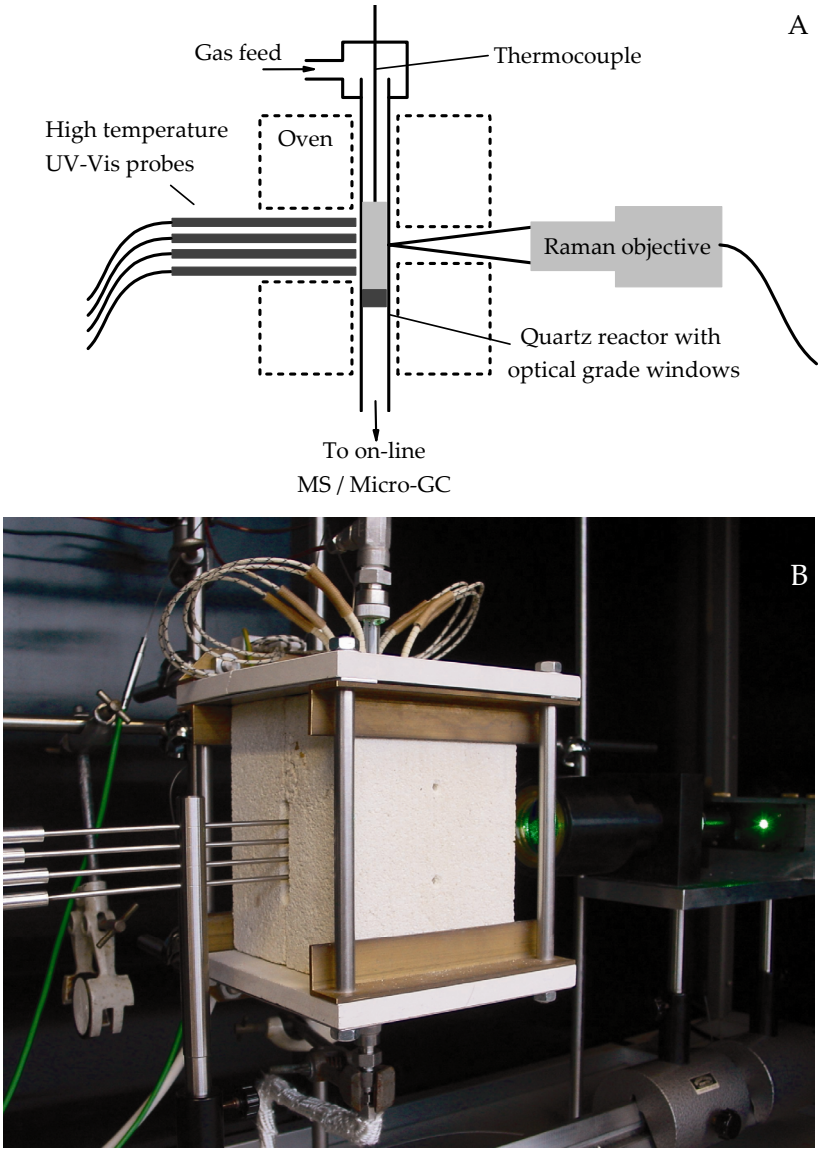

Figure 2.4 *Schematic presentation (A) and picture (B) of the reactor set-up with combined UV-Vis-NIR and Raman spectroscopy. Four UV-Vis-NIR probes are present for measuring at different heights in the catalyst bed.*

A reactor is typically loaded with 1 gram of catalyst (total bed height of 45 mm) and placed in the center of a 15-cm long tubular oven block. A thermocouple can be inserted in the catalyst to monitor on-line the temperature. A hole on one side is used to measure Raman spectra, while on the opposite side a vertical slit (5 * 50 mm) is present for UV-Vis-NIR analysis. The slit is used to focus 4 Ocean Optics Bi-FL600 optical fiber probes (each containing two 600 μm fibers, usable up to 700 °C) at the catalyst bed at a vertical spacing of 10 mm. This makes it possible to determine spatial profiles over the catalyst bed. Of each probe, one fiber is connected to one of

the four channels of an Avaspec-2048-4 spectrometer (Avantes) and another fiber is connected to a DH-2000 BAL halogen-deuterium light source (Ocean optics). The Raman system is the same system as described earlier for the first set-up. In this set-up on-line gas analysis is performed via a Compact GC (Interscience) equipped with a Porabond-Q and a Molsieve-5A column. The GC is capable of performing analyses within 60 s.

Application of the set-up

After construction of the set-ups, their strength in combining multiple spectroscopic techniques, under reaction conditions, were tested for the dehydrogenation of propane over an industrial-like 13 wt% Cr / Al_2O_3 catalyst for a series of dehydrogenation-regeneration cycles. The reactor was heated at 10 °C min^{-1} from room temperature to a catalyst temperature of 550 °C in a gas stream of 3 ml min^{-1} of O_2 (Hoek Loos, 99.995%) in 12 ml min^{-1} of He (Hoek Loos, 99,996%). After heating, the reactor was operated isothermally at a pressure of 1.5 bar in cycles of alternating dehydrogenation for ca. 50 min with 2 ml propane (Hoek Loos, 99.92%) in 20 ml min^{-1} of He and regenerating for ca. 50 min with 3 ml min^{-1} of O_2 in 12 ml min^{-1} of He. During the first 120 s of each cycle UV-Vis-NIR measurements were performed with a 1 s interval to track the rapid changes on the catalyst, after this time measurements were carried out at a 1 min interval. The UV-Vis-NIR spectrometer was used with an integration time of 28 ms and typically 40 spectra were averaged to improve the signal to noise ratio and a Halon white disk was used as a white reference. The resulting time resolution was, therefore, ≈ 1 s. Raman spectra were recorded with an exposure time of 3 s, while 10 spectra were accumulated. This resulted in a spectral recording time of 180 s. Measurements were performed at 5 min intervals. During the entire experiment the product gas composition was monitored using the MS. The temperature of the catalyst was monitored using a small thermocouple in the middle of the bed.

In the second set-up the catalyst was heated to 550 °C (10°C min^{-1}) in a gas stream of 10 ml min^{-1} of O_2 and 40 ml min^{-1} of He. After heating, dehydrogenation cycles of 50 minutes (10 ml min^{-1} of C_3H_8 and 40 ml min^{-1} of He) were alternated with regeneration cycles (10 ml min^{-1} of O_2 and 40 ml min^{-1} of He). During the first 120 s of each cycle UV-Vis-NIR spectra were measured with a 1 s interval. After this time, measurements were performed with a 60 s interval. Raman spectra were taken every

300 s. During the entire experiment the product gas composition was monitored via GC.

Results and Discussion

Monitoring a catalyst during the dehydrogenation of propane

The catalytic results of the experiment are shown in Figure 2.5 for a 13 wt% Cr / Al_2O_3 catalyst. The simultaneously measured spectroscopic data are presented in Figure 2.6.

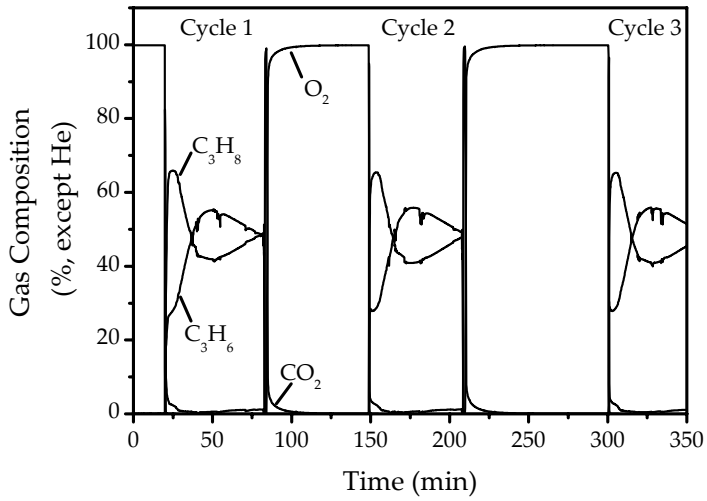

Figure 2.5 *Catalytic activity measurements for three dehydrogenation-regeneration cycles during propane dehydrogenation over a 13 wt% Cr on alumina catalyst (1 bar, 550 °C).*

The catalytic activity data in Figure 2.5 are displayed for three consecutive dehydrogenation-regeneration cycles. It can be seen that the catalytic performance is only subject to changes within one dehydrogenation cycle. Within one cycle the conversion to propene increases gradually with increasing time-on-stream and reaches a maximum of 55% after 28 min. Longer reaction times result in a gradual decrease in propene formation. The comparison of different cycles does not reveal changes in activity. The stable performance of the catalyst over the different cycles is in agreement with expectations, since a commercial catalyst is used in industry for ca. two years before it is replaced. In that case a catalyst will have undergone well over 30000 cycles.

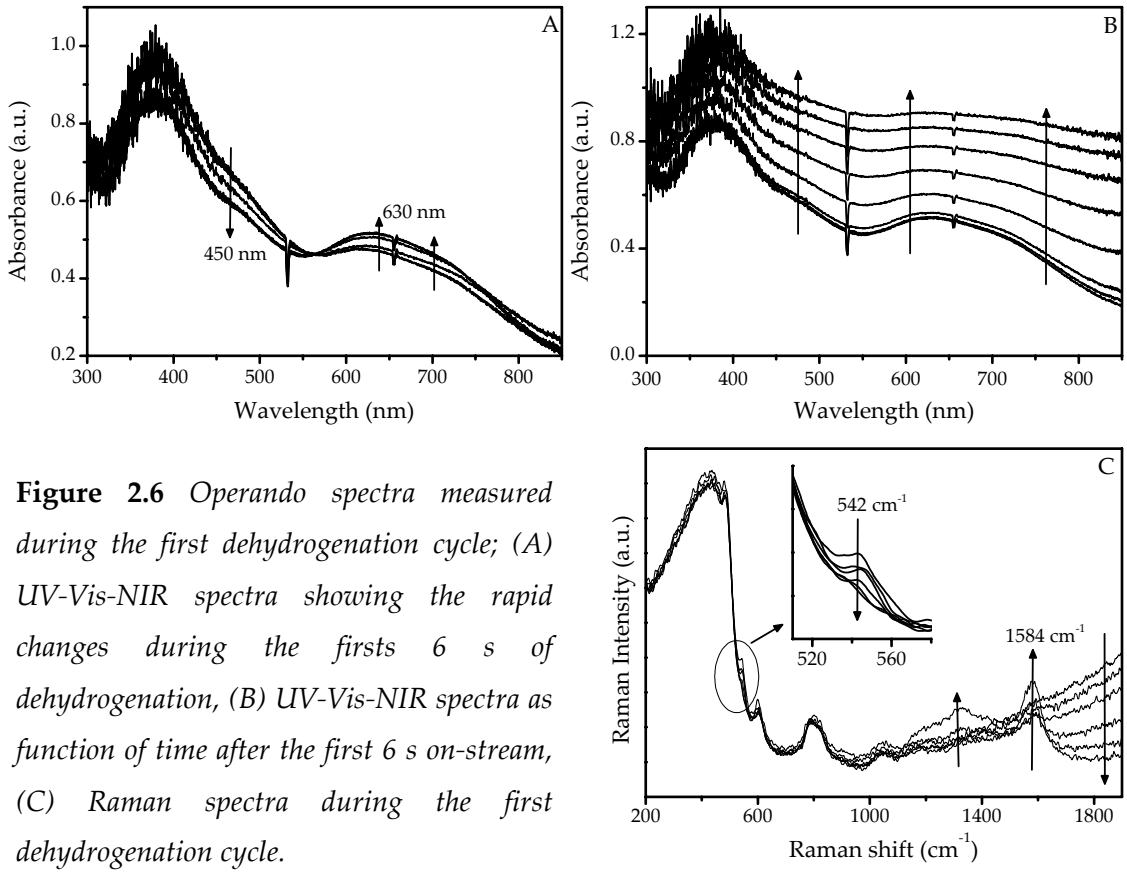

Figure 2.6 *Operando spectra measured during the first dehydrogenation cycle; (A) UV-Vis-NIR spectra showing the rapid changes during the firsts 6 s of dehydrogenation, (B) UV-Vis-NIR spectra as function of time after the first 6 s on-stream, (C) Raman spectra during the first dehydrogenation cycle.*

Figure 2.6 A shows the fast changes taking place in the UV-Vis-NIR spectra in the first 6 s of the dehydrogenation reaction. There is an isobestic point present at 565 nm, indicative for the presence of at least two distinct chromium oxide species. It can be seen that the charge transfer bands of Cr^{6+}, located at 380 and 450 nm, decrease in intensity with increasing reaction time. At the same time, the Cr^{3+} d-d transition at 630 nm increases in intensity. This decrease in absorption at 380 and 450 nm and the increase of the band at 630 nm are in agreement with the reduction of CrO_3 to Cr_2O_3 when the catalyst is switched from an oxidizing to a reducing environment. Furthermore, a shoulder at about 700-750 nm becomes visible.

This band can be attributed to the interaction of Cr^{3+} with adsorbates.[22] The sharp dip in the UV-Vis-NIR spectrum at 532 nm is due to stray light of the Raman laser scattered at the catalyst particles, while the spike at 656 nm is an artefact of the UV-Vis-NIR photometer system (most intense light emitted from the deuterium lamp). Figure 2.6 B shows the UV-Vis-NIR spectrum changing over a longer time (50 min) in the propane dehydrogenation cycle. It is clear that no major peak intensity changes can be observed. On the other hand, the overall absorbance of the sample increases and this is related to the formation of coke. The Cr^{3+} d-d transition band at 630 nm

becomes less pronounced over time. This can also be explained by the coverage of the chromium oxide by coke. Coke formation is evident from the Raman spectra in Figure 2.6 C. The bands that appear in the region 1200-1650 cm^{-1} are attributed to (poly)aromatic ring stretching C-C vibrations.[19,23-31] Fluorescence of the catalyst, causing the increasing baseline at high wavenumbers, decreases during the dehydrogenation cycle. It is likely that this phenomenon is also due to the coke formation on the catalyst. The bands at 200, 605, 810 and 1060 cm^{-1}, which can be observed in the Raman spectra, are originating from the quartz windows of the reactor. Another interesting Raman band could be observed at 542 cm^{-1}. This Raman band is assigned to the presence of Cr_2O_3[32,33] and gradually decreases with increasing reaction time. Since Cr^{3+} is unlikely to be reduced further at the applied reaction conditions, this disappearance is most probably associated with the formation of coke covering the Cr_2O_3 surface as it limits Raman scattering of the underlying layer.

In combining the spectroscopic information of Figure 2.6 with the catalytic information of Figure 2.5, coke formation, as observed by both Raman and UV-Vis-NIR, is the most likely cause of the decrease in catalyst activity over time. In the oxidation cycles this coke is combusted from the catalyst as can be concluded from the formation of CO_2 in the beginning of the regeneration cycle and from the increase in the catalyst bed temperature of about 10 - 15 °C (Figure 2.7). During the catalyst regeneration the UV-Vis-NIR spectra return completely to the initial state of Figure 2.6 A in less than 15 s. Both coke combustion and (partial) chromium oxide reoxidation take place simultaneously. This rapid change in the observed state of the catalyst is in agreement with the fact that the mass spectrometer detects a short carbon dioxide production immediately after the start of the oxidation cycle. Also, the increased catalyst temperature resulting from the heat released by the coke combustion is observed only for a short time. The smaller CO_2 production peak observed by the mass spectrometer at the beginning of the propane dehydrogenation cycle is caused by the reduction of the Cr^{6+} to Cr^{3+} by propane. In industry, this loss of propane is often circumvented by a short catalyst reduction using hydrogen immediately before switching to propane.

Both the UV-Vis-NIR and Raman spectra after dehydrogenation and regeneration show a reversible behavior of the catalyst. This is in good agreement with the activity data, which shows an identical performance of the catalyst in subsequent cycles.

The strength of the set-up is the application of two spectroscopic techniques together with on-line product analysis. Therefore an overview of the most important information is presented in Figure 2.7 for one dehydrogenation-regeneration cycle.

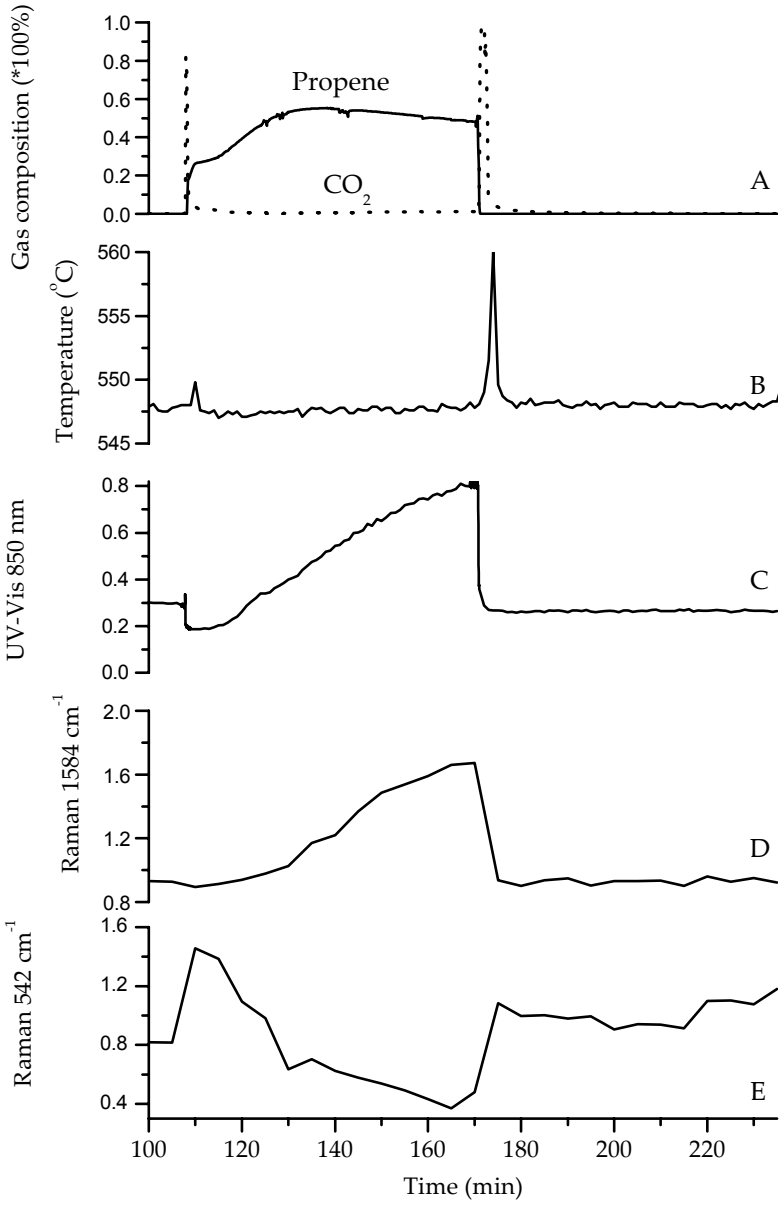

Figure 2.7 *Overview of the most relevant observed changes in measured signals during a complete dehydrogenation-regeneration cycle of propane over a 13 wt% Cr-on-alumina catalyst. (A) Observed propene (solid) and CO_2 (dots) fraction in the gas phase; (B) catalyst bed temperature; (C) UV-Vis-NIR absorbance at 850 nm, corresponding to the overall increase in absorbance due to coke formation on the catalyst; (D) Raman signal at 1584 cm^{-1} Raman shift corresponding to the major coke component formed; (E) Raman signal at 542 cm^{-1} corresponding to crystalline Cr_2O_3.*

From Figure 2.7 the consistence of the applied spectroscopic techniques can be concluded. The UV-Vis-NIR signal at 850 nm (indicative of the increasing overall absorbance of the sample due to coke formation) increases similarly fast as the Raman signal at 1584 cm^{-1} and at a similar rate as the Raman band at 542 cm^{-1} disappears due to coke coverage of Cr_2O_3. Furthermore, it can be seen that the decreasing catalyst activity observed using on-line mass spectrometry activity data agrees well with the spectroscopically observed coke build-up on the catalyst. For the combustion of coke in the catalyst regeneration steps, the information obtained using MS, UV-Vis-NIR, Raman and reactor temperature is also in excellent agreement.

Differences in coke formation over the catalyst bed measured during the dehydrogenation of propane.

The second *operando* Raman / UV-Vis-NIR set-up is capable of measuring UV-Vis-NIR spectra, not only as a function of time, but also as a function of the catalyst bed height. Therefore a dehydrogenation experiment was performed with a 13 wt% Cr / Al_2O_3 catalyst and during this experiment the catalyst was monitored via 4 UV-Vis-NIR probes according to Figure 2.4. Simultaneously the activity was measured via GC measurements and Raman spectra were collected. The activity data measured via GC is presented in Figure 2.8.

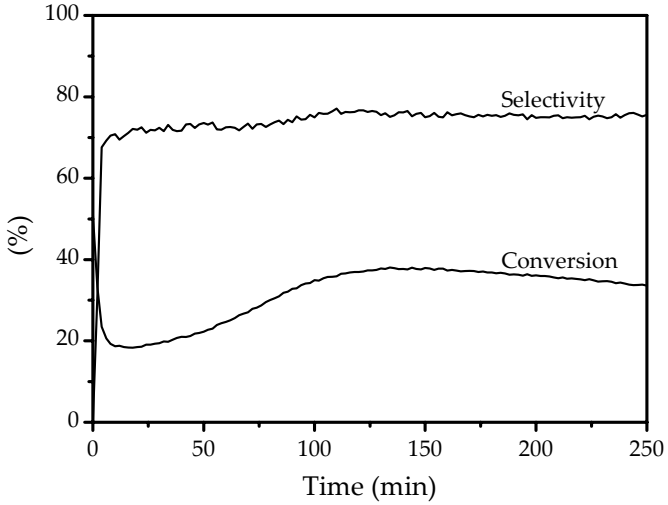

Figure 2.8 *Activity data of a 13 wt% Cr / Al_2O_3 catalyst measured during propane dehydrogenation.*

The activity data in Figure 2.8 are in good agreement with the catalytic results of Figure 2.5. The activity goes through a maximum before decreasing again.

Furthermore coke is formed decreasing the selectivity to ca. 75 %. Also the Raman data in Figure 2.9 show no differences compared to the previously described experiment in the other set-up. The two coke bands at Raman shifts of 1330 and 1580 cm^{-1} increase during propane dehydrogenation and disappear again during regeneration of the catalyst. The resemblance so far is not surprising since the same catalyst was used in the previously described experiment. The bands at 800, 1050 and 1200 cm^{-1} originate from the quartz cell used in these experiments. The sharp band at 1555 cm^{-1} can be assigned to O_2. This O_2 is present in the air outside the reactor between the reactor and objective (5.5″) and thus NOT present inside the reactor. By measuring Raman via this objective, the detection of this peak is unavoidable.

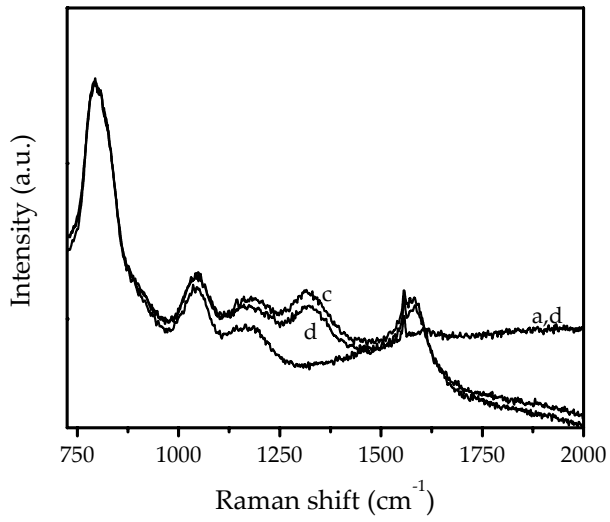

Figure 2.9 *Raman data of a 13 wt% Cr / Al_2O_3 catalyst a) before switching to propane dehydrogenation, b) after 2 h and c) 4 h of dehydrogenation and d) after complete reoxidation.*

However, with this set-up it is also possible to measure UV-Vis-NIR spectroscopy as a function of the catalyst bed height. When looking at the individual UV-Vis-NIR spectra similar spectra are obtained as presented in Figures 2.6A and B. However, these similarities end when the development of coke is monitored as function of time via the course of the baseline at 1000 nm. Figure 2.10 shows the course of the background level in the UV-Vis-NIR spectra at different heights of the catalyst.

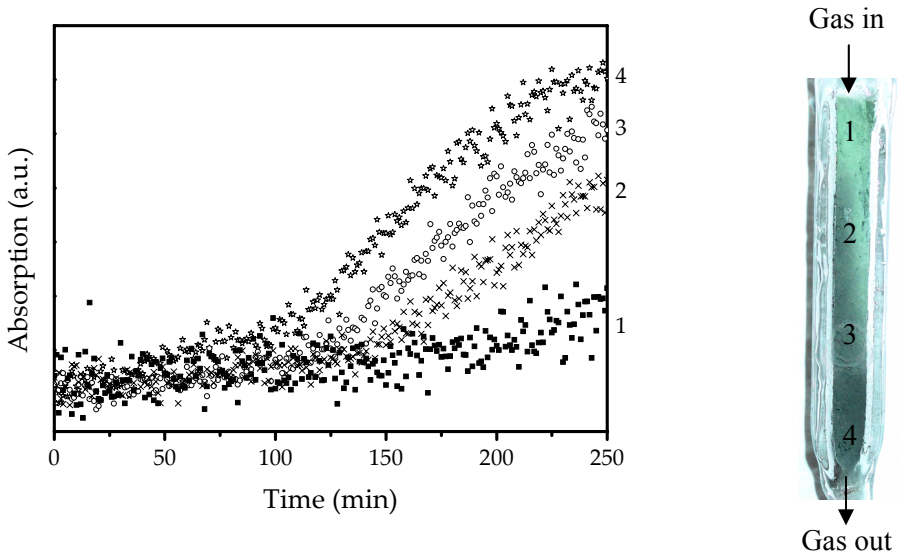

Figure 2.10 *UV-Vis-NIR trends of sample absorbance at 1000 nm over time measured at different heights in the reactor (1 = top, 4 = bottom).*

From this figure it is clear that a large difference exists in the background signal between the top and the bottom of the reactor. Since the background signal is indicative for the blackening of the catalyst, and thus the amount of coke formed on the catalyst, this suggests that the amount of coke at the bottom of the reactor is larger than at the top.

This is in agreement with observations performed after cooling the reactor to room temperature in helium at the end of the dehydrogenation cycle. After removal of the reactor from the oven a clear coke gradient could be observed visually over the catalyst bed. The top of the bed was light green, slowly changing into dark gray towards the bottom of the catalyst. Thermogravimetric analysis (coke combustion in air) showed a coke content on the catalyst increasing from 0.1 wt% at the top of the catalyst bed to 1.0 wt% at the bottom of the bed.

Implications of combining spectroscopic information to catalytic data simultaneously with the described experiments it is shown that it is possible to obtain *operando* Raman and UV-Vis-NIR spectra and correlate the features to activity data. With the possibility of monitoring coke in a dynamical way, this information can be implemented in a process control system, which adjusts cycle times for the dehydrogenation process to optimally run the process. Before this is reality, it would be best if the qualitative Raman information on the amount of coke present on the catalyst could be quantified.

Operando UV-Vis-NIR measurements can be used to monitor the long-term deactivation of the catalyst. Puurunen and Weckhuysen[34] have reported that the active chromium oxide species in the dehydrogenation is most likely the chromium oxide, which undergoes a redox cycle in the dehydrogenation-regeneration cycles. Permanent deactivation of the catalyst is linked to a decrease in the amount of this redox type chromium oxide. Therefore, the change in the relative peak intensities of the 450 and 630 nm bands on switching from air to propane can be used to determine when the catalyst needs to be replaced. The capability of *operando* UV-Vis-NIR measurements to determine long-term deactivation was verified by performing an experiment in which the catalyst was purposely deactivated. Therefore, the catalyst was put in an oven at 1200 °C. It is known that at this temperature the chromium incorporates the alumina and is deactivated, which is similar to the 'lost' of chromium during the catalyst life. In Figure 2.11 the UV-Vis-NIR spectra of the fresh and deactivated catalysts are presented. Chromium oxide is slowly 'loss' during the catalyst life and as a result is migrated into the alumina support. This results in the absorption shifting to higher energies. This change in the UV-Vis-NIR spectrum shows that *operando* measurements can provide essential information on the catalyst activity and the related deactivation phenomena.

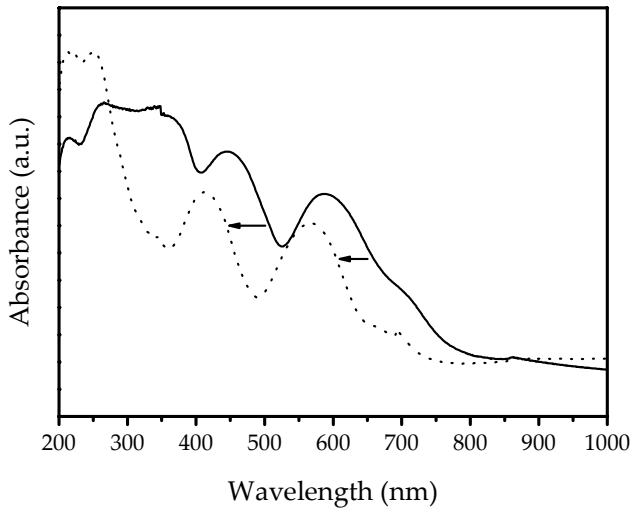

Figure 2.11 *Comparison between the UV–Vis spectra of a fresh 13 wt% chromium on alumina catalyst (solid) and a deactivated catalyst in which the chromium has moved into the alumina lattice by a high-temperature treatment (dotted, 1473 K, 12 h).*

Conclusions

The results in this chapter show the value of combining *operando* spectroscopic techniques with on-line product analysis using mass spectrometry and / or micro-GC. It has been shown that o*perando* spectroscopy is an effective method to study the dynamics of a chromium oxide catalyst during the dehydrogenation of propane. UV-Vis-NIR spectroscopy is able to monitor the oxidation state of the catalyst and the changing background signal is indicative for the coke content on the catalyst. Raman spectroscopy provides information on the coke content on the catalyst, which is in agreement with UV-Vis-NIR spectroscopy. Increasing the number of UV-Vis-NIR probes makes it possible to monitor the catalyst as a function of the catalyst bed height. It is suggested that the system could be up-scaled to an industrial environment if the amount of coke can be determined, i.e. if on-line quantitative information could be gathered.

References

1. Eramo, M., Asia Petrochemical Industry Conference Raw Materials Committee Meeting, Kuala Lumpur, Malaysia, 2004.
2. Short, P. L., Chem. Eng. News, 2005, 83, 30.
3. Milmo, S., Chem. World, 2005, 2, 36.
4. Tullo, A. H., Chem. Eng. News, 2003, 81, 15.
5. Aitani, A. M., Oil Gas Eur. Mag., 2004, 30, 36.
6. Parkinson, G., CEPmagazine, 2004.
7. Walther, M., Oil & Gas J., 2003, 101, 52.
8. Houdek, J. M.; Andersen, J., ARTC 8th Annual Meeting, Kuala Lumpur, 2005.
9. Tan, L., Asia Petrochemical Industry Conference Raw Materials Committee Meeting, Kuala Lumpur, Malaysia, 2004.
10. Calamur, N.; Carrera, M. Propylene. In Kirk-Othmer Encyclopedia of Chemical Technology; online edition ed.; John Wiley & Sons, Inc, 1996.
11. Bhasin, M. M.; Mccain, J. H.; Vora, B. V.; Imai, T.; Pujado, P. R., Appl. Catal. A-Gen., 2001, 221, 397.
12. Eisele, P.; Killpack, R. Propene. In Ullmann's Encyclopedia of Industrial Chemistry; online edition ed.; Wiley-VCH Verlag GmbH & Co., 2000.
13. Catofin Dehydrogenation, 2005 at www.ABB.com
14. Oleflex tm Process for Propylene Production, 2004 at www.UOP.com
15. Buyanov, R. A.; Pakhomov, N. A., Kinet. Catal., 2001, 42, 64.
16. The Uhde Star Process 'Oxydehydrogenation of light paraffins to olefins', 2003 at www.uhde.de.

17. Uhde's STAR process - Oxydehydrogenation of propane or butanes to olefins, 2004 at www.uhde.de.
18. Buonomo, F.; Sanfilippo, D.; Trifiro, F. Dehydrogenation Reactions. In Handbook of Heterogeneous Catalysis; Ertl, G., Knozinger, H., Weitkamp, J., Eds.; VCH: Weinheim, 1997; Vol. 5.
19. Chua, Y. T.; Stair, P. C., J. Catal., 2003, 213, 39.
20. Nijhuis, T. A.; Tinnemans, S. J.; Visser, T.; Weckhuysen, B. M., Phys. Chem. Chem. Phys., 2003, 5, 4361.
21. Nijhuis, T. A.; Tinnemans, S. J.; Visser, T.; Weckhuysen, B. M., Chem. Eng. Sci., 2004, 59, 5487.
22. Scarano, D.; Spoto, G.; Bordiga, S.; Carnelli, L.; Ricchiardi, G.; Zecchina, A., Langmuir, 1994, 10, 3094.
23. Vidano, R. P.; Fischbach, D. B.; Willis, L. J.; Loehr, T. M., Solid State Commun., 1981, 39, 341.
24. Lespade, P.; Marchand, A.; Couzi, M.; Cruege, F., Carbon, 1984, 22, 375.
25. Ager, J. W.; Veirs, D. K.; Shamir, J.; Rosenblatt, G. M., J. Appl. Phys., 1990, 68, 3598.
26. Kong, F.; Kostecki, R.; Nadeau, G.; Song, X.; Zaghib, K.; Kinoshita, K.; McLarnon, F., J. Power Sources, 2001, 97-8, 58.
27. Sze, S. K.; Siddique, N.; Sloan, J. J.; Escribano, R., Atmos. Environ., 2001, 35, 561.
28. Compagnini, G.; Puglisi, O.; Foti, G., Carbon, 1997, 35, 1793.
29. Escribano, R.; Sloan, J. J.; Siddique, N.; Sze, N.; Dudev, T., Vibr. Spectrosc., 2001, 26, 179.
30. Mertes, S.; Dippel, B.; Schwarzenbock, A., J. Aerosol Sci., 2004, 35, 347.
31. Wang, Y.; Alsmeyer, D. C.; McCreery, R. L., Chem. Mat., 1990, 2, 557.
32. Vuurman, M. A.; Hardcastle, F. D.; Wachs, I. E., J. Mol. Catal., 1993, 84, 193.
33. Weckhuysen, B. M.; Wachs, I. E.; Schoonheydt, R. A., Chem. Rev., 1996, 96, 3327.
34. Puurunen, R. L.; Weckhuysen, B. M., J. Catal., 2002, 210, 418.

3

Quantitative *operando* Raman spectroscopy without the need of an internal standard

Abstract

The diffuse reflectance properties of a catalyst may change during catalyst operation. A common cause is a changing oxidation state of or coke formation on the catalyst. As a result the observed Raman intensity is affected and the signal cannot be used in a quantitative manner. A method was developed in which the change of color measured via UV-Vis-NIR is related to the 'observed' Raman intensity. This results in a 'true' Raman intensity, which comprises quantitative information. To verify this method, it was compared to the quantification using an internal standard. Both methods were applied to the formation of coke on a Cr / Al_2O_3 catalyst during propane dehydrogenation. It was found that the results were in good agreement. Therefore, this newly developed method proved to be an elegant manner for the qualitative as well as quantitative monitoring of the amount of coke in a reactor.

Introduction

Raman spectroscopy is a useful characterization tool. However, most studies based on Raman spectroscopy are applied in a qualitative manner. The number of quantitative studies is limited. A reason for this is that besides a change in concentration of the scattering species also other parameters like variations in laser excitation intensity, instrumental settings, sample positioning, temperature fluctuations, etc. might influence the Raman intensities. Furthermore, Raman intensities also depend on the scattering and absorption properties of the sample. As a consequence, progressive darkening of a catalyst during reaction by *e.g.* coke formation may strongly affect the intensities of the Raman spectra.

One way to quantify Raman spectra is by normalizing the Raman bands of a species of interest to those of a specific scattering standard, which is assumed to remain unaffected during reaction. In principle, for supported metal oxide catalysts, the Raman bands of the bulk support material can be used. Several supports, like for instance zirconia, contain intense Raman bands. However, the relative ratio between the support band and metal oxide band can change due to temperature differences making them not suitable for use as an internal standard.[1] Also reduction of the support would change the ratio of the bands, making the support not applicable as internal standard. A third example is the coverage of the sample with for instance coke. This affects the 'visible amount' of bulk material. Closely related to this is a possible change in self absorption of the sample during dehydrogenation. Black materials are known to suffer from self absorption. In this process the scattered radiation is absorbed by neighboring black (dark) particles and cannot be detected anymore. As a result the observed Raman intensity is not related to a concentration, and thus cannot be used in a quantitative manner.

To correct for these possible changes, an unreactive standard of known concentration can be mixed homogeneously with the catalyst. Such internal standards should not interact with the catalyst material, or perturb the spectrum of the supported metal oxide catalyst. Internal standards should also be strong Raman scatterers, so that a small quantity produces a signal of adequate intensity. Several successful applications of an internal standard are known in the literature.[2-9] An example of such a compound is boron nitride (BN), which is known to exhibit only one intense Raman band at 1367 cm^{-1}, while the vibrational bands of most supported metal oxides appear below 1200 cm^{-1}.

An alternative approach could be to measure the color of the sample directly with UV-Vis-NIR spectroscopy. It is known that the scattering and absorption properties

of a catalytic solid can be described by the diffuse reflectance R_∞ of the solid.[10-13] Progressive darkening of the catalytic solid due to *e.g.* coke formation during a dehydrogenation reaction may lead to a decreasing R_∞ and, as a result, the proportionality between the Raman band intensities and the concentration of the corresponding species is no longer valid. In order to compare Raman intensities at different times-on-stream inside a catalytic reactor, the relationship between the diffuse reflectance of the catalytic solid of infinite thickness (R_∞) and the Raman intensity (Ψ_∞) must be known. Already in 1967 Schrader and Bergmann[14] derived an approximate expression to correlate the Raman intensity (Ψ_∞) to the diffuse reflectance (R_∞) based on the Kubelka-Munk formalism. This was later improved by Waters[15] and Kuba and Knözinger[16] into the following expression:

$$\Psi_\infty = \frac{\rho I_0}{s} \cdot G(R_\infty) \qquad \text{(eq. 3.1)}$$

$$G(R_\infty) = \frac{R_\infty(1+R_\infty)}{(1-R_\infty)} \qquad \text{(eq. 3.2)}$$

In Equation 3.1, Ψ_∞ represents the observed Raman intensity for a powdered sample of infinite thickness, I_0 the exciting Raman laser intensity, ρ the coefficient of Raman generation (Raman cross-section) and s the scattering coefficient. The equation is valid based on the assumption that the scattering of the solid s does not change. This implies *e.g.* that the catalyst particles may not aggregate during reaction leaving the scattering coefficient s unaltered. $G(R_\infty)$ can then be directly determined via Equation 3.2 by measuring R_∞ with UV-Vis-NIR diffuse reflectance spectroscopy.

Figure 3.1 illustrates the dependence of $G(R_\infty)$ on R_∞. It is evident that when $R_\infty \rightarrow 100$ % the function $G(R_\infty)$ goes to infinity. Furthermore, small changes of R_∞ between 90 and 100% strongly affect the observed Raman intensity Ψ_∞. Thus, Raman intensities may decrease significantly as a function of time during reaction although the density of the corresponding Raman sensitive species remains unchanged. Fortunately, Equations 3.1 and 3.2 allow then to calculate the correction for the Raman intensity of such species assuming s to be constant. This means that Ψ_∞ has to be divided by $G(R_\infty)$. The combined *operando* Raman / UV-Vis-NIR set-up described in Chapter 2 is capable of measuring both Raman and UV-Vis-NIR spectroscopy simultaneously under working conditions. In Chapter 2 only the qualitative potential of this set-up is discussed.

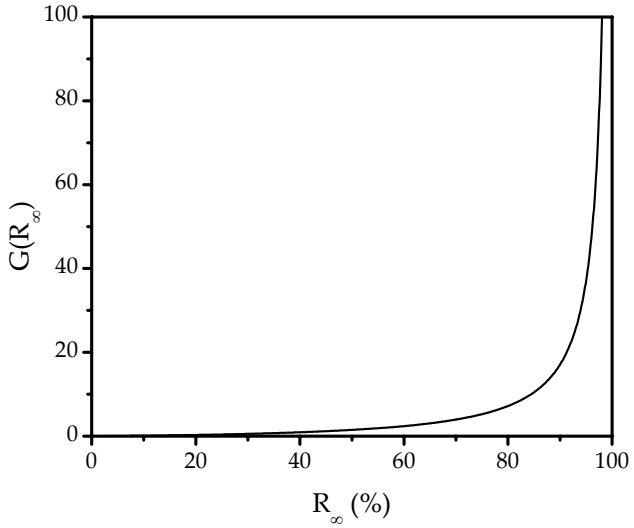

Figure 3.1 *G(R∞) as a function of R∞.*

However, with this set-up, one should be able to apply Raman spectroscopy not only in a qualitative, but also in a quantitative manner since the change in *G(R∞)* of the catalytic solid can be simultaneously measured with UV-Vis-NIR as a function of reaction time. Therefore, the goal of this chapter is to illustrate the possibilities for performing quantitative Raman spectroscopy with the developed set-up. The dehydrogenation of propane over an industrial-like Cr / Al_2O_3 dehydrogenation catalyst is taken as a case study. The results obtained with the developed methodology will be compared with the results based on the use of BN as an internal standard. To ensure that BN has no influence on the catalytic material under investigation, the influence on the Raman intensity of both loading and temperature was explored for BN enriched samples. Also the inertness of these catalysts was tested for various gasses. Ideally these experiments are performed with materials, which have great resemblance with the actual catalyst, i.e. with BN enriched Cr / Al_2O_3. Unfortunately, these type of materials have weak Raman signals. This makes them not suitable for investigating the possibility of using BN as an internal standard. To circumvent this problem an alternative support with strong Raman bands was chosen, namely TiO_2 having intense Raman bands at 396, 516 and 638 cm^{-1}. By mixing different amounts of BN with TiO_2 the validity of BN as an internal standard was evaluated.

Experimental

Physical mixtures of BN (Aldrich, 99%) and TiO_2 (Aerolyst 7711, 50 m^2 g^{-1}) were prepared and measured with Raman spectroscopy. The ratio TiO_2 : BN in the samples varied from 0.1 to 50. Besides, different amounts of BN were added to 0.5 wt% Cr / TiO_2 (calcined) catalysts, which were prepared via incipient wetness impregnation. Raman spectra were recorded using a Kaiser RXN spectrometer equipped with a 532 nm diode laser (output power of 70 mW). A 5.5″ objective was used for beam focusing and collection of the scattered radiation. The exposure time of the CCD was 2 s while 25 accumulations were averaged to obtain a reasonable signal to noise ratio. Spectra were taken every 300 s. Subsequently, propane dehydrogenation experiments were performed with an industrial-like 13 wt% Cr / Al_2O_3 catalyst enriched with 4 wt% BN (Aldrich, 99%). The mixture was ball-milled for 15 min to obtain a homogeneously mixed powder. The furnace of the reactor was heated to 585 °C (catalyst temperature of 550 °C) with 10 °C min^{-1} in a 20 vol% oxygen (Hoek Loos, 99.995 %) in He (Hoek Loos, 99.996 %) flow of 15 ml min^{-1}. After heating, He was purged to remove all oxygen in the system and subsequently a 9 vol% propane (Hoek Loos, 99.92 %) stream with a total flow of 22 ml min^{-1} was applied. All flows given are at standard temperature and pressure. On-line gas analysis was performed using a Varian CP-4900 Micro GC equipped with a Poraplot Q and a Molsieve 5A column and TCD detectors. UV-Vis-NIR diffuse reflectance (DRS) spectra were measured using a DH-2000 light source (Avantes) combined with an Avaspec 2048 CCD spectrometer (Avantes) and a BI-FL400 high temperature resistant probe (Ocean Optics).[17,18] Additional measurements were performed to measure the coke formation as a function of catalyst bed height during and after reaction. All Raman spectra were first baseline-corrected in the spectral region 1100 - 1700 cm^{-1} using Thermo Galactic Grams AI v. 7.0 software. This software package was also used to determine the Raman peak areas. Tapered element oscillating microbalance (TEOM) experiments have been performed with a Rupprecht & Pataschnick TEOM 1500 PMA equipment using 100 mg of catalyst and a gas mixture of propane (7 ml min^{-1}, Hoek Loos, 99.92 %)) and argon (20 ml min^{-1}, Hoek Loos, 99.995 %). Prior to the uptake experiment, the catalytic solid was dried and calcined under oxygen (5 ml min^{-1}, Hoek Loos, 99.995 %) and argon (10 ml min^{-1}, Hoek Loos, 99.995 %) at 600 °C. The start of the uptake experiment (t = 0) was defined as the last data point before the first mass change. All mass changes were corrected for effects of gas density and temperature by performing a blank run over a reactor filled with

quartz chips. Thermogravimetrical analysis (TGA) has been performed using a Mettler Toledo TGA/SDTA 851e instrument.

Results and Discussion

The use of boron nitride as internal standard

The relative intensities of the TiO_2 bands were determined, since a different focusing of the samples, inevitable with measuring different samples, always results in a different absolute intensity. The results are shown in Figure 3.2.

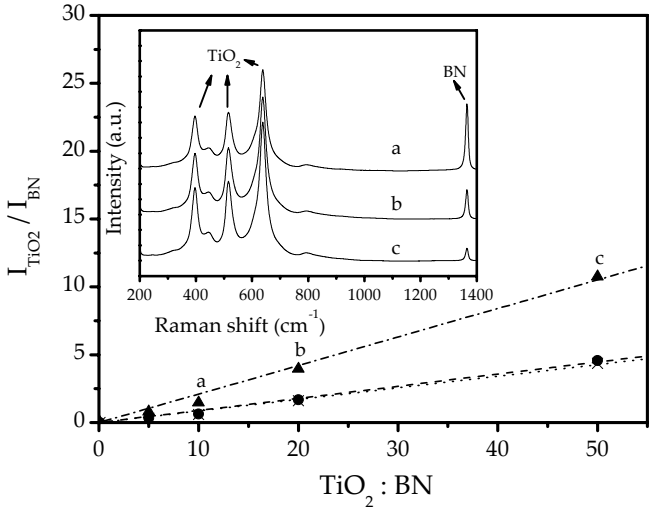

Figure 3.2 *Normalized Raman peak intensities of the Raman shifts at 396 (×), 516 (●) and 638 (▲) cm^{-1}, using BN as internal standard. In the insert Raman spectra are shown with TiO_2 : BN ratios of a) 10, b) 20 and c) 50.*

From Figure 3.2 it is evident that there is a linear relationship between the amount of BN present in the sample and the relative (integrated) peak intensity of titania. The difference in slope for the different bands can be addressed to a difference in scattering efficiency of that particular band. In a next step the behavior of these materials at elevated temperatures was investigated. Upon heating these catalysts in air, it is expected that the relative intensities remain unaltered, i.e. that the temperature has no influence. This result is presented in Figure 3.3 for the 516 cm^{-1} Raman band of TiO_2.

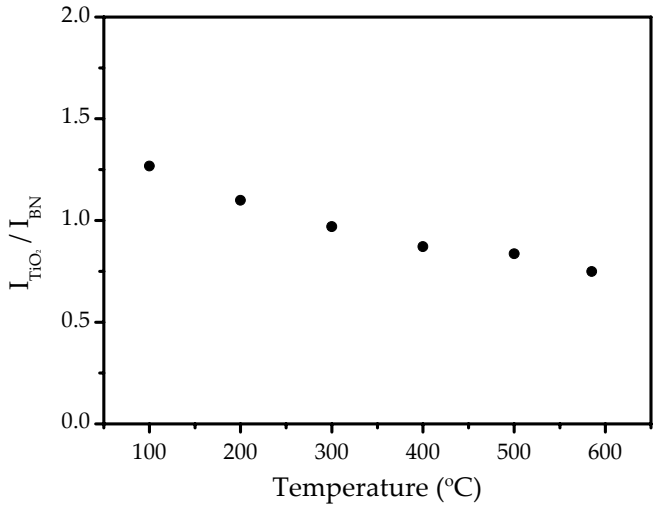

Figure 3.3 *Temperature dependency of the 516 cm^{-1} band of TiO_2 (TiO_2 : BN = 20 : 1).*

From this Figure it is evident that the influence of temperature on the relative intensity is small at temperatures above ca. 350 °C. After cooling it appeared that the process is completely reversible and therefore the use of BN as an internal standard, especially at higher temperatures, is possible. Besides, during heating the band of BN shifted gradually to 1350 cm^{-1}. After cooling this band was at its original position of 1367 cm^{-1}. Since the temperature is of little influence it is of course important to check the inertness of BN. Feeding different gasses like propane and hydrogen over the reactor at temperatures up to 600 °C revealed that BN does not take part in any reaction at these conditions. Therefore it can be concluded that BN is applicable as an internal standard for supported metal oxide catalysts during dehydrogenation reactions.

Monitoring the propane dehydrogenation of a boron nitride enriched Cr / Al_2O_3 catalyst during propane dehydrogenation

Figure 3.4 shows a representative set of time-resolved Raman spectra of an industrial-like 13 wt% Cr/Al_2O_3 propane dehydrogenation catalyst mixed with BN under working conditions at 550 °C. It can be concluded from this Figure that the Raman band of BN, located at 1350 cm^{-1} (slightly shifted from the 1367 cm^{-1} position due to temperature effects) decreases in intensity as the reaction proceeds. The formation of coke is seen most easily by the upcoming (broad) Raman bands located at 1580 cm^{-1} and at 1330 cm^{-1}, the latter close to the Raman band position of the BN standard, which may hamper quantification. These two Raman bands can be

assigned based on literature data of relevant reference compounds to the gradual formation of polyaromatic compounds.[19-24] However, as coke is expected to be developing throughout the reaction, the amount of coke should increase over time, resulting in increasing intensities of the Raman bands at 1580 and 1330 cm^{-1}.

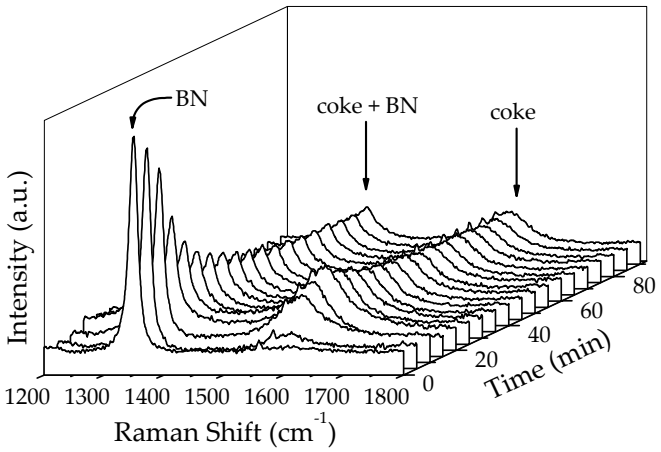

Figure 3.4 *Operando Raman spectra of a 13 wt% Cr / Al_2O_3 catalyst during 90 min. of propane dehydrogenation at 550 °C.*

However, this is not observed in Figure 3.4. Based on the band intensities, the amount of coke (best seen by the intensity of the 1580 cm^{-1} band) seems to increase up to 30 min followed by a gradual decrease before leveling off. However, it is unlikely that the amount of coke first increases and later on decreases during a propane dehydrogenation cycle. In order to validate this hypothesis, TEOM experiments have been performed on the same catalytic solid under experimental conditions, as close as possible to those used in the operando Raman/UV-Vis-NIR reactor set-up (100 mg, 550 °C, 26 vol% C_3H_8 in Ar). The obtained data are given in Figure 3.5.

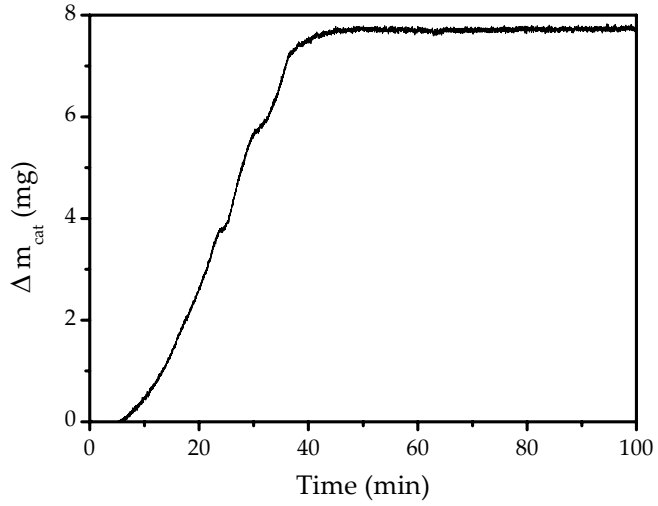

Figure 3.5 *Mass uptake of a 13 wt% Cr / Al_2O_3 catalyst as a function of time-on-stream as measured with TEOM (m_{cat} = 100 mg).*

It was found that the mass of the catalyst during a propane dehydrogenation cycle at 550 °C gradually increases with increasing reaction time up to 40 min-on-stream and then remains constant. Since coke is responsible for the mass uptake, this is in contrast to the Raman observations where the amount of coke appears to go through a maximum. A possible explanation for the different behavior of the intensity of the Raman spectra is a gradual darkening of the catalytic solid during propane dehydrogenation, which results in a reduction of the Rayleigh and Raman scattered light (self-absorption). This can be verified by analyzing the corresponding UV-Vis-NIR diffuse reflectance spectra (Figure 3.6).

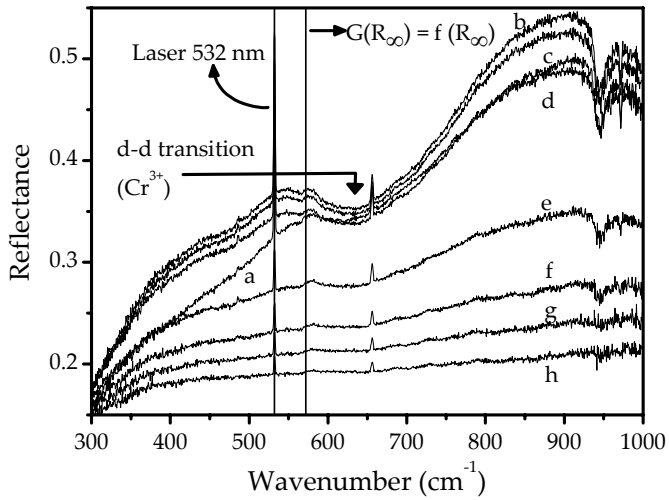

Figure 3.6 *Operando UV-Vis-NIR reflectance spectra measured during 90 min of propane dehydrogenation at 550 °C on a 13 wt% Cr / Al_2O_3 catalyst. Representative spectra are taken after a) 0, b) 5, c) 10, d) 15, e) 30, f) 45, g) 60, and h) 90 min.*

In Figure 3.6, spectrum *a* represents the spectrum of the catalytic solid prior to exposure to a stream of propane at 550 °C. At this starting point, the d-d transition of supported Cr_2O_3-like oxides is indicated with an arrow at around 640 nm.[25,26] The spike at 532 nm is observed due to the Raman laser light picked up by the UV-Vis-NIR detector. The reduction of Cr^{6+} to Cr^{3+} in the beginning of the reaction is presented in Figure 3.6 *a-b*. Figures 3.6 *b-h* show a decrease in the diffuse reflectance of the catalytic solid as propane dehydrogenation proceeds. This decrease is due to darkening of the catalyst by coke. This coke covers the Cr_2O_3-like oxides and as a result the d-d transitions becomes undetectable as time proceeds. This is not surprising since the Raman spectra show that carbonaceous species are formed at the active catalyst surface during reaction. This results in a gradual coverage of the supported Cr_2O_3-like oxides, which are becoming less accessible to the UV-Vis-NIR and Raman light source probing the catalyst and an increasing self-absorption. Finally, Figure 3.7 shows the results of the on-line activity measurements of the catalytic solid.

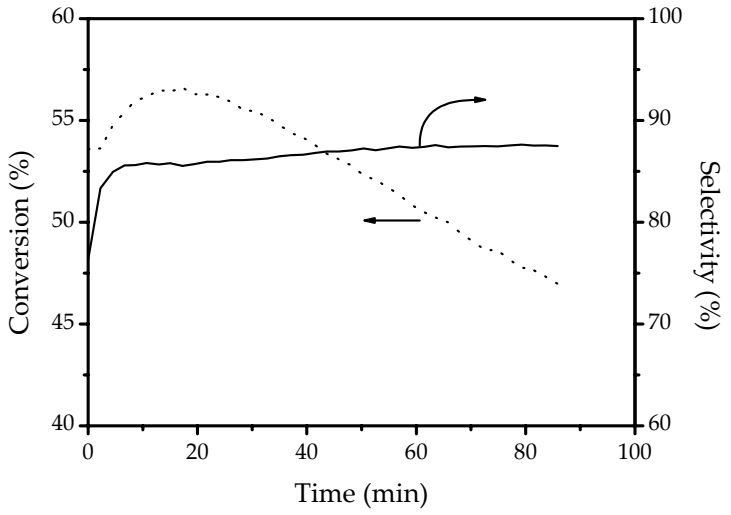

Figure 3.7 *On-line activity and selectivity data for a 13 wt% Cr/Al_2O_3 dehydrogenation catalyst plotted against time-on-stream for a propane dehydrogenation cycle at 550 °C.*

It is clear that the propane conversion increases with reaction time to reach a maximum activity of 56% after 17 min and then gradually decreases with increasing time-on-stream. At the same time, the selectivity towards propene slightly increases and reaches a rather stable value of about 87%.

Quantitation of operando Raman spectra based on the G(R∞) correction factor and boron nitride as an internal standard

As stated in the introduction, two different approaches to quantify time-resolved Raman spectra are compared in this work. The first method makes use of a correction factor based on the UV-Vis-NIR diffuse reflectance spectra, further denoted as the $G(R_\infty)$ correction factor. This correction factor is determined for each Raman spectrum by calculating the $G(R_\infty)$ value using Equation 3.2 at 580 nm. This position in the UV-Vis-NIR spectrum corresponds to the coke band at a Raman shift of 1580 cm^{-1} in case a Raman laser wavelength of 532 nm (18 800 cm^{-1}) is used. (Figure 3.6) The values of $G(R_\infty)$, calculated from the UV-Vis-NIR spectra are presented in Figure 3.8.

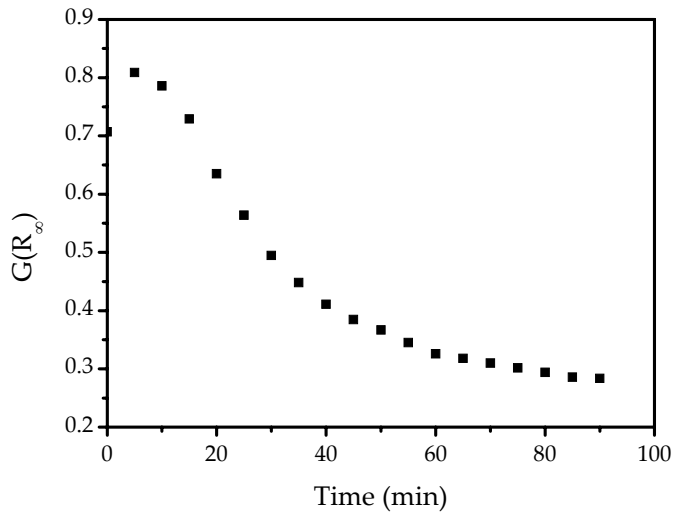

Figure 3.8 *$G(R_\infty)$ as a function of time during 90 min of propane dehydrogenation*

It was found that R_∞ and thus $G(R_\infty)$ decreases as the reaction time proceeds except for the first min-on-stream. Here, the reduction of Cr^{6+} to Cr^{3+} is mainly responsible for a small increase in $G(R_\infty)$. After this initial reduction, the catalyst becomes darker due to a build up of coke on the surface. This darkening results in more absorption and thus less reflection and as a result $G(R_\infty)$ decreases. The nature of the color change, in this case either reduction or blackening, does not influence the correctness of the values, since $G(R_\infty)$ is only dependant on the color of the catalyst. It should be mentioned that, although R_∞ only drops from values of around 0.35 to 0.19, still this corresponds with a decrease of $G(R_\infty)$ of more than 50%. In a second step, the corresponding Raman spectra of Figure 3.4 were divided by the corresponding values of $G(R_\infty)$ according to Equation 3.1 to obtain the true Raman intensities taking

into account the increased self absorption of the darkened sample. The result of this operation is shown in Figure 3.9.

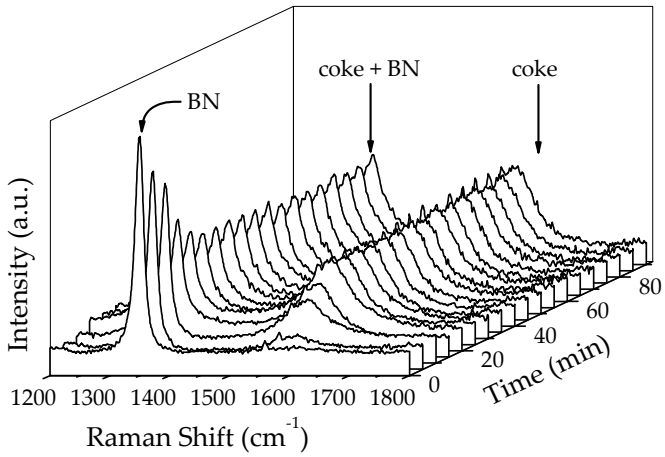

Figure 3.9 *Raman spectra measured during 90 min of propane dehydrogenation over a 13 wt% Cr / Al_2O_3 catalyst after application of a $G(R_\infty)$ correction factor.*

Now, it is evident from Figure 3.9 that the Raman bands due to coke formation at 1580 cm^{-1} gradually develop as a function of reaction time, while the Raman band of BN decreases during the first 30 min and remains constant thereafter. Evaluation of the band at 1330 cm^{-1} (after deconvolution of the BN and coke band) shows a similar trend compared to the 1580 cm^{-1} coke band. The course of the BN band suggests that the absolute amount of BN is initially decreasing. Since BN is inert, this means that the BN is covered by coke. Assuming that the coke is not preferentially formed on either the catalyst or the BN, this does not influence the applicability of using BN as an internal standard in this case. Therefore, Figure 3.10 shows the Raman spectra of Figure 3.4 obtained after normalizing the Raman bands of the carbonaceous deposits to those of the inert internal standard BN.

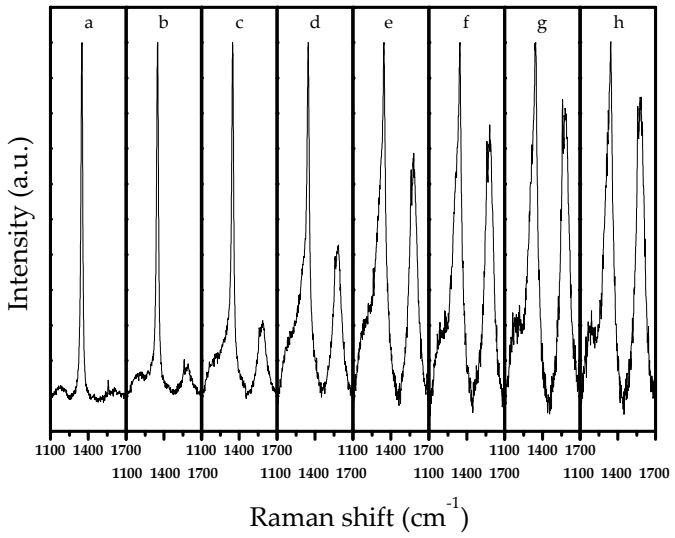

Figure 3.10 *Raman spectra measured during 90 min of propane dehydrogenation over a 13 wt% Cr / Al_2O_3 catalyst after normalization on the band of BN.(T = 550 °C) Spectra are taken after a) 0, b) 5, c) 10, d) 15, e) 30, f) 45, g) 60, and h) 90 min-on-stream.*

In this figure it is clearly visible that next to the increasing intensity of the 1580 cm^{-1} band, a shoulder appears at around 1330 cm^{-1} next to the BN band due to the formation of coke and this band grows in intensity during the whole dehydrogenation period indicating that the amount of coke increases. To compare the two quantitation methods, the integrated Raman peak intensities of the coke band at 1580 cm^{-1} of both procedures are plotted against reaction time in Figure 3.11. In this figure also the intensities of the uncorrected (raw) spectra are presented. Similar results are obtained for the 1330 cm^{-1} band, but because this band overlaps with the Raman BN peak the values are more scattered.

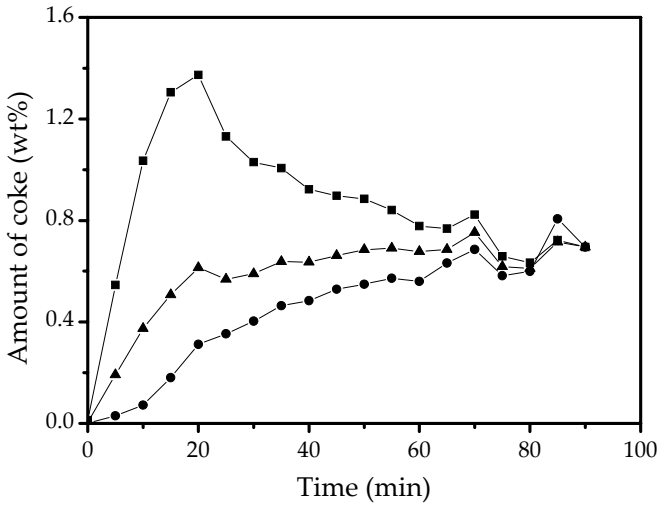

Figure 3.11 *Intensity profile of the 1580 cm^{-1} Raman band during propane dehydrogenation without any correction (■), after G(R_∞) correction (▲) and after BN based correction (●).*

The relative amounts of coke measured with Raman spectroscopy have been transformed into the exact amount of coke present in the solid by measuring the catalyst samples after reactions with TGA. This allows us to put real values to the amount of coke in the catalyst sample as a function of reaction time, assuming that a linear response is present. This linear response can be assumed since no major changes in the intensity (and thus Raman cross-section) are present during the reaction. It is evident that without any correction applied the band intensities do not reflect the reality. The amount of coke seems to go through a maximum, an observation, which is conflicting with the TEOM data. However, the data obtained after applying one of the correction methods results in coke uptake patterns, similar to those obtained with the TEOM technique. In accordance, quantitative Raman spectroscopy indicates that a maximum amount of coke is formed after about 40-50 min-on-stream. Indeed, small differences in coke formation between the TEOM method and both Raman quantitation methods are present, but these can be assigned to the different reactor designs used.

Quantitative Raman spectroscopy and on-line activity measurements of a Cr / Al_2O_3 propane dehydrogenation catalyst, without using an internal boron nitride standard

In order to prove the inertness of BN in the reaction, the experiment was repeated without the addition of BN to the catalyst. Also the overlap in coke band (1330 cm^{-1})

and BN (1350 cm^{-1}) is then absent. The obtained catalytic performances are shown in Figure 3.12 together with the development of the $G(R_\infty)$ corrected Raman bands of 1330 and 1580 cm^{-1}.

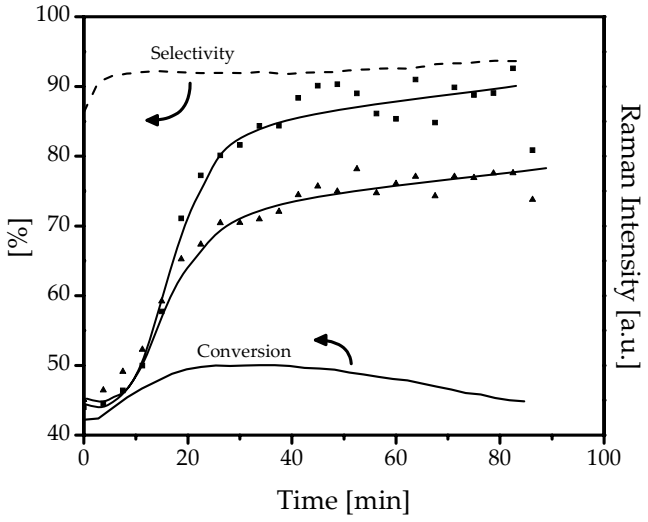

Figure 3.12 *Activity and selectivity data of a 13 wt% Cr / Al_2O_3 catalyst without BN, as well as the intensity profile of the $G(R_\infty)$ corrected 1330 cm^{-1} (■) and 1580 cm^{-1} (▲)Raman bands. (T = 550 ℃, P=1.5 bar).*

It was found that the selectivity towards propene readily reaches a value around 92%, while the conversion increases to a maximum value of about 50% after 34 min-on-stream. Trend wise, these results are identical to those obtained for a catalyst containing BN, although the exact maxima are slightly different.

Using the spectroscopic data to apply the $G(R_\infty)$ correction factor, one can quantify the 1330 and 1580 cm^{-1} bands. The obtained results are included in Figure 3.12 and are in agreement with earlier observations, indicating that the application of the $G(R_\infty)$ correction method is valid during the dehydrogenation of propane.

Coke profiles as a function of the catalyst bed height

In another experiment the Raman spectra were measured during a propane dehydrogenation cycle as a function of the catalyst bed height. The corresponding $G(R_\infty)$ corrected Raman spectra obtained after 250 min-on-stream are given in Figure 3.13 and both 1580 and 1330 cm^{-1} Raman bands are clearly visible.

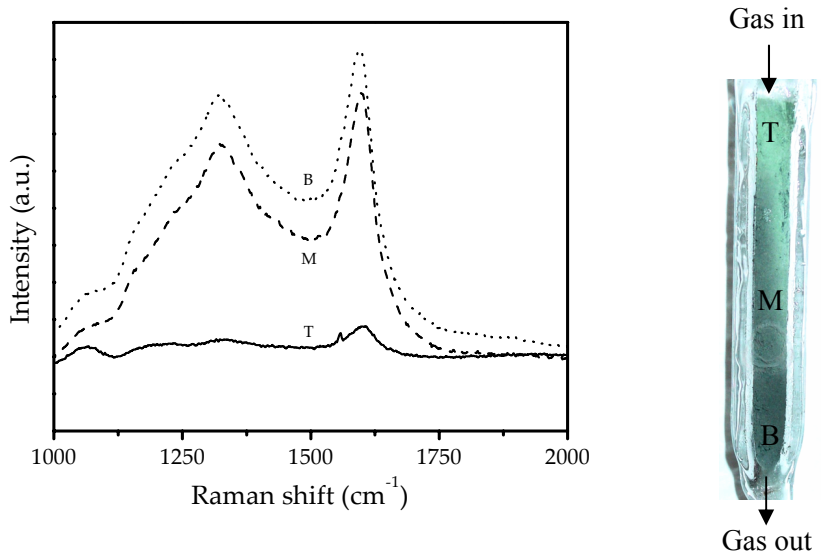

Figure 3.13 *G(R∞) corrected Raman spectra measured at different positions in the reactor after 250 min of propane dehydrogenation at 550 °C. The spectra were taken at the top (T), middle (M) and bottom (B) of the reactor.*

The relative intensity of the Raman spectra increases from top (reactor inlet) to bottom (reactor outlet). This is an indication that propene is a precursor for coke formation at the catalytic surface. After the dehydrogenation cycle the catalyst was removed from the reactor and the amount of coke was determined by TGA at different bed heights. The results are shown in Figure 3.14.

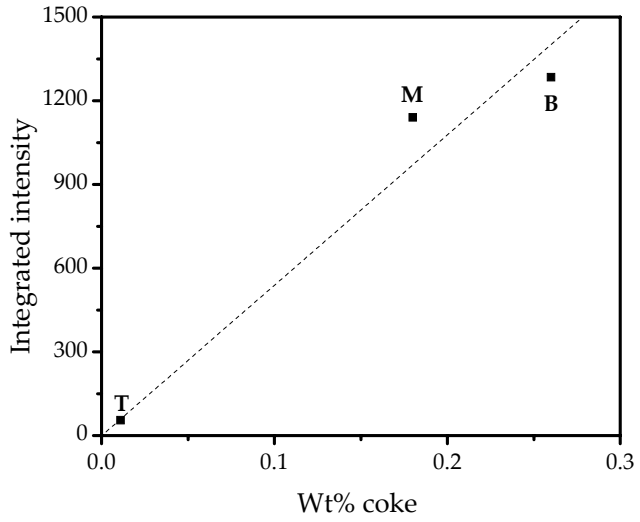

Figure 3.14 *G(R∞) corrected Raman intensity of the 1580 cm-1 band plotted against the amount of coke as measured with TGA for different reactor bed heights.*

If the $G(R_\infty)$ correction is a valid method, a trend is expected between the amount of coke observed with Raman spectroscopy and measured with TGA analysis. It appears that a correlation between the amount of coke determined with both methods is present, assuming the earlier mentioned linear relation between the coke content and the corrected intensity. According to this plot the error in the measurements is close to 10%.

Evaluation of Raman quantitation based on the $G(R_\infty)$ correction factor

The proposed method based on the $G(R_\infty)$ correction factor provides an elegant procedure to determine in a quantitative manner the amount of coke inside a catalytic reactor as a function of the reaction time and catalyst bed height. The main advantage of the method is that an internal standard is not required to quantify the measured Raman spectra. In retrospection of this particular set of experiments, BN, although catalytically inert, is not a good internal standard since its Raman peak overlaps with one of the coke bands. An internal standard with a sharp band at a slightly different position would be better, but has not been found.[*] The application conditions of an internal standard are highly specific to the system in which it is applied making the choice of a suitable compound more difficult.

The assumption for Raman quantitation using the $G(R_\infty)$ correction factor is that the scattering coefficient s is constant during the experiment. It implies that quantitation is possible within one experiment, but is not straightforward when different catalyst samples in different runs have to be compared.

Conclusions

Two different methods of Raman quantitation have been explored to determine the amount of coke present in a catalytic reactor during a propane dehydrogenation cycle, i.e. (1) the use of an internal boron nitride standard and (2) a $G(R_\infty)$ correction factor. It was found that both methods are suitable, but the use of a combined operando Raman / UV-Vis-NIR set-up has the advantage that the addition of an internal standard is not necessary. Comparing the results to TGA / TEOM data has proven the validity of the methods. Both are in good agreement with each other, making method 2 the preferred one. The new method, in which a $G(R_\infty)$ factor is applied, allows with an estimated error of approximately 10% to quantify the

[*] Other possible internal standards, that have been explored in this study are SiC and TiN. It appeared that the Raman bands were either not strong enough (TiN) or located at a position, overlapping other bands (SiC).

amount of coke formed during a propane dehydrogenation reaction as a function of catalyst bed height as well as the reaction time in an industrial-like reactor.

Acknowledgements

B. van der Linden (Delft University of Technology) and F. Broersma (Utrecht University) are acknowledged for performing the TGA and TEOM measurements described in this chapter.

References

1. Li, C.; Li, M., *J. Raman Spectrosc.*, **2002**, *33*, 301.
2. Aarnoutse, P. J.; Westerhuis, J. A., *Anal. Chem.*, **2005**, *77*, 1228.
3. Baltrus, J. P.; Makovsky, L. E.; Stencel, J. M.; Hercules, D. M., *Anal. Chem.*, **1985**, *57*, 2500.
4. Bergwerff, J. A.; Visser, T.; Leliveld, B. R. G.; Rossenaar, B. D.; de Jong, K. P.; Weckhuysen, B. M., *J. Am. Chem. Soc.*, **2004**, *126*, 14548.
5. Chan, S. S.; Bell, A. T., *J. Catal.*, **1984**, *89*, 433.
6. Schmidt, K. J.; Zhang, S. L.; Michaelian, K. H.; Webb, M. A.; Loppnow, G. R., *Appl. Spectrosc.*, **1999**, *53*, 1206.
7. Vankeirsbilck, T.; Vercauteren, A.; Baeyens, W.; Van der Weken, G.; Verpoort, F.; Vergote, G.; Remon, J. P., *Trends Anal. Chem.*, **2002**, *21*, 869.
8. Zheng, X.; Fu, W.; Albin, S.; Wise, K. L.; Javey, A.; Cooper, J. B., *Appl. Spectrosc.*, **2001**, *55*, 382.
9. Wu, Z.; Zhang, C.; Stair, P. C., *Catal. Today*, **2006**, in press.
10. Kellerman, R. In *Spectroscopy in Heterogeneous Catalysis*; Delgass, W. N., L., H. G., Kellerman, R., Lunsford, J. H., Eds.; Academic Press: New York, 1979.
11. Kortum, G. *Reflectance Spectroscopy: Principles, Methods and Applications*; Springer-Verlag: Berlin, Heidelberg and New York, **1969.**
12. Schoonheydt, R. A. In *Characterization of Heterogeneous Catalysts*; Delannay, F., Ed.; Marcel Dekker Inc: New York and Basel, 1984.
13. Weckhuysen, B. M., Ed.; *In-situ Spectroscopy of Catalysts*; American Scientific Publishers: Stevenson Ranch, 2004, pp 255.
14. Schrader, B.; Bergmann, G., *Z Anal. Chem*, **1967**, *225*, 230.
15. Waters, D. N., *Spectroc. Acta Pt. A-Molec. Biomolec. Spectr.*, **1994**, *50*, 1833.
16. Kuba, S.; Knozinger, H., *J. Raman Spectrosc.*, **2002**, *33*, 325.
17. Nijhuis, T. A.; Tinnemans, S. J.; Visser, T.; Weckhuysen, B. M., *Phys. Chem. Chem. Phys.*, **2003**, *5*, 4361.

18. Nijhuis, T. A.; Tinnemans, S. J.; Visser, T.; Weckhuysen, B. M., *Chem. Eng. Sci.*, **2004**, *59*, 5487.
19. Sze, S. K.; Siddique, N.; Sloan, J. J.; Escribano, R., *Atmos. Environ.*, **2001**, *35*, 561.
20. Mertes, S.; Dippel, B.; Schwarzenbock, A., *J. Aerosol Sci.*, **2004**, *35*, 347.
21. Kong, F.; Kostecki, R.; Nadeau, G.; Song, X.; Zaghib, K.; Kinoshita, K.; McLarnon, F., *J. Power Sources*, **2001**, *97-8*, 58.
22. Escribano, R.; Sloan, J. J.; Siddique, N.; Sze, N.; Dudev, T., *Vibr. Spectrosc.*, **2001**, *26*, 179.
23. Compagnini, G.; Puglisi, O.; Foti, G., *Carbon*, **1997**, *35*, 1793.
24. Chua, Y. T.; Stair, P. C., *J. Catal.*, **2003**, *213*, 39.
25. Weckhuysen, B. M.; Wachs, I. E.; Schoonheydt, R. A., *Chem. Rev.*, **1996**, *96*, 3327.
26. Puurunen, R. L.; Weckhuysen, B. M., *J. Catal.*, **2002**, *210*, 418.

4

Quantitative Raman spectroscopy of supported metal oxide catalysts: On-line determination of the amount of Cr^{6+} in a catalytic reactor

Abstract

In continuation of previous work on the applicability of the $G(R_\infty)$ correction factor for the quantification of Raman spectra of coke during propane dehydrogenation experiments, research has been carried out on the potential of this correction factor for the quantification of supported metal oxides during reduction experiments. For this purpose, supported chromium oxide catalysts have been studied by combined *in-situ* Raman and UV-Vis-NIR spectroscopy during temperature programmed reduction experiments with hydrogen as reducing agent. The goal was to quantify on-line the amount of Cr^{6+} in a reactor based on the measured *in-situ* Raman spectra. During these experiments, a significant temperature effect was observed, which has been investigated in more detail with a thermal imaging technique. The results revealed a temperature increase 'on the spot' that can exceed 100°C. It implies that Raman spectroscopy can have a considerable effect on the local reaction conditions and explains observed inconsistencies between the *in-situ* UV-Vis-NIR and Raman data. In order to minimize this heating effect, reduction of the laser power, mathematical matching of the spectroscopic data, a different cell design and a change in reaction conditions has been evaluated. It is demonstrated that increasing the reactor temperature is the most feasible method to solve the heating problem. Next, it allows the application of *in-situ* Raman spectroscopy in a reliable quantitative way without the need of an internal standard.

Introduction

In Chapter 3, it has been demonstrated that the amount of coke, that is formed on a Cr/Al_2O_3 propane dehydrogenation catalyst, can be quantified with *in-situ* Raman spectroscopy by using a $G(R_\infty)$ correction factor.[1] This factor can be directly determined with *in-situ* UV-Vis-NIR spectroscopy using a previously developed combined Raman / UV-Vis-NIR set-up.[2,3] The results turned out to be in good agreement with those obtained by applying boron nitride as an internal standard. Furthermore, they are consistent with independently conducted thermogravimetrical results along the reactor bed. At that time, it was that the $G(R_\infty)$ correction factor method should in principle work for every active Raman active species present in the catalyst sample.

In order to determine the correctness of this hypothesis, the temperature programmed reduction of a series of Cr / Al_2O_3 catalysts in the presence of hydrogen as reducing agent are investigated. The colour of this catalyst system is known to change as a result of the reduction treatment and the conversion of Cr^{6+} to Cr^{3+} can be monitored with *in-situ* UV-Vis-NIR spectroscopy by measuring the intensity changes of the Cr^{6+} charge transfer (CT) and Cr^{3+} d-d transition bands. These spectral features should be accompanied by an intensity decrease of the characteristic Cr=O (Cr^{6+}) stretching vibration at around 996 cm^{-1} as measured with *in-situ* Raman spectroscopy. The goal of this work is to show the general validity of the $G(R_\infty)$ correction factor for the Raman quantification of this Cr^{6+}-species during temperature programmed reduction experiments. It will, however, be shown that a local Raman heating effect complicates this quantitative approach.

Experimental

A series of catalyst materials was prepared by the incipient wetness impregnation method using CrO_3 solutions and an alumina support (Sasol, Puralox SCCA-5/200, 188 m^2 g^{-1}). After impregnation the catalysts were dried for 12 h at 60 °C and subsequently for 12 h at 120 °C. The catalysts were then calcined in air at 550°C (10°C min^{-1}) for 5 h. After calcination, 0.1 wt% of boron nitride (BN, Aldrich, 99%) was added to the catalysts as an internal standard and they were ball-milled for 15 min to obtain a homogeneously mixed powder at a speed of 2000 rpm.

For a reduction experiment typically 300 mg of catalyst was loaded in a quartz reactor, which forms part of the combined *in-situ* Raman / UV-Vis-NIR set-up described in previous papers.[2,3] First, the catalyst was heated to 550°C at a rate of 10°C min^{-1} in a mixture of 3 ml min^{-1} O_2 (Hoek Loos, 99.995%) and 12 ml min^{-1} He

(Hoek Loos, 99.996%). The temperature was kept at 550°C for 5 h before cooling down to 100°C. After this drying step, He was purged to remove all O_2 from the system. Subsequently, the reduction was started in parallel with on-line Raman and UV-Vis-NIR analysis, by flowing 0.5 ml min^{-1} of a reducing agent (H_2, Hoekloos, 99.0%) in 39.5 ml min^{-1} of He, unless otherwise stated.

UV-Vis-NIR spectra were measured using a DH2000 light source (Avantes) combined with an Avaspec 2048 CCD spectrometer (Avantes) and a BI-FL400 high temperature resistant probe (Ocean Optics). Raman spectra were recorded using a Kaiser RXN spectrometer equipped with a 532 nm diode laser (output power could be varied up to 60 mW). The laser power was measured via an Orion PD display detector (Ophir Optronics Ltd). A 5.5" objective was used for beam focusing and collection of the scattered radiation. Typically the exposure time of the CCD camera was 2 s and 25 spectra were accumulated to obtain a reasonable signal to noise ratio. The spectra were analyzed with Thermo Galactic Grams AI v. 7.0 software. In addition, IR-thermography experiments were carried out with a Jade J550M InSb BB Camera (CEDIP Infrared Systems) equipped with a 50 mm lens and a 20 mm extension ring. The applied camera wavelength was 3.9 μm with an estimated temperature sensitivity of 20 mK. An ex-situ TPR measurement was performed using an Autochem II 2920 (Micromiretics). The catalyst was heated from 25 °C to 600 °C at a rate of 5 °C min^{-1} in a gas stream of 5 % H_2 in Ar.

Results and Discussion

Development of a calibration line

A first step towards the application of a spectroscopic technique in a quantitative manner is the development of a calibration line. In Raman spectroscopy, Cr^{6+} has a characteristic Raman shift around 996 cm^{-1} originating from the Cr=O vibration.[4-7] However, from our previous work where the amount of coke has been quantified with *in-situ* Raman spectroscopy it is known that the observed Raman intensity is not always in agreement with the 'true' Raman intensity.[1] Therefore, BN was added to the catalyst samples as an internal standard. The choice for BN was made because it is inert, and a strong Raman scatterer. A calibration line of the chromium band in a series of alumina-supported chromium oxide catalysts, enriched with BN as internal standard, differing in their chromium oxide loading is presented in Figure 4.1.

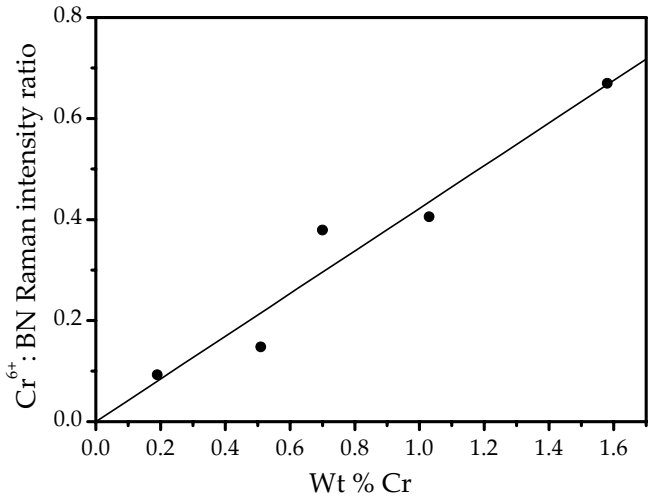

Figure 4.1 *Calibration line of the Cr=O band plotted against the loading of a supported Cr / Al_2O_3 catalyst after BN-correction. ($y = 0.42\ x$, $R^2 = 0.941$).*

Figure 4.1 depicts the Cr^{6+}:BN ratio as a function of the Cr loading. Each point in the graph represents an average of 6 consecutive measurements. In each measurement the Raman was completely refocused. To ensure that the catalyst remained completely oxidized, the catalyst was kept in an oxidizing environment (O_2 flow) during these measurements. The obtained spectra were averaged, which was necessary because a change in focusing, inherent to the applied *in-situ* set-up, resulted in slightly different Cr^{6+}:BN ratios. By averaging the results of multiple spectra measured at a different focusing spot, this effect can be overcome. The straight line of Figure 4.1 shows a correlation between the observed Raman intensity and the amount of Cr^{6+} in the catalyst in the range 0–1.5 wt% and suggests that the amount of Cr^{6+} can be monitored quantitatively by using *in-situ* Raman spectroscopy. Recently, a similar calibration line for low-loaded supported vanadium oxide catalysts has been presented by Wu *et al*.[8] From a practical point of view, however, it would be advantageous if no internal standard has to be added for Raman quantification. Thus, in line with the previous work, the diffuse reflectance measured at 562 nm with UV-Vis-NIR spectroscopy (corresponding to a Raman shift of 996 cm^{-1}, i.e. the location of the Cr^{6+} band) can be used to derive the 'true' Raman intensity.[1] Unfortunately, this holds only as long as the focusing of the UV-Vis-NIR-probe is constant. A difference in focusing, which is unavoidable when measuring different catalyst materials, results in a different baseline. As a consequence, the relative intensity of the Cr^{6+} charge transfer (CT) band around 407 nm changes as well. In

addition, it is not possible to simply shift the baseline followed by a multiplication factor dependent on the concentration. The reason for all this is that the multiplication factor is unknown and cannot be experimentally determined. Nevertheless, within one experiment the $G(R_\infty)$ correction is still applicable since relative changes in diffuse reflectance can still be measured with UV-Vis-NIR spectroscopy.

Qualitative Raman spectroscopy on supported chromium oxide catalysts during temperature programmed reduction experiments

To prove that the use of the $G(R_\infty)$ correction factor is a valid approach to monitor the amount of Cr^{6+} during a reduction process in a catalytic reactor, a 0.5 wt% Cr/Al_2O_3 catalyst, enriched with BN, was exposed to a 20% H_2 in He mixture (total flow of 15 ml min^{-1}). The catalyst was heated in steps of 20°C and at every temperature step, *in-situ* Raman and UV-Vis-NIR spectra were measured. The results of this experiment are presented in Figure 4.2.

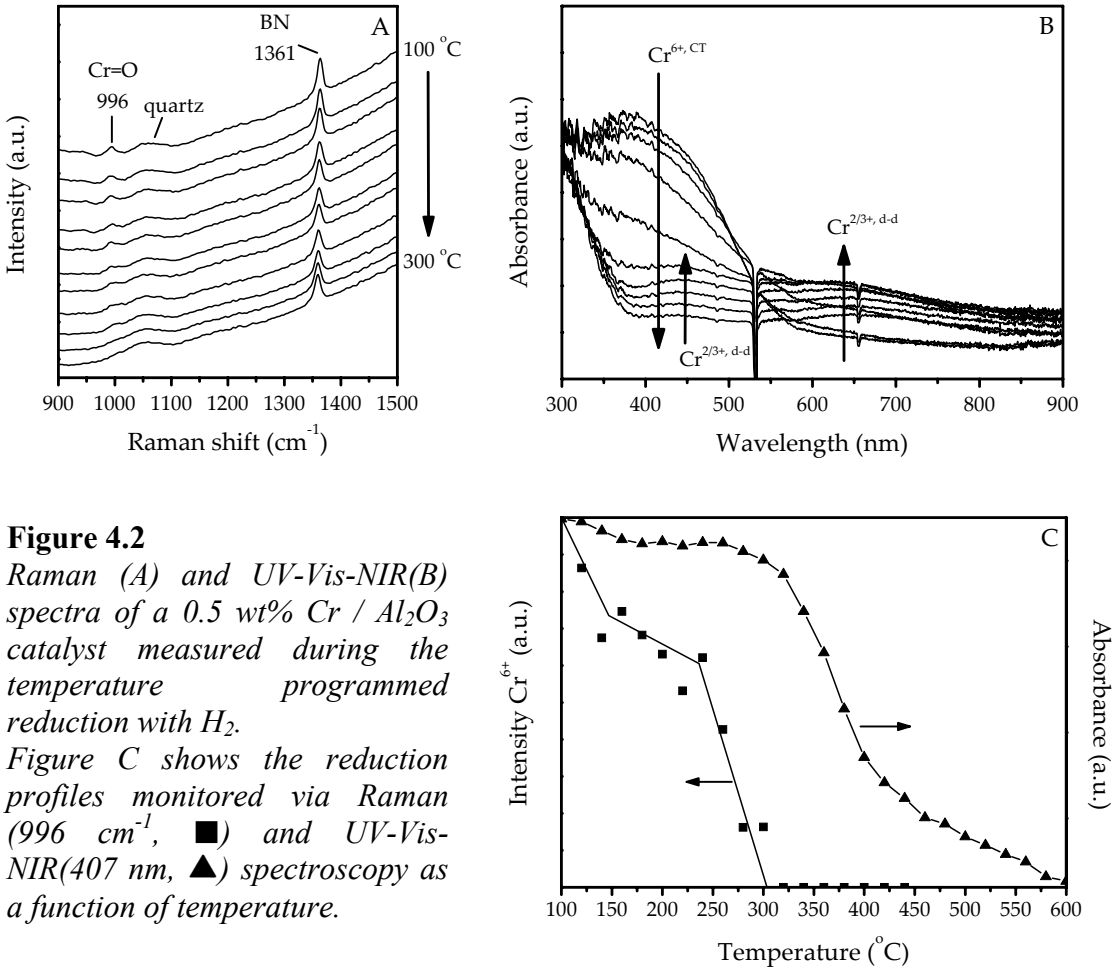

Figure 4.2
Raman (A) and UV-Vis-NIR(B) spectra of a 0.5 wt% Cr / Al_2O_3 catalyst measured during the temperature programmed reduction with H_2.
Figure C shows the reduction profiles monitored via Raman (996 cm^{-1}, ■) and UV-Vis-NIR(407 nm, ▲) spectroscopy as a function of temperature.

Figure 4.2 A shows a selection of Raman spectra measured at different temperatures during the reduction process. The reduction of Cr^{6+} can be monitored via the decrease of the Cr=O band at 996 cm^{-1}. The reduction can also be monitored via the decrease of the Cr^{6+} charge transfer band at around 407 nm and the appearance of a Cr^{3+} d-d transition at around 650 nm (Figure 4.2B). Since Figure 4.2 A and B provide insufficient insight into the course of the reduction profiles, this information is presented in Figure 4.2C. On the left hand axis the intensity of the Cr^{6+} band is plotted, whereas on the right hand axis the reduction with UV-Vis-NIR spectroscopy is monitored via the course of the 407 nm Cr^{6+} CT band intensity. From this figure it can be concluded that the two observed reduction temperatures differ ca. 100-150°C. For two spectroscopic techniques monitoring the same species (i.e. Cr^{6+}), this is not an expected result. A plausible explanation for the observed difference in reduction temperature is the presence of a local heating effect in the laser spot. This means that UV-Vis-NIR spectroscopy must be used to verify the results obtained by Raman spectroscopy. This is clearly another advantage of combining multiple spectroscopic techniques in one set-up for studying catalytic solids at work. A similar advantage of combining techniques has recently been described for a ED-XAFS/UV-Vis-NIR set-up by Mesu *et al.*, where beam damage was assessed when probing a catalyst system with X-rays.[9,10]

Raman laser heating effect

It is well-known that Raman lasers may heat a sample, especially when high laser powers are applied.[11-17] To prove that a local heating effect was indeed responsible for the discrepancies between the *in-situ* Raman and UV-Vis-NIR data, additional experiments were carried out. First of all, the same experiment was performed, but now the reduction process was stopped at 280°C. It turned out that at this temperature, the reduction process was only observed with Raman spectroscopy and not yet with UV-Vis-NIR spectroscopy. After this temperature treatment, the reactor was cooled down to room temperature and removed from the furnace under an inert gas flow (He). After removal of the reactor, a dark grey-coloured spot was visible at the position where the Raman laser had been focused on the catalyst sample. When measuring a new Raman spectrum at a shifted position, the Cr^{6+} band became visible again. This is illustrated in Figure 4.3.

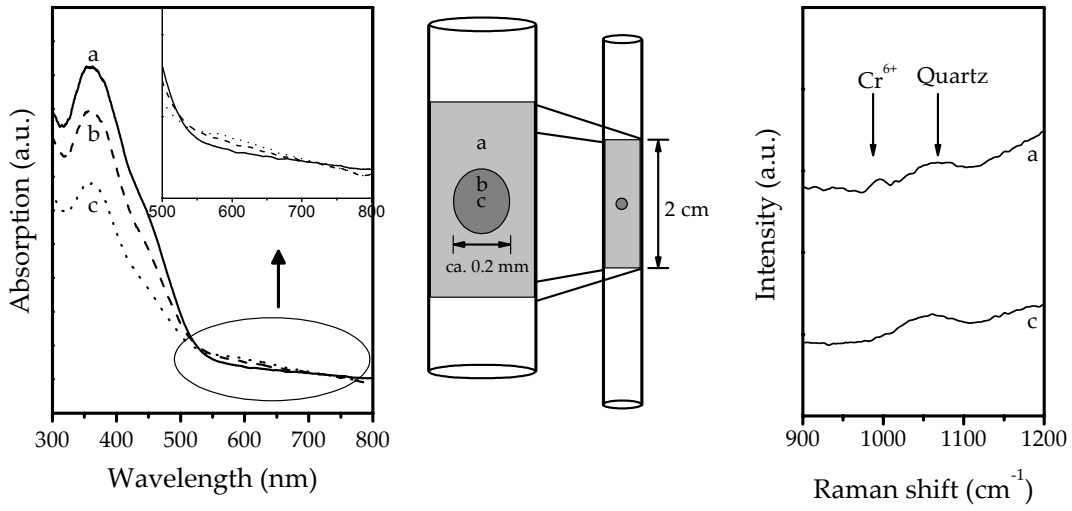

Figure 4.3 *UV-Vis-NIR (left) and Raman (right) spectra measured at different locations in the laser spot after reduction of a 0.5 wt% Cr / Al_2O_3 catalyst at 280 °C.*

To confirm this observation UV-Vis-NIR microspectroscopy was performed.[18] In Figure 4.3 UV-Vis-NIR spectra are shown, which are measured at different locations towards the center of the laser spot. Spectrum *a* is measured in the bulk of the catalyst just outside the coloured spot, whereas spectra *b* and *c* are measured more towards the center of the spot. Going from spectrum *a* to *c* in this graph, the CT band of Cr^{6+} decreases in intensity, while simultaneously the d-d transition of Cr^{3+} becomes visible. These UV-Vis-NIR data, in combination with the observations from Raman spectroscopy, show that at the position of the laser spot, the catalyst is reduced and that it is likely that a local temperature increase has occurred to achieve this. With this result in mind, it would be useful if the temperature inside the laserspot could be determined, and in this way correlate the UV-Vis-NIR spectra to the Raman data.

In principle, the sample temperature in a laser spot can be determined via the relative intensities of the Stokes and anti-Stokes shifts in a spectrum making use of Boltzmann's Law.[19,20] Unfortunately, only the Stokes radiation can be measured with the available Raman spectrometer and thus the actual sample temperature in the laser spot could not be determined in this way. Instead, IR-thermography was applied to measure the temperature of the laserspot on a completely oxidized and dehydrated catalyst sample and on a spent catalyst. For this purpose, pellets were pressed of the catalyst materials. For the (white-yellow) dehydrated catalyst, a small effect became visible (ca. 15 °C), but a much larger effect was observed obtained for the spent catalyst (having a dark grey colour). A thermographical image of this sample is presented in Figure 4.4 A.

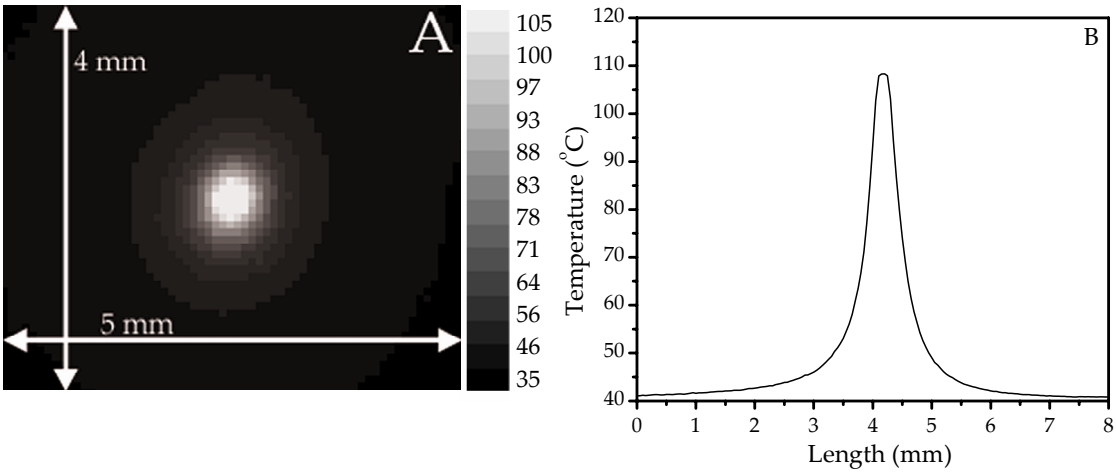

Figure 4.4 A) *IR-thermographic image of a catalyst pellet after exposure to propane for 90 min.* **B)** *Observed temperature at the catalytic surface when a 532 nm laser (50 mW) is focused at this material.*

The bright spot in this image clearly shows that the Raman laser is heating the catalyst sample locally, an effect which was already expected from the previous experiments. Figure 4.4 B was obtained when analyzing the data along the diameter of the laser spot, indicating that a local temperature increase of 70°C is possible. Furthermore, extrapolating the slopes in these graphs, suggest that even larger temperature effects (> 100°C) are not unlikely, in line with the data presented in Figure 4.2 C.

Application of quantitative Raman spectroscopy during a series of temperature programmed reduction cycles

It will be clear from the heat effect, observed during the temperature programmed reduction experiments, that this complicates the application of the $G(R_\infty)$ correction factor. Recall that this factor corrects for the actual colour of the catalyst sample. In the laser spot, the catalyst will be heated and reduced and the colour consequently will change. However, simultaneously measured *in-situ* UV-Vis-NIR spectra do not show a colour change, which is due to the lower temperature of the remaining part of the catalyst material. Therefore, it is not possible to calculate the $G(R_\infty)$ correction factor directly. This problem can be overcome by 'shifting' the course of the reduction of the Cr^{6+} band to lower temperatures, in order to let this reduction coincide with the observed reduction in Raman spectroscopy. In other words, shift the UV-Vis-NIR spectra of Figure 4.2C to lower temperatures in such a way that the heat effect is eliminated. After doing this, the $G(R_\infty)$ correction can be applied. The

result of this operation is presented in Figure 4.5 for 5 consecutive temperature programmed reduction cycles alternated with a re-oxidation step at 500°C with O_2. In each redox cycle the temperature is raised 20°C every 30 min in the range 100–500°C.

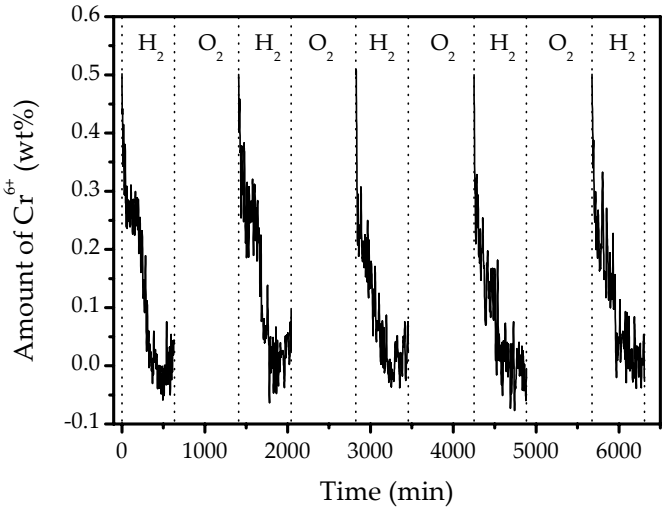

Figure 4.5 *The amount of Cr^{6+} present during 5 cycles of temperature programmed reduction with H_2 and reoxidation with O_2 on a 0.5 wt% Cr / Al_2O_3 catalyst after application of the $G(R_\infty)$ correction factor.*

Figure 4.5 shows that a gradual reduction is observed during all reduction cycles, although in the first part of every cycle (thus at lower temperatures) the reduction of supported chromium oxide species seems to be faster.† This could be an indication that two different chromium oxide species are probed with Raman spectroscopy, one being more easily reducible than the other. An explanation can be the presence of both monomeric and polymeric chromium oxide species, which are likely to have a different reduction behavior. This idea is in agreement with data of Weckhuysen *et al*. and Airaksinen *et al.* where both chromate and polychromates are reported to exist for Cr / Al_2O_3 catalysts.[21-23]

An ex-situ TPR experiment on the same sample could not prove the presence of two distinguisable species, which is in accordance with earlier studies of Kanervo and Krause.[24]

The data of Figure 4.5 also show that the use of the $G(R_\infty)$ correction factor allows to determine on-line the amount of Cr^{6+} during a reduction process in a reactor. The applied method (shifting the reduction profile to lower temperatures) is, however,

† It would be advantageous if the reoxidation step could also be monitored. However, after switching the gas from H_2 to O_2 the Raman scattering properties of the solid were dramatically changed. As a consequence, the application of a correction factor was not anymore possible.

rather subjective. Therefore, it is preferable that the Raman data are not shifted, i.e. change the conditions inside the reactor in such a manner that both *in-situ* Raman and UV-Vis-NIR data are measuring the catalyst material under identical conditions and thus eliminate the temperature effect.

Exploration of experimental conditions at which the local Raman heating effect is negligible

There are many ways of circumventing the observed local Raman heating effect. It is possible to 1) decrease the laser power, 2) defocus the Raman laser, 3) rotate the sample, 4) use a chopper or pulsed laser, 5) probe the same volume with UV-Vis-NIR and Raman spectroscopy, and 6) increase the overall reaction temperature. A selection of these methods (1, 5 and 6) was investigated in the course of this study. Some comments are made on the other methods as well.

The simplest way of decreasing the local Raman heating effect is by reducing the photon-flux on the catalyst sample. As a result the difference in the observed reduction temperature in Raman and UV-Vis-NIR spectroscopy decreases. However, the laser power cannot be reduced ceaselessly as a secondary effect is taking place, which is illustrated in Figure 4.6.

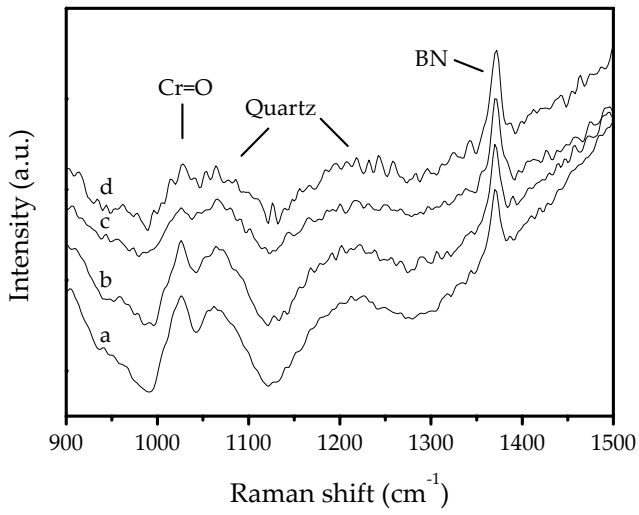

Figure 4.6 *Raman spectra of a 0.5 wt% Cr / Al_2O_3 catalyst measured with an exposure time of 1 s; 10 spectra were averaged for S / N improvement; a) 35 mW, b) 20 mW c) 10 mW and d) 5 mW. The spectra are normalized on the BN band.*

On reducing the laser power, the features remain the same, but the signal-to-noise ratio becomes worse. For static experiments this is not a problem, since more Raman spectra can be averaged to maintain a good signal-to-noise ratio. However, for *in-situ*

experiments, this will increase the time necessary for measuring one Raman spectrum and as a result dynamic information on the catalyst behavior might be lost.
Closely related to this method is a defocusing of the Raman laser. In this way the photons are spread on a larger surface, but also at the expense of the signal-to-noise ratio. This method has been applied by Macdonald and co-workers.[25] Other methods to decrease the photon flux on the sample are using a chopper, a pulsed laser or moving the sample around in the focus spot of the beam. A rotating disk is an example, which can be used to prevent beam damage.[26,27] However, for the developed Raman / UV-Vis-NIR set-up sample spinning is not an option and other methods for dealing with the local heat effect have to be explored.
A possibility might be changing the reactor configuration. In the normally used reactor tubes, the probed volumes by Raman and UV-Vis-NIR spectroscopy do no coincide. If the internal diameter can be reduced to an extent that both techniques probe the same volume, the heat effect can be neglected and the $G(R_\infty)$ correction factor can be applied directly. To understand this, one needs to realize that the Raman laser will still heat the catalyst locally, but since UV-Vis-NIR spectroscopy is now probing the same catalyst particles, it is no longer causing differences. This is schematically depicted in Figure 4.7.

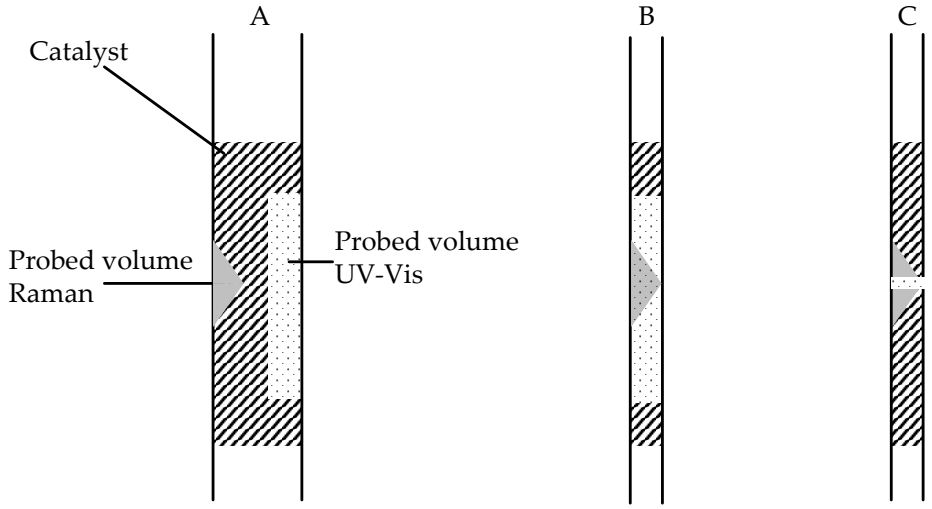

Figure 4.7 *Schematic representation of the probed catalyst volume with A) a 'normal' reactor (Ø = 6 mm) and a standard UV-Vis-NIR probe (400 μm fibers), B) a reactor with a smaller inner diameter (Ø =1 mm) and a 'standard' UV-Vis-NIR probe (400 μm fibers) and C) a reactor with a smaller inner diameter (Ø =1 mm) and a micro-UV-Vis-NIR probe (100 μm fibers).*

As illustrated in Figure 4.7 A, in a normal reactor, the volume probed by UV-Vis-NIR spectroscopy is relatively far away from the volume that is probed by the Raman

spectrometer. Since the heat effect of the Raman laser is very local a temperature effect will not be detected with UV-Vis-NIR spectroscopy at the opposite side of the reactor. If the inner diameter of the reactor is reduced, as in Figure 4.7B, the situation changes. The small volume probed by Raman spectroscopy is now overlapping with the sample volume probed by UV-Vis-NIR spectroscopy. However, only a very small portion of the volume probed with UV-Vis-NIR consists of reduced chromium oxide species and therefore the reduction will still be difficult te detect. Instead, if the probed volume is more or less the same for both spectroscopic techniques, the reduction, caused by the laser might be observable with UV-Vis-NIR spectroscopy (Figure 4.7 C).

Unfortunately, an investigation using a reactor with an internal diameter of 1 mm and a micro-UV-Vis-NIR probe[28] showed that the difference in observed reduction temperature is still present and close to 100°C. This observation can be explained by the limited penetration depth of the laser which makes that the volumes probed by Raman and UV-Vis-NIR spectroscopy are not identical. Since solid phase Raman spectroscopy is merely a surface technique, this would require a reactor with an inner diameter in the order of microns, but such reactor tube would easily be plugged. This means that, although it is theoretically possible to create a reactor in which the temperature effect is minimized, this reactor tube could never be used for *in-situ* experiments in a practical manner.

Finally, circumventing the local heating effect was studied by changing the reaction conditions. Since it is shown that it is necessary to get a homogeneous temperature distribution throughout the reactor tube, this means that the overall reaction temperature must be increased. The influence of the temperature of the reactor on the difference in observed reduction behavior was investigated by performing isothermal reductions with hydrogen at different temperatures in the range 400-500°C. The results of these experiments are given in Figure 4.8.

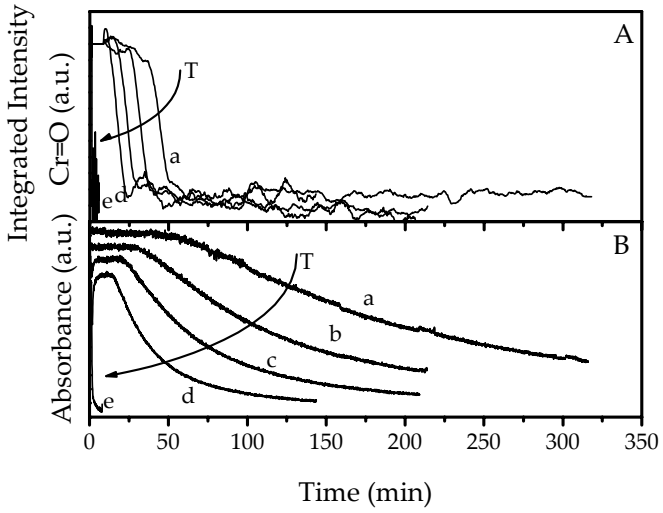

Figure 4.8 *Isothermal reduction profile of a 0.5 wt % Cr / Al_2O_3 catalyst treated in H_2 and measured at 400 (a), 420 (b), 440 (c), 460 (d), and 500 ℃ (e). The top figure represents the decrease of the Cr=O band observed in Raman spectroscopy. In the bottom figure the intensity of the UV-Vis-NIR band at 407 nm is presented as a function of time.*

Figure 4.8A illustrates the course of the Cr=O band intensity as determined with *in-situ* Raman spectroscopy, while in Figure 4.8B the course of the 407 nm UV-Vis-NIR band intensity is plotted. Combining these two figures indicates that the difference in observed reduction temperature by UV-Vis-NIR and Raman spectroscopy decreases if the temperature of the furnace is increased. The results show that at relatively low temperatures the Raman heating effect is still substantial, but at temperatures close to 500°C these differences become negligible. This also means that the application of the $G(R_\infty)$ correction factor is limited to high temperature reactions for this type of catalytic materials.

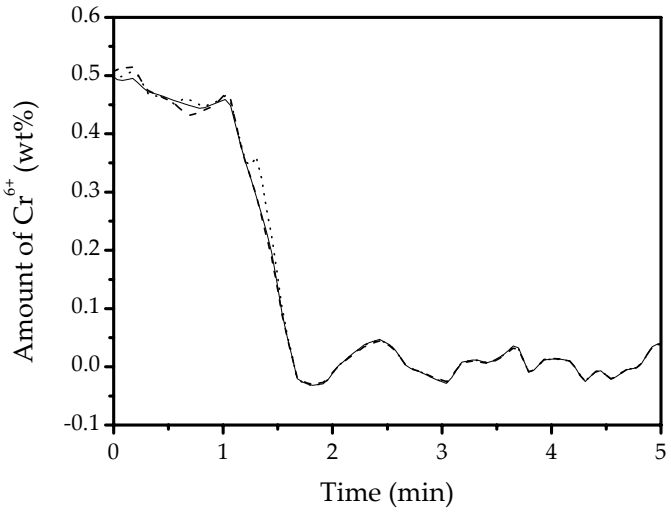

Figure 4.9 *Amount of Cr^{6+} present in a 0.5 wt% Cr / Al_2O_3 catalyst during reduction with H_2 at 500 °C after application of the $G(R_\infty)$ correction factor (dots) and the application of BN as internal standard (dash). The solid line represents the uncorrected data.*

Finally, the amount of Cr^{6+} was determined during a hydrogen reduction at 500°C by using the $G(R_\infty)$ correction factor. The results are compared with those obtained when using BN as internal standard in Figure 4.9. It is clear that both correction methods show good agreement with each other. However, a remark must be made that during the reduction of Cr^{6+} the relative changes occurring at 562 nm are rather small, and as a consequence, the influence of the $G(R_\infty)$ correction factor on the raw Raman data is relatively small. Nevertheless, it is shown that it is indeed possible to develop the technique of quantitative *in-situ* Raman spectroscopy without the use of an internal standard, such as BN.

Recently, we have discussed the quantification of the amount of coke formed during a catalytic reaction as measured with *in-situ* Raman spectroscopy.[1] The methodology was based on the use of the $G(R_\infty)$ correction factor. It is of course important to check whether the obtained knowledge about the local Raman heating effect affects the conclusions made. As shown in this paper, the local Raman heating effect is negligible at temperatures above 500°C. Since the dehydrogenation reaction of propane is typically performed at 550°C it can be anticipated that the Raman laser did not have any significant effect. In other words, the application of the $G(R_\infty)$ factor, on-line measured with *in-situ* UV-Vis-NIR spectroscopy, provides an elegant way of quantifying *in-situ* Raman spectra in a catalytic reactor.

Conclusions

It is shown that a combined *in-situ* Raman / UV-Vis-NIR set-up allows the on-line monitoring of the redox process of a supported chromium oxide catalyst during a series of temperature programmed reduction cycles. The UV-Vis-NIR spectra can be used to quantify the Raman spectra by performing a $G(R_\infty)$ correction with an uncertainty of less than 10%. It is shown that this method is always applicable as long as the temperature is homogeneously distributed throughout the reactor bed. This is of great importance since a Raman laser is able to cause a local heating effect, which in one of our experiments resulted in a difference in observed reduction temperature of more than 100°C for both spectroscopic techniques. In other words, a combined set-up allows with one technique (UV-Vis-NIR) to verify the results obtained with another technique (Raman).

Furthermore, it is shown that circumventing this local Raman heating effect is far from trivial as is often assumed. Reducing the laser power results in a reduced sample heating, but at the expense of the signal-to-noise ratio. If the observed reaction processes are slow, this is not really a problem. However, with fast reaction processes taking place in a reactor, one might loose important information. Changing the cell design is only useful if the same sample volume can be probed by both spectroscopic techniques. In heterogeneous catalysis, this method is generally inapplicable since the required inner diameter of the reactor would cause severe reactor plugging. Increasing the overall reaction temperature clearly reduces the Raman heating effect, but limits the applicability of the experimental set-up to high-temperature catalytic reactions. It is shown that for the systems under investigation the heat effect becomes negligible when the reactor temperature is close to 500°C. Nevertheless, carefully selecting the reaction parameters makes it possible to use *in-situ* Raman spectroscopy in a quantitative manner making use of the $G(R_\infty)$ correction factor.

Acknowledgements

Dr. P. Brémond (CEDIP Infrared Systems) and P. van Riel (L-A-P Specialty Products & Services) are kindly acknowledged for their contribution to the IR-thermography experiments.

References

1. Tinnemans, S. J.; Kox, M. H. F.; Nijhuis, T. A.; Visser, T.; Weckhuysen, B. M., *Phys. Chem. Chem. Phys.*, **2005**, *7*, 211.
2. Nijhuis, T. A.; Tinnemans, S. J.; Visser, T.; Weckhuysen, B. M., *Phys. Chem. Chem. Phys.*, **2003**, *5*, 4361.
3. Nijhuis, T. A.; Tinnemans, S. J.; Visser, T.; Weckhuysen, B. M., *Chem. Eng. Sci.*, **2004**, *59*, 5487.
4. Vuurman, M. A.; Hardcastle, F. D.; Wachs, I. E., *J. Mol. Catal.*, **1993**, *84*, 193.
5. Vuurman, M. A.; Stufkens, D. J.; Oskam, A.; Moulijn, J. A.; Kapteijn, F., *J. Mol. Catal.*, **1990**, *60*, 83.
6. Weckhuysen, B. M.; Wachs, I. E.; Schoonheydt, R. A., *Chem. Rev.*, **1996**, *96*, 3327.
7. Weckhuysen, B. M.; Schoonheydt, R. A.; Jehng, J. M.; Wachs, I. E.; Cho, S. J.; Ryoo, R.; Kijlstra, S.; Poels, E., *J. Chem. Soc. Faraday Trans.*, **1995**, *91*, 3245.
8. Wu, Z.; Zhang, C.; Stair, P. C., *Catal. Today*, **2006**, in press.
9. Mesu, J. G.; van der Eerden, A. M. J.; de Groot, F. M. F.; Weckhuysen, B. M., *J. Phys. Chem. B*, **2005**, *109*, 4042.
10. Tinnemans, S. J.; Mesu, J. G.; Kervinen, K.; Visser, T.; Nijhuis, T. A.; Beale, A. M.; Keller, D. E.; van der Eerden, A. M. J.; Weckhuysen, B. M., *Catal. Today*, **2006**, *113*, 3.
11. Bowie, B. T.; Chase, D. B.; Griffiths, P. R., *Appl. Spectrosc.*, **2000**, *54*, 164A.
12. Everall, N. J.; Lumsdon, J.; Christopher, D. J., *Carbon*, **1991**, *29*, 133.
13. Johansson, J.; Pettersson, S.; Taylor, L. S., *J. Pharm. Biom. Anal.*, **2002**, *30*, 1223.
14. Kagi, H.; Tsuchida, I.; Wakatsuki, M.; Takahashi, K.; Kamimura, N.; Iuchi, K.; Wada, H., *Geochim. Cosmochim. Acta*, **1994**, *58*, 3527.
15. Paolone, A.; Sacchetti, A.; Corridoni, T.; Postorino, P.; Cantelli, R.; Rousse, G.; Masquelier, C., *Solid State Ionics*, **2004**, *170*, 135.
16. Schrader, B.; Hoffmann, A.; Keller, S., *Spectrochim. acta. prt. A,* **1991**, *47*, 1135.
17. Shebanova, O. N.; Lazor, P., *J. Raman Spectrosc.*, **2003**, *34*, 845.
18. van de Water, L. G.; Bergwerff, J. A.; Nijhuis, T. A.; de Jong, K. P.; Weckhuysen, B. M., *J. Am. Chem. Soc.*, **2005**, *127*, 5024.
19. Long, D. A. *Raman Spectroscopy*; McGraw-Hill Inc.: Great Britain, **1977.**
20. Kip, B. J.; Meier, R. J., *Appl. Spectrosc.*, **1990**, *44*, 707.
21. Weckhuysen, B. M.; Verberckmoes, A. A.; Buttiens, A. L.; Schoonheydt, R. A., *J. Phys. Chem.*, **1994**, *98*, 579.
22. Weckhuysen, B. M.; De Ridder, L. M.; Schoonheydt, R. A., *J. Phys. Chem.*, **1993**, *97*, 4756.

23. Airaksinen, S. M. K.; Krause, A. O. I.; Sainio, J.; Lahtinen, J.; Chao, K. J.; Guerrero-Perez, M. O.; Banares, M. A., *Phys. Chem. Chem. Phys.*, **2003**, *5*, 4371.
24. Kanervo, J. M.; Krause, A. O. I., *J. Catal.*, **2002**, *207*, 57.
25. Macdonald, A. M.; Vaughan, A. S.; Wyeth, P., *J. Raman Spectrosc.*, **2005**, *36*, 185.
26. Kiefer, W.; Bernstein, H. J., *Appl. Spectrosc.*, **1971**, *25*, 500.
27. Sloane, H. J.; Cook, R. B., *Appl. Spectrosc.*, **1972**, *26*, 589.
28. Beale, A. M.; Van der Eerden, A. M. J.; Kervinen, K.; Newton, M. A.; Weckhuysen, B. M., *Chem. Comm.*, **2005**, *24*, 3015.

5

The role of coke on light alkane dehydrogenation reactions over supported chromium oxide catalysts

Abstract

Research has been carried out on the role of coke in the catalytic dehydrogenation of light alkanes. For this purpose, the formation of coke during the catalytic cycle has been monitored as a function of time by two combined *operando* techniques, i.e., Raman / UV-Vis-NIR and EPR / UV-Vis-NIR spectroscopy. The results of both methods are in good agreement. The Raman / UV-Vis-NIR set-up showed a maximum in activity after ca. 35 min-on-stream. EPR spectroscopy could not confirm this maximum due to inherent differences in reaction conditions. From independent dehydrogenation experiments with ^{13}C-ethane, it was found that the coke, formed on the catalyst surface, is not involved in the dehydrogenation mechanism. However, by combining the activity data with the simultaneously obtained spectroscopic information, it is demonstrated that coke is important to facilitate propane adsorption near the active chromium site.

Introduction

In Chapters 2 and 3, it has been shown that the activity of a propane dehydrogenation catalyst goes through a maximum after approximately 20 min-on-stream, while the selectivity towards propene remains constant. When looking at the catalyst with UV-Vis-NIR spectroscopy, Cr^{6+} is reduced in the first minutes of the cycle and thereafter coke is formed on the surface. This is confirmed by Raman spectroscopy. Combining this information indicates that coke plays an important role in the reaction. This is supported by recent work of the group of Schlögl, in which it is shown that carbon nanomaterials are active in the dehydrogenation of ethylbenzene to styrene.[1,2] However, the results of Chapters 2 and 3 can also be explained by a mechanism, in which coke facilitates an enhanced propane adsorption near the active site. A way to enlarge insight into the precise role of coke during dehydrogenation is to combine spectroscopic information with activity data. Since electron paramagnetic resonance (EPR) spectroscopy is capable of measuring both paramagnetic chromium species and coke radicals[3-17], it was decided to perform such a study on the role of coke by means of *operando* EPR / UV-Vis-NIR spectroscopy in parallel with the previously described combined Raman / UV-Vis-NIR method. Since valuable additional information can be extracted from experiments with isotopic labeled gasses, it was also decided to study the catalytic process using ^{13}C containing hydrocarbons and D_2. With respect to isotopic labeling experiments, it is remarkable to note that such labeling experiments have only been reported for unsupported chromium oxide catalysts, namely Cr_2O_3.[18,19]

Experimental

Experiments were carried out in three different set-ups: 1) *operando* Raman / UV-Vis-NIR , 2) *operando* EPR / UV-Vis-NIR set-up and 3) fixed bed.

Raman / UV-Vis-NIR

In the Raman / UV –Vis set-up, 300 mg of a 13 wt% Cr / Al_2O_3 catalyst was typically placed in quartz reactor and heated at a rate of 10 °C min^{-1} to 550 °C in a 20 vol% O_2 (Hoek Loos, 99.995%) in He (99.996%) flow. After heating, He was purged to remove all O_2 in the system and subsequently a 9 vol% propane (Hoek Loos, 99.92 %) stream with a total flow of 22 ml min^{-1} was applied. All flows given are at standard temperature and pressure. On-line gas analysis was performed using a Varian CP-4900 Micro GC equipped with a Poraplot Q and a Molsieve 5A column and TCD detectors. UV-Vis-NIR diffuse reflectance (DRS) spectra were measured using a DH-

2000 light source (Avantes) combined with an Avaspec 2048 CCD spectrometer (Avantes) and a BI-FL400 high temperature resistant probe (Ocean Optics).[20] Raman spectra were recorded using a Kaiser RXN spectrometer equipped with a 532 nm diode laser (output power of 60 mW). A 5.5″ objective was used for beam focusing and collection of the scattered radiation.[21] The exposure time of the CCD detector was 2 s, while 25 accumulations were averaged to obtain a reasonable signal to noise ratio. Spectra were taken every 225 s. The intensities of the Raman bands were determined using Thermo Galactic Grams AI v. 7.0 software.

EPR / UV-Vis-NIR

Operando EPR / UV-Vis-NIR was performed with a fixed-bed tubular quartz reactor with an inner diameter of 3 mm, located within a double-wall quartz dewar. This reactor was placed into the rectangular cavity of an ELEXSYS 500-10/12 EPR spectrometer (Bruker). A preheated stream of nitrogen was used to heat the sample. EPR spectra were recorded in X-band (ν = 9.28 GHz) using a microwave power of 15 mW, a modulation frequency of 100 kHz and a modulation amplitude of 0.5 mT. As reference, the signal of 2,2-diphenyl-1-picrylhydracyl hydrate (DPPH) was used. UV-Vis-NIR spectra were recorded with an AVASPEC spectrometer (Avantes) in combination with a DH 2000 deuterium-halogen light source (Avantes). The probe is a cylindrical quartz sensor (Optran UV 1500/1800 T, length 200 mm, diameter 1.5 mm, CeramOptec GmbH), which is focused on top of the reactor bed. More details about this setup can be found in the literature.[3,4] Experiments in this set-up were carried out at 500 °C.[†]

Fixed bed

Experiments with labeled compounds were carried out in a tubular fixed bed quartz reactor with an inner diameter of 7 mm. The temperature in the catalyst bed was measured by a thermocouple contained in a quartz well (outer diameter of 3 mm), which was placed directly under the catalyst bed. The same catalyst as described above was pretreated by heating to 580 °C in a He stream and exposure to 20 vol% O_2 in He for 30 min at 580 °C before flushing with He. Unless otherwise specified, the reaction mixture was composed of 2 ml min^{-1} ethane and 20 ml min^{-1} He. Catalyst regeneration was performed by exposure to a 20 vol% O_2 in He stream for 30 min at

[†] Unfortunately, measuring in this set-up at higher temperatures was not possible. At 500 °C the dehydrogenation activity will be low. Nevertheless, the catalyst will show reduction behavior and coke will be formed on the surface due to cracking.

580 °C. Transient experiments were performed by switching a 4-way, He-actuated valve (Valco Inc.) between two sets of feed lines, before the reactor. Feed and product gas composition was analyzed by using an on-line HP Quad Micro-Gas Chromatograph (GC) with 3 separate channels containing Molsieve-5A, PoraPlot-U and AluminaPlot columns, respectively, and thermal conductivity detectors. The mass spectrum of the reactor effluent was continuously monitored by an on-line Pfeiffer Omnistar Mass Spectrometer. The isotopic composition of each gas component was determined by using an off-line HP 6890 GC with a GS GasPro column and a HP 5973 Mass Selective Detector. Isotopic labeling experiments were performed after pretreatment and exposure to the standard reactant mixture for 10–20 min at 580 °C, followed by flushing in He. D_2 gas (99.8%) was obtained from Linde Gas AG. Mono-labeled ethane (mono-^{13}C, 99%) was obtained from Cambridge Isotope Laboratories Inc. Simulated mass fragmentation spectra were calculated by assuming a statistical distribution of corresponding fragments (such as $C_2H_3^+$ versus $C_2H_2D^+$), not taking into account kinetic isotope effects.

Results and Discussion

Figure 5.1 shows the EPR spectra of a 13 wt% Cr / Al_2O_3 catalyst during C_3H_8 dehydrogenation recorded after 0 min (spectrum *a*) and 35 min-on-stream (*b*).

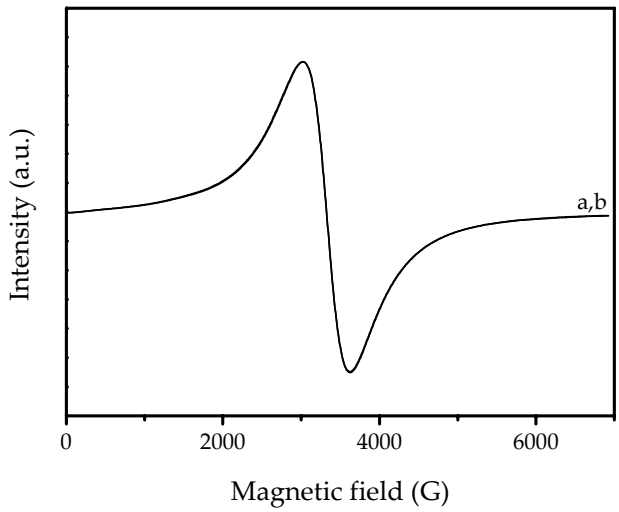

Figure 5.1 *Operando EPR spectra during C_3H_8 dehydrogenation over a 13 wt% Cr / Al_2O_3 industrial-like catalyst at 500 °C recorded after a) 0 and b) 35 min-on-stream.*

As can be seen, the spectra are completely overlapping, both showing a strong β-signal at a g-value of 1.98 (line width 600 G) characteristic for Cr_2O_3-like clusters.[9,11,17]

If coke is formed on the catalyst, it is expected to form a band at a *g*-value close to 2.01[14-16] , but such an additional band is clearly not observed in Figure 5.1. Besides, changes in the amount of Cr are not detected. At first glance, it suggests that the catalytic surface has not changed. However, this conclusion is not permitted, since it is known that, especially high loaded samples (and this sample is a 13 wt% Cr / Al_2O_3) have strong spin-spin interactions. This leads to broadening of the signals thus preventing detection of more specific EPR data. To reduce the problem of signal broadening, a similar experiment with a low loaded catalyst, i.e., a 0.1 wt% Cr / Al_2O_3 sample was performed and the results of these measurements are presented in Figure 5.2.

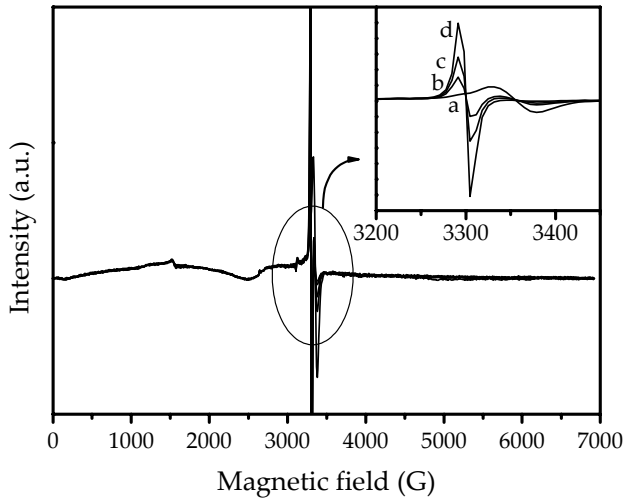

Figure 5.2 *Operando EPR spectra recorded during C_3H_8 dehydrogenation. Spectra were recorded after a) 0, b) 7, c) 14 and d) 42 min-on-stream.*

As can be seen, the EPR signals are considerably narrowed. The Cr^{5+} is seen at the same *g*-value of 1.97, but now it has a line width of 40 G (γ-phase)[9,11,17]. It should be noted that this signal is sometimes attributed to a mixed phase of Cr^{6+}-Cr^{3+}-Cr^{6+} clusters.[7,8] As can be seen from the inset (exploded view), the Cr^{5+} signal decreases during dehydrogenation, which indicates that oxidized Cr-species are being reduced at these conditions. Simultaneously, a second signal appears at a *g*-value of 2.0025 (line width 14 G) and continues growing, as is best seen in the inset in Figure 5.2 (spectrum *a* to *d*). It can be attributed to the formation of coke radicals[14-16] and the line width indicates that the carbon content (C : H ratio) is close to 100 %, and thus that a graphitic type of coke is formed.[16] To obtain a more quantitative insight into the reduction of Cr^{5+} and the simultaneous formation of coke, the EPR signals recorded

at 7 different points during the reaction, have been double integrated and plotted against time in Figure 5.3.

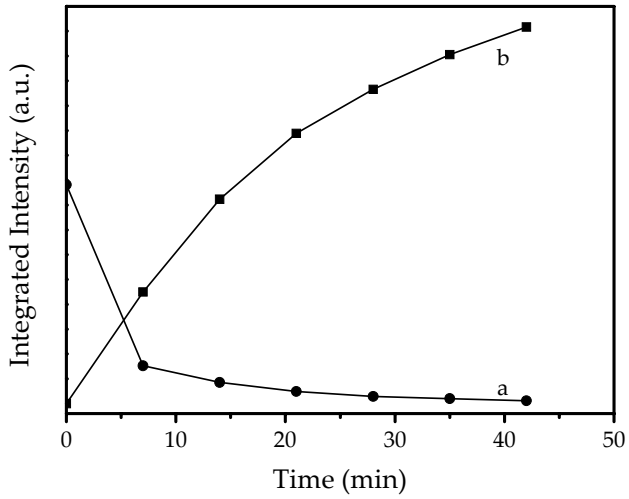

Figure 5.3 *The course of the amount of Cr^{5+} (a) and coke (b) plotted as function of time during propane dehydrogenation at 500 °C.*

As appears, the amount of Cr^{5+} rapidly decreases in the first minutes on-stream. Furthermore, the amount of coke gradually increases during the experiment. These observations are in line with the results of the experiments in which the amount of coke was determined via Raman spectroscopy. The Raman spectra, showing the development of the characteristic coke bands at 1330 and 1580 cm^{-1} are presented in Figure 5.4. The spectra have been corrected for the changing color according to the $G(R_\infty)$ method.

As already mentioned in Chapter 3, the amount of coke formed increases from the top to the bottom of the catalyst bed. This observation is in contrast to the results of modeling work of Jackson and Stitt who calculated that the largest amount of coke deposits are present at the inlet of a reactor during an isothermal propane dehydrogenation reaction.[22] Nevertheless, the dark color at the bottom of the reactor after an experiment indicates that coke is primarily formed out of propene. This hypothesis was verified by feeding a mixture of propene in He over the 13% catalyst at the same conditions. The complete catalyst bed became now darker and a gradient was not observed.

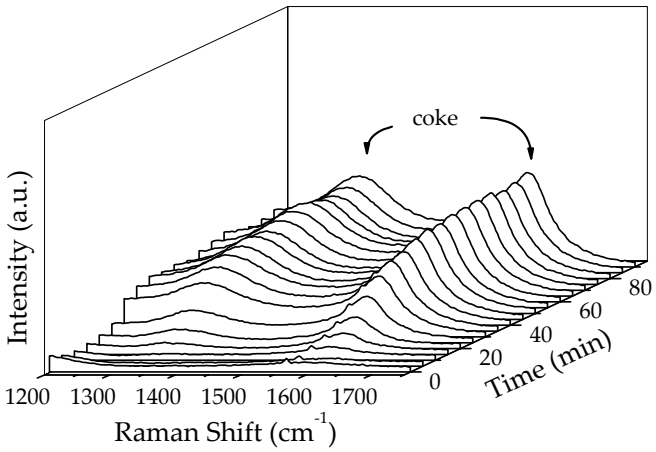

Figure 5.4 *Coke formation monitored on a 13 wt% Cr / Al_2O_3 catalyst during 90 min of propane dehydrogenation. The $G(R_\infty)$ method has been applied to correct the Raman spectra.*

From literature, it is known that the two Raman bands of coke not only provide information on the amount of coke present on the catalyst, but also on its the nature. More graphitic type of coke has a band around 1580 cm^{-1}, whereas more disordered types of coke have a contribution around 1330 cm^{-1}.[23-32] Therefore, the intensity course and mutual ratio of these bands provide valuable information on the type of coke formed on the surface. In Figure 5.5 the course of the coke bands is plotted against time.

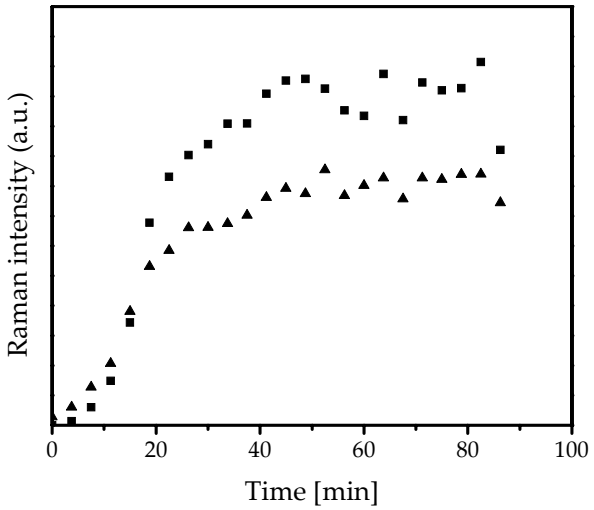

Figure 5.5 *Raman intensity profile of the coke bands located at 1330 cm^{-1} (■) and 1580 cm^{-1} (▲) after $G(R_\infty)$ correction.*

Evidently, both the disordered and the graphitic type of coke are increasingly formed which is in accordance with the results from EPR as depicted in Figure 5.3. Figure 5.5 also shows that the formation of coke is levelling off after approximately 35 min-on-stream. Unfortunately, corresponding EPR data at t > 40 min have not been recorded, but it is reasonable to assume that such measurements would show the same behaviour for t > 40 min. Next, the intensity ratio of the two Raman bands after $G(R_\infty)$ correction was determined, as this provides information on the type of coke that is primarily formed. The results are shown in Figure 5.6 together with the activity and selectivity data.

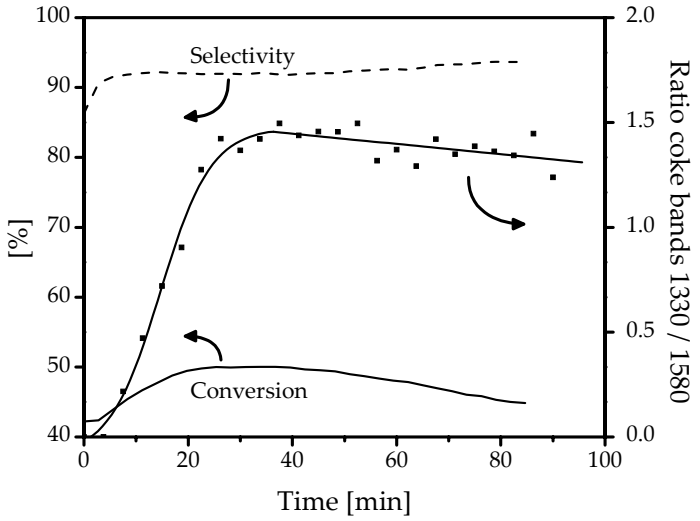

Figure 5.6 *Activity and selectivity data of a 13 wt% Cr / Al_2O_3 catalyst, as well as the intensity ratio of the $G(R_\infty)$ corrected coke bands at 1330 and 1580 cm^{-1}.*

It appears that in the beginning of the reaction a more disordered aliphatic type of coke is formed. After ca 35 min-on-stream the ratio between the 1330 and 1580 cm^{-1} bands decreases. It follows that the nature of the coke becomes more graphitic, which is in agreement with measurements of Lespade *et al.*[33] This indicates that the propene will initially form oligomers (or polymers) and aromatics, but after a while, these species loose hydrogen and become graphitic. The detection of C_4^+ hydrocarbons in the product stream during ethane dehydrogenation experiments also points to such a mechanism. Similar results have been observed by Wu and Stair.[34] They performed butane dehydrogenation experiments at different temperatures over V / θ-Al_2O_3 catalysts and observed the formation of styrene (C_8H_8) at the surface. Next, after polymerization to polystyrene, this material developed further into dense polyaromatic structures.

Figure 5.6 also shows that the change in the nature of the coke, which occurs after ca. 35 min-on-stream, coincides with a maximum in activity. Apparently, the type of coke is related to the activity of the reaction. A plausible explanation for this phenomenon is that at the start of the reaction Cr^{6+} at the surface is reduced to Cr^{3+}. This is in accordance with the results from UV/Vis and EPR spectroscopy. Next, an aliphatic type of coke is predominantly formed on the surface, which facilitates the adsorption of propane at the surface. Finally, this improved adsorption capacity results in a higher activity. This leads to the conclusion that the initially formed coke is beneficial to the reaction, which is in line with work of Menon.[35] As the reaction proceeds, more coke is formed at the surface and finally the active sites will be completely covered. At this point the active Cr sites have become less accessible and as a result the activity decreases. In the meantime, the nature of the coke becomes more graphitic. Since the complete coverage of the active centers starts at the end of the reactor and moves slowly towards the beginning, the effect on the overall activity is only limited.

Based on this hypothesis, it is proposed that coke is not actively taking part in the reaction, but only facilitates propane adsorption. However, it does not exclude that coke is also part of the active site, in analogy to the dehydrogenation of ethylbenzene to styrene.[1,2,35,36] To prove whether carbon deposits are active in the dehydrogenation of light alkanes, experiments were previous experiments. The conversion obtained, showed a maximum after 15 min-on stream before levelling off at 20 % while the selectivity remained > 94 %. This is in agreement with the observation for the propane dehydrogenation. However, the use of labeled reactants also offers the possibility to gain insight in the origin of the formed product. If an oligomer or aromatic compound would be an intermediate in the reaction, isotopic scrambling of ethane is expected during 1-^{13}C ethane dehydrogenation. Therefore the (changes in) mass fragmentation pattern of ethane and ethane in the reactor effluent were studied upon switching the gas feed from ^{12}C-C_2H_6 / He to ^{13}C-C_2H_6 / He. The results are presented in Figure 5.7.

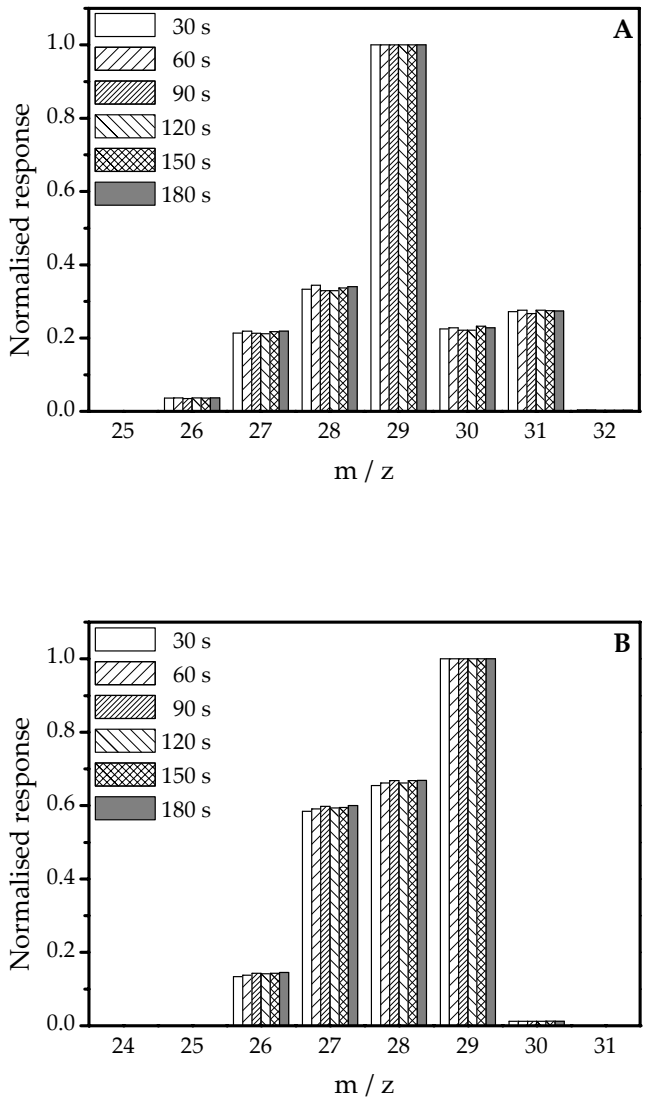

Figure 5.7 *Mass fragmentation pattern of A) ethane and B) ethene in the reactor effluent after switching from ^{12}C-C_2H_6 / He via He to 1-^{13}C-C_2H_6 / He over a 13 wt% Cr / Al_2O_3 catalyst.*

Clearly, no indication of isotopic scrambling is observed during the first 180 s after onset of the 1-^{13}C ethane feed. This is most readily illustrated by the absence of any $^{13}C_2H_6$ formation (m/z 32) or $^{13}C_2H_4$ (m/z 30) (Note that the small peaks observed for m/z 32 and m/z 30, respectively, correspond to the 1.1% natural abundance of ^{13}C in carbon). This result supports the hypothesis that coke intermediates are not part of the reaction cycle that leads to the formation of ethene. Therefore, it can be concluded that coke indeed facilitates the adsorption of light alkanes and in this way enhances the activity until the active site is covered.

This conclusion is in agreement with literature, stating that the dehydrogenation is initiated by physisorption of the alkane on coordinatively unsaturated Cr^{3+} centers.[13,19,37] A C-H bond is subsequently activated and new O-H and Cr-Alkyl bonds are formed. The alkene is then formed from a transfer of hydrogen from the alkyl to the chromium. This reaction is thought to be the rate determining step in the process. The reaction cycle is completed via the formation of H_2 and a regeneration of the Cr site. In a possible parallel mechanism, ethane coordinates to a hydrochromium site, leading to the formation of a Cr-alkyl and H_2. The cycle is completed via a β-H transfer to the Cr and ethene desorption. These mechanisms, schematically depicted in Figure 5.8, have recently been discussed by Lillehaug *et al.*, who studied this reaction via quantum chemical methods.[38]

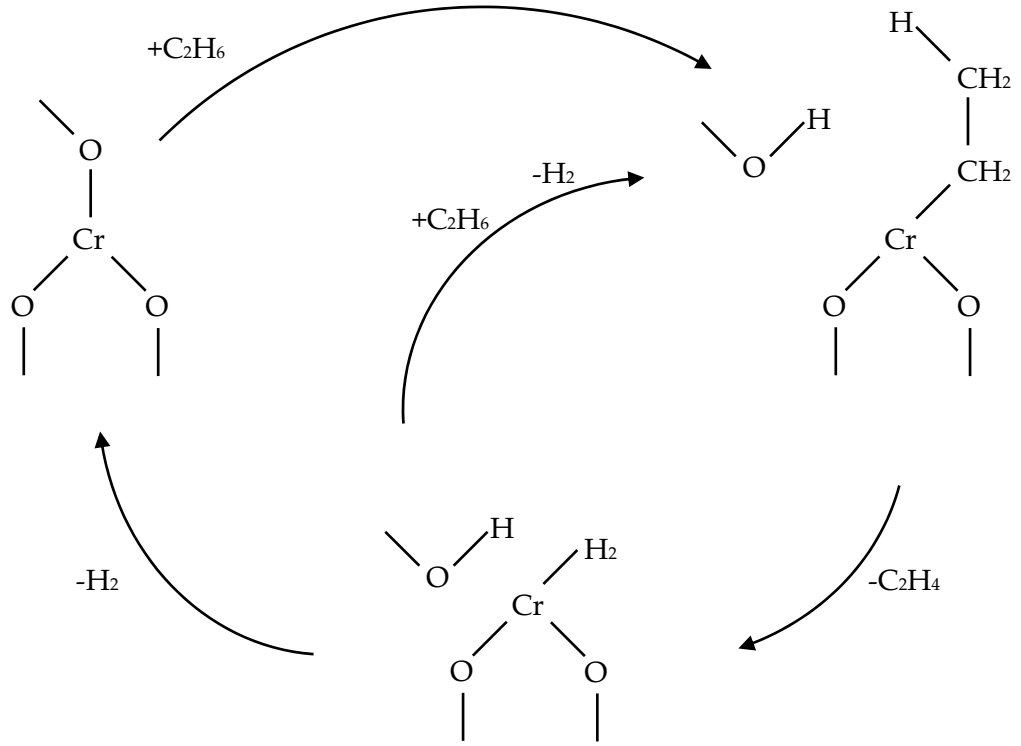

Figure 5.8 *Schematic reaction mechanism for the dehydrogenation of alkanes over a Cr / Al_2O_3 catalyst.*

To further confirm the reaction mechanism, experiments were carried out by feeding both ^{12}C ethane and D_2 over the catalyst in a 2:1:20 ratio (C_2H_6:D_2:He). The mass fragmentation patterns of ethane and ethane, obtained for this reaction, are presented in Figure 5.9 together with simulated data.

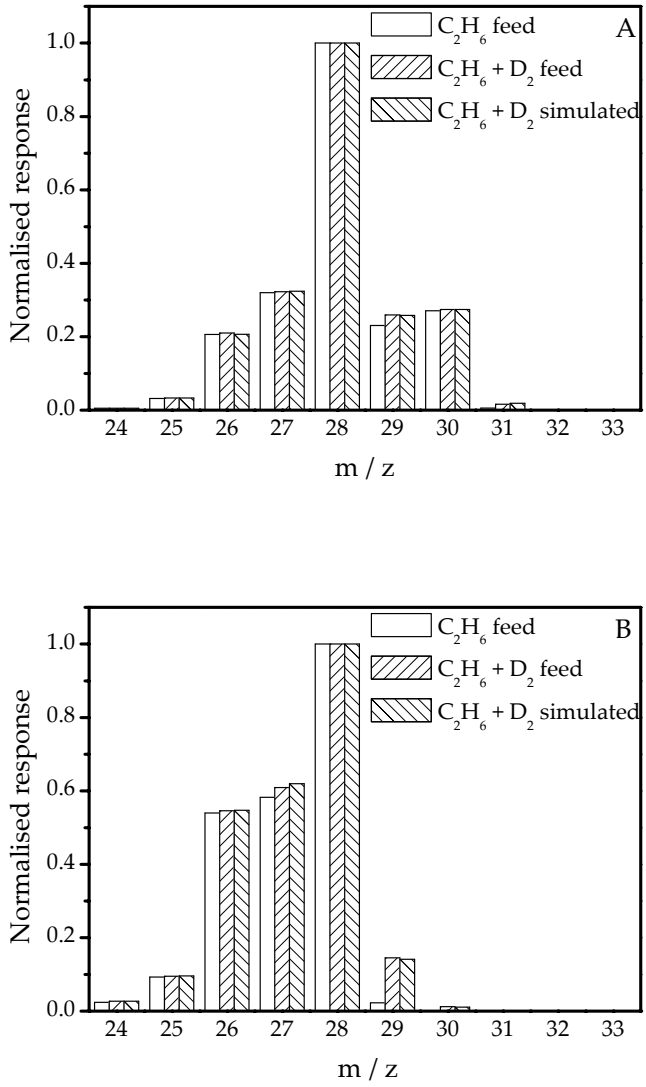

Figure 5.9 *Mass fragmentation pattern of A) ethane and B) ethene in the reactor effluent during a dehydrogenation experiment with a gas feed composition of C_2H_6:D_2:He = 2:0:20 or C_2H_6:D_2:He = 2:1:20.*

As appears, a hydrogen atom is only exchanged by a deuterium atom in a fraction (4%) of the ethane. Also, m/z = 30 increases hardly, which implies that only one hydrogen atom in the ethane is replaced. This points towards an end-on, dissociative adsorption of ethane at the catalytic surface. Furthermore, bi-deuterated ethane is not observed and hence it can be concluded that the formation of ethane from ethene does not occur at the applied conditions. When looking at the fragmentation pattern of ethene (Figure 5.9B), it can be noticed that ethene experiences more H-D exchange than ethane. The simulated data indicate the abundances to be 89 % for C_2H_4, 10 %

for C_2H_3D and 1 % for $C_2H_2D_2$. This suggests that ethene can be easily adsorbed end-on as an ethyl entity, either hydrogenating to ethane or dehydrogenating back to ethene. Another explanation can be that ethene is deuterated, and subsequently deprotonated on Bronsted-acid sites on the Al_2O_3 support, as has been observed by Amenomiya.[39] Finally, it must be noted that the overall dehydrogenation reaction is an equilibrium reaction. It implies that, in case more H_2 is added to the stream, the equilibrium will shift towards the formation of ethane with an increase in the amount of deuterated ethane as a result.

Conclusions

Operando EPR / UV-Vis-NIR spectroscopy performed in parallel to *operando* Raman / UV-Vis-NIR is a valuable way to obtain more detailed insight into events that take place during alkane dehydogenation over chromium oxide catalysts. The two-track approach allows quantitative monitoring of the oxidative state of the chromium species and the reduction and formation of coke as function of time. The results of the partly complementary methods are highly consistent, but the EPR / UV-Vis-NIR requires low loaded chromium catalysts to obtain useful data.

Isotopic labeling experiments show that ethane dehydrogenation proceeds via an end-on, dissociative adsorption of ethane on a Cr^{3+}–O active site at the catalyst surface. This experimental finding confirms the results reported by Burwell *et al*. for higher alkanes on Cr_2O_3[19] and the recent theoretical work of Lillehaug *et al.*[38] Furthermore, it is concluded that coke deposits, formed during the activation, are not actively involved in the ethane dehydrogenation cycle. The current view is that coke facilitates propane adsorption in the initial stage of the catalytic process. Next, after the activation period, coke covers the active Cr site and as a result the activity drops. This is substantiated by the Raman spectroscopic data which demonstrate that the type of coke evolves from a disordered aliphatic form to a more graphitic type.

Acknowledgements

Prof. Olsbye, A. Virnovskaia and Ø. Prytz are kindly acknowledged for performing the measurements with labeled compounds. The Ph. D. grant of A.V. is financed by Statoil through the VISTA program, contract no. 6446.

References

1. Mestl, G.; Maksimova, N. I.; Keller, N.; Roddatis, V. V.; Schlögl, R., *Angew. Chem. Int. Ed.*, **2001**, *40*, 2066.
2. Keller, N.; Maksimova, N. I.; Roddatis, V. V.; Schur, M.; Mestl, G.; Butenko, Y. V.; Kuznetsov, V. L.; Schlögl, R., *Angew. Chem. Int. Edit.*, **2002**, *41*, 1885.
3. Bruckner, A., *Phys. Chem. Chem. Phys.*, **2003**, *5*, 4461.
4. Bruckner, A.; Kondratenko, E., *Catal. Today*, **2006**, in press.
5. Mentasty, L. R.; Gorriz, O. F.; Cadus, L. E., *Ind. Eng. Chem. Res.*, **1999**, *38*, 396.
6. Cimino, A.; Cordischi, D.; Derossi, S.; Ferraris, G.; Gazzoli, D.; Indovina, V.; Occhiuzzi, M.; Valigi, M., *J. Catal.*, **1991**, *127*, 761.
7. Ellison, A.; Sing, K. S. W., *J. Chem. Soc. Faraday Trans.*, **1978**, *74*, 2807.
8. Ellison, A.; Sing, K. S. W., *J. Chem. Soc. Faraday Trans.*, **1978**, *74*, 2017.
9. Khaddar-Zine, S.; Ghorbel, A.; Naccache, C., *J. Mol. Catal. A-Chem.*, **1999**, *150*, 223.
10. Yanez-Limon, J. M.; Perez-Roblez, J. F.; Gonzalez-Hernandez, J.; Zamorano-Ulloa, R.; Ramirez-Rosales, D., *Thin Solid Films*, **2000**, *373*, 184.
11. Weckhuysen, B. M.; Wachs, I. E.; Schoonheydt, R. A., *Chem. Rev.*, **1996**, *96*, 3327.
12. Weckhuysen, B. M.; Wachs, I. E.; Schoonheydt, R. A., *Stud. Surf. Sci. Catal.*, **1994**, *91*, 151.
13. Weckhuysen, B. M.; Schoonheydt, R. A., *Catal. Today*, **1999**, *51*, 223.
14. Karge, H. G.; Lange, J.-P.; Gutsze, A.; Laniecki, M., *J. Catal.*, **1988**, *114*, 114.
15. Li, C.; Takanohashi, T.; Saito, I., *Energy and Fuels*, **2002**, *16*, 1116.
16. Ingram, D., *Third biennial carbon conference*, **1957**, 93.
17. O'Reilly, D. E.; Mac Iver, D. S., *J. Phys. Chem.*, **1962**, *66*, 276.
18. Burwell, R. L.; L., H. G.; Taylor, K. C.; Read, J. F., *Adv. Catal.*, **1969**, *20*, 1.
19. Burwell, R. L.; Littlewood, A. B.; Cardew, M.; Pass, G.; Stoddart, C. T. H., *J. Am. Chem. Soc.*, **1960**, *82*, 6272.
20. Nijhuis, T. A.; Tinnemans, S. J.; Visser, T.; Weckhuysen, B. M., *Chem. Eng. Sci.*, **2004**, *59*, 5487.
21. Nijhuis, T. A.; Tinnemans, S. J.; Visser, T.; Weckhuysen, B. M., *Phys. Chem. Chem. Phys.*, **2003**, *5*, 4361.
22. Jackson, S. D.; Stitt, E. H., *Curr. Top. Catal.*, **2002**, *3*, 245.
23. Ager, J. W.; Veirs, D. K.; Shamir, J.; Rosenblatt, G. M., *J. Appl. Phys.*, **1990**, *68*, 3598.
24. Bowling, R. J.; Packard, R. T.; McCreery, R. L., *J. Am. Chem. Soc.*, **1989**, *111*, 1217.
25. Katagiri, G.; Ishida, H.; Ishitani, A., *Carbon*, **1988**, *26*, 565.
26. Nakamizo, M.; Tamai, K., *Carbon*, **1984**, *22*, 197.

27. Escribano, R.; Sloan, J. J.; Siddique, N.; Sze, N.; Dudev, T., *Vibr. Spectrosc.*, **2001**, *26*, 179.
28. Kong, F.; Kostecki, R.; Nadeau, G.; Song, X.; Zaghib, K.; Kinoshita, K.; McLarnon, F., *J. Power Sources*, **2001**, *97-8*, 58.
29. Mertes, S.; Dippel, B.; Schwarzenbock, A., *J. Aerosol Sci.*, **2004**, *35*, 347.
30. Wang, Y.; Alsmeyer, D. C.; McCreery, R. L., *Chem. Mat.*, **1990**, *2*, 557.
31. Compagnini, G.; Puglisi, O.; Foti, G., *Carbon*, **1997**, *35*, 1793.
32. Sze, S. K.; Siddique, N.; Sloan, J. J.; Escribano, R., *Atmos. Environ.*, **2001**, *35*, 561.
33. Lespade, P.; Marchand, A.; Couzi, M.; Cruege, F., *Carbon*, **1984**, *22*, 375.
34. Wu, Z.; Stair, P. C., *J. Catal.*, **2006**, *237*, 220.
35. Menon, P. G., *J. Mol. Catal.*, **1990**, *59*, 207.
36. Echigoya, E.; Sano, H.; Tanaka, M., *8th International Congress on Catalysis*, Berlin, **1984**,V623.
37. Derossi, S.; Ferraris, G.; Fremiotti, S.; Garrone, E.; Ghiotti, G.; Campa, M. C.; Indovina, V., *J. Catal.*, **1994**, *148*, 36.
38. Lillehaug, S.; Borve, K. J.; Sierka, M.; Sauer, J. A., *J. Phys. Org. Chem.*, **2004**, *17*, 990.
39. Amenomiya, Y., *J. Catal.*, **1968**, *12*, 198.

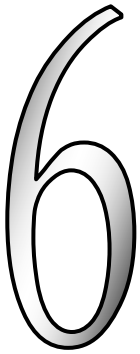

Summary and Concluding Remarks

Spectroscopic techniques can provide characteristic information about a catalytic material. These techniques can be applied at different stages of the catalyst lifetime, for instance before and after deactivation and this results in valuable information. However, information about the nature of the deactivation is not obtained and it would be interesting to investigate a catalyst during a reaction, i.e. to perform *operando* spectroscopy. The combination of different *operando* spectroscopic techniques provides even more information as long as the applied techniques are complementary. Therefore the aim of this work was to combine two complementary spectroscopic techniques, namely Raman and UV-Vis-NIR, into one *operando* reaction set-up. Raman spectroscopy provides vibrational information, whereas information about electronic transitions can be gathered with UV-Vis-NIR. In **Chapter 2** the development of this combination is described. The developed set-up was tested for the dehydrogenation of propane over a Cr / Al_2O_3 catalyst. Traditionally, propene is a side product formed in ethylene steam crackers and fluidized catalytic crackers. However, the requested amount of propene is outgrowing the production capacity, making new routes, like the dehydrogenation, vital to comply with the demand. It is shown that coke species, formed on the catalytic surface, can be monitored with Raman spectroscopy. Furthermore, it is shown that simultaneously measured UV-Vis-NIR spectra provide information about the chromium site on the catalyst. Unfortunately, the obtained information was qualitative and it would be very advantageous if the information could also be used in a quantitative manner. Especially since the *operando* Raman spectra, measured during dehydrogenation, suggested a role for coke in the dehydrogenation process. In **Chapter 3** the amount of coke formed on the catalyst during dehydrogenation, was determined via quantitative Raman spectroscopy. A new method was developed, in which the observed Raman intensity was corrected for the changing color (absorption) of the catalyst. By measuring simultaneously the changing color (absorption at a specific wavelength) of the catalyst via UV-Vis-NIR spectroscopy, a $G(R_\infty)$ correction factor could be determined. This factor was used to quantify the Raman signal. The results of the application of the $G(R_\infty)$ correction factor were compared with the quantification of the Raman data making use of BN as an internal standard. The

latter approach is a more commonly known procedure to quantify Raman signals. It appeared that both methods showed good agreement, making the newly developed method preferable since the addition of an extra compound (namely the internal standard) is not required. It is stated that the method is generally applicable. Therefore, in **Chapter 4** the amount of Cr^{6+} in Cr / Al_2O_3 catalysts was monitored during temperature programmed reduction experiments. It appeared that the laser was capable of heating the sample locally and as a consequence; the color was not the same throughout the reactor. This made the application of the $G(R_\infty)$ correction not straightforward. Several attempts were made to circumvent this heat effect and every method had its own strengths and limitations. Furthermore, it is shown that if the experimental conditions are chosen carefully, Raman spectroscopy can be performed in a quantitative manner. Finally, in **Chapter 5** the role of coke was explored in more detail. Experiments with labeled compounds revealed that ethane dehydrogenation proceeds via an end-on dissociative adsorption of ethane on a Cr^{3+}–O active site at the catalyst surface. No evidence was found that coke deposits, formed during the activation, are involved in the ethane dehydrogenation cycle. Furthermore, it appeared propene is precursor for coke formed on the catalyst during the dehydrogenation. Initially, this coke enhances the propane adsorption and as a result the activity increases. Here after, coke starts blocking the active site, and as a result the activity will drop making a regeneration step necessary. Raman spectroscopy showed that during reaction the type of coke present changes from a more aliphatic to a more graphitic type of coke.

In other words, combining multiple *operando* spectroscopic techniques into one set-up proves to be a very useful approach in gathering information on catalytic reactions. Someone may state that the information can also be gathered by performing separate experiments. To some extent this is true for qualitative information. However, different experiments are likely to result in different reaction conditions. Furthermore, it is very useful if one technique can be used to verify the results obtained by a second technique. In this way it was possible to observe the heat affect, and address it to the heating of the Raman laser. This effect of a high energy radiation source on a catalyst is often neglected. Furthermore, it is shown

that, if the heat effect can be eliminated, it is possible to use the UV-Vis-NIR data for the quantification of the Raman signals. An application that would not have been possible if different experiments were performed.

For the reasons mentioned above, combining spectroscopic techniques is very useful. New set-ups combining three *operando* characterization techniques (e.g. EPR / Raman / UV-Vis-NIR and ED-XAFS / Raman / UV-Vis-NIR) have the potential of providing even more insight about a catalyst in action. However, one must realize that the addition of a spectroscopic technique is not straightforward. Every technique has its own sensitivity and thus concentration range in which useful data can be gathered. This must be taken into account when building a new set-up.

These examples show the value of *operando* spectroscopy in a research environment for rational catalyst design. However, in industrial companies the application of multiple spectroscopic techniques could also be very useful. Instead of controlling the reactor via the analysis of the product stream, the catalyst can be directly monitored. The condition of the catalyst is known at any time and an optimal performance can be maintained by intervening in a very early stage, if necessary. As an example one could think of the combination of UV-Vis-NIR and Raman spectroscopy for the control of a propane dehydrogenation plant. Together, they provide information on the amount of coke present on the catalyst and this information can be used to start a regeneration cycle. In other words, *operando* spectroscopy has great potential for on-line catalyst monitoring and reaction control.

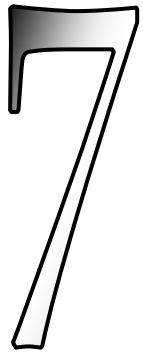

Samenvatting and Slotopmerkingen

De toepassing van spectroscopische technieken kan karakteristieke informatie verschaffen over een katalysator. Dit kan worden gedaan door te meten in de verschillende stadia van de levensduur van de katalysator. Bijvoorbeeld voor en na het deactiveren. Op deze manier wordt waardevolle informatie verkregen. Echter, informatie over de oorsprong van de deactivering zal onmeetbaar zijn. Daarom is het nuttig om een katalysator tijdens een reactie te meten, oftewel het toepassen van *operando* spectroscopie. Indien meerdere complementaire *operando* spectroscopische technieken worden gecombineerd, zal nog meer informatie verkregen worden. Daarom was het doel van dit onderzoek het combineren van twee complementaire spectroscopische technieken, te weten Raman en UV-Vis-NIR, in één *operando* opstelling. Raman verschaft informatie over de vibratietoestanden van moleculen, terwijl electronische overgangen gemeten kunnen worden met UV-Vis-NIR. In **Hoofdstuk 2** is de ontwikkeling van de opstelling beschreven en is deze getest tijdens de dehydrogenering van propaan. Propene wordt typisch gemaakt als bijproduct in etheen stoomkrakers en katalytische vloeistofkrakers. Aangezien de vraag naar propeen de productiecapaciteit overtreft, worden nieuwe productieroutes zoals de dehydrogenering steeds belangrijker. Het is aangetoond dat de vorming van poly-aromatische koolwaterstoffen (coke) op het oppervlak van de katalysator, gevolgd kan worden met Raman spectroscopy. Tegelijkertijd gemeten UV-Vis-NIR spectra geven informatie over de aanwezige chroom-site. Helaas is al deze informatie kwalitatief. Het zou echter waardevol zijn als ook deze informatie over kwantitatief gebruikt zou kunnen worden. Temeer daar de Raman spectra een actieve rol voor coke in het proces suggereren. Een kwantitatieve bepaling van het coke gehalte, gemeten met Raman spectroscopie, is beschreven in **Hoofdstuk 3**. Een nieuwe methode is ontwikkeld, waarin the Raman intensiteit gecorrigeerd wordt voor de veranderde kleur van katalysator. Deze verandering van kleur (absorptie bij een specifieke golflengte) is tegelijk gemeten met UV-Vis-NIR spectroscopie en resulteerde in een $G(R_\infty)$ correctie factor. Met behulp van deze factor is het mogelijk om het Raman signaal te kwantificeren. De op deze manier behaalde resultaten zijn vergeleken met de toepassing van een interne standaard. Deze laatste methode is een meer traditionele manier om Raman signalen te kwantificeren. Beide methoden

geven overeenkomstige resultaten. Dit maakt dat de nieuw ontwikkelde $G(R_\infty)$ correctie-factor de voorkeur geniet. In dat geval hoeft geen extra stof, zoals een interne standaard, te worden toegevoegd. Tevens wordt gesteld dat deze methode algemeen toepasbaar is. Om die reden is in **Hoofdstuk 4** de hoeveelheid Cr^{6+} in een Cr / Al_2O_3 katalysator gemeten tijdens reductie-experimenten waarbij de temperatuur langzaam wordt verhoogd. Hierbij bleek dat de laser in staat was om het monster locaal te verwarmen. Dit had als consequentie dat de kleur in de reactor niet langer homogeen verdeeld was en dus dat de toepassing van de ontwikkelde $G(R_\infty)$ correctie factor niet direct mogelijk was. Meerdere pogingen zijn ondernomen om dit effect te omzeilen waarbij bleek dat iedere methode zijn eigen voor- en nadelen kende. Er is tevens aangetoond dat bij zorgvuldig gekozen reactie omstandigheden het mogelijk is om Raman spectroscopie op een kwantitatieve manier toe te passen. Tot slot wordt in **Hoofdstuk 5** dieper ingegaan op de rol van coke tijdens de dehydrogenering. Uit experimenten met gelabelde reactanten blijkt dat de dehydrogenering van ethaan geschiedt via een end-on dissociatieve adsorptie van ethaan op een Cr^{3+}-O actieve site op het oppervlak. Er is geen bewijs gevonden dat coke residuen, gevormd tijdens de activering, actief betrokken zijn in het reactie-mechanisme. Verder bleek dat propeen pre-cursor is voor de gevormde coke op het oppervlak. De coke zorgt voor een initieel toenemende adsorptie van propaan op het oppervlak, met een toenemende activiteit tot gevolg. Op een gegeven moment is er teveel coke en zullen tevens actieve sites geblokkeerd worden met als resultaat een afnemende activiteit en de noodzaak voor een regeneratie. Uit de Raman data bleek verder dat tijdens de reactie het type coke veranderde van alifatisch naar grafitisch.

Al met al blijkt dat het toepassen van meerdere *operando* spectroscopische technieken in één opstelling zeer waardevol is voor het bestuderen van katalysatoren. Natuurlijk zou iemand de kritiek kunnen uiten dat deze informatie ook in aparte experimenten verzameld kan worden. Dit geldt tot op zekere hoogte voor de kwalitatieve informatie. Echter hierbij moet worden aangetekend dat het zeer moeilijk is om echt identieke reactiecondities te waarborgen. Daarbij komt nog dat het waardevol kan zijn om de ene techniek de andere te laten controleren. Op deze manier was het mogelijk om het warmte-effect toe te schrijven aan de Raman laser. Dit belangrijke

effect van hoog energetische straling wordt vaak verwaarloosd. Tevens is aangetoond dat, wanneer het warmte-effect uitgeschakeld kan worden, het mogelijk is om met behulp van UV-Vis-NIR spectroscopie het Raman signaal te kwantificeren. Om deze redenen is het combineren van meerdere technieken zeer nuttig. Nog meer informatie komt beschikbaar met de opstellingen waarbij drie technieken (EPR / Raman / UV-Vis-NIR en ED-XAFS / Raman / UV-Vis-NIR) zijn geïntegreerd. Hierbij moet wel worden opgemerkt dat het niet altijd gemakkelijk is om meerdere technieken te implementeren. Iedere techniek heeft immers zijn eigen specifieke gevoeligheid en hierop zullen de monsters moeten worden aangepast. Een compromis is dan ook vaak noodzakelijk.

De hierboven beschreven voorbeelden geven een inzicht in de waarde van *operando* spectroscopie in een onderzoeksomgeving. Echter, ook in een industriële omgeving kan het toepassen van meerdere technieken zeer waardevol zijn. In plaats van te sturen op basis van productstroom, zal het mogelijk worden om de katalysator direct te bestuderen. Hierbij wordt het mogelijk om eerder in te grijpen als de katalysator tekenen van deactivering laat zien om een optimale conditie te behouden. Hierbij valt te denken aan bijvoorbeeld processturing van de dehydrogenering van propaan met behulp van Raman en UV-Vis-NIR. Samen zijn zij in staat om de hoeveelheid coke op de katalysator te meten en deze informatie kan worden teruggekoppeld voor het starten van een regeneratie. De toekomst van *operando* spectroscopie ligt dus zowel bij het analyseren van een proces als het aansturen.

List of Publications and Presentations

Publications

T.A. Nijhuis, S.J. Tinnemans, T. Visser, B.M. Weckhuysen, *Operando spectroscopic investigation of supported metal oxide catalysts by combined time-resolved UV-VIS/Raman/on-line mass spectrometry,* Phys. Chem. Chem. Phys., **2003**, *5*, 4361-4365.

T.A. Nijhuis, S.J. Tinnemans, T. Visser, B.M. Weckhuysen, *Towards real-time spectroscopic process control for the dehydrogenation of propane over supported chromium oxide catalysts,* Chem. Eng. Sci., **2004**, *59*, 5487.

O.L.J. Gijzeman, J.N.J. van Lingen, J.H. van Lenthe, S.J. Tinnemans, D.E. Keller and B.M. Weckhuysen, *A new model for the molecular structure of supported vanadium oxide catalysts,* Chem. Phys. Lett., **2004**, *397*, 277.

S. J. Tinnemans, M. H. F. Kox, T. A. Nijhuis, T. Visser, B. M. Weckhuysen, *Real time quantitative Raman spectroscopy of supported metal oxide catalysts without the need of an internal standard,* Phys. Chem. Chem. Phys., **2005**, **7**, 211.

U. Olsbye, A. Virnovskaia, Ø. Prytz, S.J. Tinnemans, B.M. Weckhuysen, *Mechanistic insight in the ethane dehydrogenation reaction over Cr/Al_2O_3 catalysts,* Catal. Lett., **2005**, *103, 1-2,* 143.

S.J. Tinnemans, J.G. Mesu, K. Kervinen, T. Visser., T.A. Nijhuis, A.M. Beale, D.E. Keller, A.M.J van der Eerden, B.M. Weckhuysen, *Combining operando techniques in one spectroscopic-reaction cell: New opportunities for elucidating the active site and related reaction mechanism in catalysis,* Catal. Today, **2006**, *113*, 3.

S. J. Tinnemans, M.H.F. Kox, M.W. Sletering, T.A. Nijhuis, T.Visser and B.M. Weckhuysen, *Dealing with a local heating effect when measuring catalytic solids in a reactor with Raman spectroscopy,* Phys. Chem. Chem. Phys., **2006**, *accepted.*

Presentations

S.J. Tinnemans, T.A. Nijhuis, T. Visser, B.M. Weckhuysen, *Synchronised Operando UV-Vis and Raman Spectroscopy on Catalytic Solids,* Poster presented at the First International Congress on Operando Spectroscopy, Lunteren, March 2003.

S.J. Tinnemans, T.A. Nijhuis, T. Visser, B.M. Weckhuysen, *Synchronised Operando UV-Vis and Raman Spectroscopy on Catalytic Solids,* Poster presented at the 4th Netherlands' Catalysis and Chemistry Conference, Noordwijkerhout, March 2003.

S.J. Tinnemans, T.A. Nijhuis, T. Visser, B.M. Weckhuysen, *Synchronised Operando UV-Vis and Raman Spectroscopy on Catalytic Solids,* Poster presented at the On-line Analyser symposium: Spectroscopy as on-line measuring tool, Antwerp, Belgium, February 2004.

S.J. Tinnemans, T.A. Nijhuis, T. Visser, B.M. Weckhuysen, *Operando UV-Vis-NIR and Raman spectroscopy on supported metal oxides during propane dehydrogenation,* Lecture given at the 5th Netherlands' Catalysis and Chemistry Conference, Noordwijkerhout, March 2004.

S.J. Tinnemans, T.A. Nijhuis, T. Visser, B.M. Weckhuysen, *Synchronised Operando UV-Vis and Raman Spectroscopy on Catalytic Solids,* Poster presented at the COST D15 workshop, La Colle sur Loup, France, October 2004.

S.J. Tinnemans, T.A. Nijhuis, T. Visser, B.M. Weckhuysen, *Towards real-time spectroscopic process control for propane dehydrogenation,* Lecture given at the First Conference of the European Union Coordination Action "CO-ordination of Nanostructured Catalytic Oxides Research and Development in Europe": CONCORDE, Louvain-la-Neuve, Belgium, January 2005.

Dankwoord

Nu zit het er na vier jaar dan echt bijna op. Voor mij betekent dit dat ik nu de kans krijg om een aantal mensen in het bijzonder te bedanken die hebben bijgedragen aan de totstandkoming van dit proefschrift. Allereerst mijn promotor prof. Weckhuysen. Beste Bert, bedankt dat jij mij de kans hebt gegeven om te promoveren en tevens om mezelf verder te ontwikkelen. Het waren soms roerige tijden waarbij jij altijd achter mij hebt gestaan. Ik kan niet beschrijven hoeveel dat voor mij betekend heeft. Tevens ben ik zeer blij geweest met al jouw snelle correctiewerk (Waar haal je toch de tijd vandaan?). Natuurlijk wil ik ook mijn beide co-promotoren bedanken. Xander^{N}, bedankt voor alle hulp die ik heb ontvangen. Zonder jou zou de set-up niet zo makkelijk te bedienen zijn. Tevens heb jij mij geïntroduceerd in een hele nieuwe (af en toe verslavende) wereld. Hopelijk kom ik je nog vaak tegen (al dan niet on-line). Heel veel geluk samen met je vrouw en fijn dat je er op deze dag toch bij kan zijn. Tom, jouw deur stond altijd open voor raad of advies. Door jouw (al dan niet gevraagde) kritische opmerkingen werd ik regelmatig aan het denken gezet. Bedankt daarvoor.

Voor het ontwerpen en bouwen van de opstelling wil ik ook Ad^{M} bedanken. Mede met behulp van jouw praktische kijk hebben we een mooie opstelling kunnen bouwen. Natuurlijk wil ik jou ook bedanken voor alle overige ondersteuning die je geboden hebt.

In dit dankwoord mag ook zeker de glasblazerij niet vergeten worden. De spectroscopische cellen, door jullie gemaakt, hebben in belangrijke mate bijgedragen aan het kunnen werken met de opstelling en het verkrijgen van goede data. Voor mij is het absolute hoogtepunt van jullie kunde de speciale Mickey van glas. Hij staat nog steeds te pronken in de kast en iedereen die hem ziet is onder de indruk.

Tijdens mijn promotie heb ik het geluk gehad om twee afstudeerders te mogen begeleiden. Als eerste was daar Marianne. Ik had je verteld dat ik graag kwantitatieve Raman wilde kunnen doen en dat we daarvoor een studie naar een interne standaard nodig hadden. Het bleek allemaal toch wat ingewikkelder dan gedacht, maar jij hebt wel laten zien wat er met een interne standaard mogelijk is. Bedankt en veel succes met je eigen promotie onderzoek. Bijna aansluitend kwam Marco. Na het toepassen van kwantitatieve Raman op de coke band, wilden we nu de Cr-band kwantificeren tijdens reductie. We wisten dat de laser verantwoordelijk was voor lokale verhitting, maar we dachten dat het effect boven de 100 °C wel mee zou vallen. Dit bleek een illusie, maar het vinden van een oplossing is uiteindelijk

toch gelukt. Bedankt voor jouw inzet en veel succes bij het afronden van de laatste onderdelen van je studie.
Dr. Brückner, I would like to thank you for giving me the opportunity of measuring *operando* EPR / Raman / UV-Vis spectroscopy in Berlin. Working with a different *operando* set-up learned me that more of these type of set-ups are necessary.
I also wish to thank prof. Olsbye for all the labeling experiments she performed in her group and the email discussions.
Natuurlijk wil ik ook mijn kamergenoten bedanken voor alle gezelligheid die zij mij altijd hebben gegeven. Willem, het was altijd leuk om met jou te discussiëren over de meest uiteenlopende onderwerpen. Cristina, de snelheid waarmee jij Nederlands hebt geleerd, verbaast me nog steeds. Niels, wanneer leer je nu eindelijk eens muziek (dus geen herrie) te waarderen?
Naast deze mensen wil ik natuurlijk ook de rest van de collega's bedanken voor alle gezelligheid en overige zaken die op directe of indirecte wijze hebben bijgedragen aan dit boekje.
Xander[T], ik heb jou leren kennen tijdens mijn studie. Altijd kon ik terecht voor een praatje en onze lunches zal ik missen. Hopelijk blijf je zo verstandig om af en toe je rust te nemen zodat je mij niet meer zo hoeft te laten schrikken. Fijn dat jij op deze dag naast mij wilt staan. Hopelijk lukt het je jouw ambities waar te maken.
Daphne, aan het begin van mijn promotietijd kende ik jou nog niet. In de loop van de tijd werd jij een hele goede vriendin waarbij ik maar een minpunt kan bedenken: Je blijft maar bezig met je Vanadium. Ik zal onze (bijna) dagelijkse kop thee missen . Ook heb ik nooit begrepen waarom andere mensen onze gesprekken niet konden volgen. Dat wisselen van gespreksonderwerpen sprak toch voor zich. Dat jij mijn getuige wilde zijn tijdens mijn bruiloft heeft veel voor mij betekend evenals het feit dat jij tijdens mijn promotie naast mij wil staan. Hopelijk blijven we elkaar nog regelmatig spreken en zien.
In een dankwoord kunnen natuurlijk de meest dierbaren om mij heen niet ontbreken. Pa, als pater familias heb jij altijd klaar gestaan met je wijze raad. Ofschoon ik wellicht niet altijd (meteen) luisterde, heb ik er toch veel aan gehad. Bedankt voor je steun. Marjon en Yvonne, betere zussen kan ik me niet wensen. Bedankt dat jullie altijd naar mij hebben willen luisteren als ik daar behoefte aan had. Jullie gegil toen je hoorde dat je (een echte) tante zou worden, zal ik nooit vergeten.
Ma (de Jager), altijd stond u klaar voor mij als ik daar behoefte aan had. (Ook als dat betekende om 6.00 uur opstaan om mij op de trein te zetten). Bedankt! Myrna, Erwin, Lisa en Marc, bij jullie kon ik altijd terecht voor een kop thee. Het raar doen met de

tweeling, daar zijn ooms tenslotte voor, zorgde dat ik mijn hoofd weer even helemaal leeg kon maken.

Het laatste stuk in dit dankwoord is gereserveerd voor de mij meest dierbare persoon. Ilona, eerst als verloofde en later als echtgenote heb jij mij altijd gesteund en bent altijd in mij blijven geloven. Na een geweldige trouwdag vorig jaar, zullen we op de dag van mijn promotie kersverse ouders zijn. Een compleet nieuwe dimensie in ons mooie leven. Hopelijk zullen we er samen nog lang van mogen genieten.

Stan

Curriculum Vitae

Stanislaus Josepus Tinnemans werd op 14 februari 1978 geboren in Deurne. In 1997 behaalde hij het VWO diploma aan het Christelijk College Zeist. Aansluitend werd de opleiding Scheikunde gedaan aan de Universiteit Utrecht. Met universitaire stages bij de vakgroepen Fysisch Organische Chemie en Anorganische Chemie en Katalyse werd het doctoraal diploma in 2002 behaald. In de periode 2002-2006 werd een promotieonderzoek uitgevoerd in de vakgroep Anorganische Chemie en Katalyse (Universiteit Utrecht) onder supervisie van prof. Dr. Ir. B.M. Weckhuysen, Dr. T.A. Nijuis en Dr. T. Visser. De resultaten van dat onderzoek hebben geleid tot dit proefschrift.